SCUOLA NORMALE SUPERIORE

Classe di Scienze

Corso di perfezionamento in

Neuroscienze

XXXII ciclo

“Protein aggregation, ageing and neurodegeneration in the emerging model *Nothobranchius furzeri*”

Settore Scientifico Disciplinare **BIO/09**

Candidato
dr. Sara Bagnoli

Relatore
Eva Terzibasi Tozzini, PhD

Supervisore interno
prof. Alessandro Cellerino

Anno accademico 2020/2021

Abstract

The teleost *Nothobranchius furzeri* is an annual fish and is the shortest-lived vertebrate that can be cultured in captivity. The longer-lived strains of *N. furzeri* show a median lifespan of 40 weeks making it a unique model organism for ageing research. *N. furzeri* recapitulates the major features of mammalian brain ageing, such as gliosis, lipofuscin and iron accumulation and also more global changes at transcriptomic- and proteomic-level.

Neurodegenerative diseases such as Alzheimer's disease (AD), Parkinson's disease (PD) and Fronto-Temporal Dementia (FTD), are the prevalent causes of dementia and are currently viewed as cerebral proteopathies, having age as the major risk factor and in which the accumulation of specific misfolded proteins is the most relevant causative factor.

In the initial part of my thesis, I detected age-dependent protein aggregation, and in particular ribosome aggregation, in the brain of *N. furzeri* during physiological ageing. This observation is key to suggest this organism as a model for observing and studying neurodegeneration. In my thesis work, I laid the groundwork for future studies in this direction, and, in particular, I focused my attention on studying PD- related and TDP43-related protein aggregation and neurodegeneration.

Parkinson's disease is the second most common age-related neurodegenerative disorder after Alzheimer's disease with an estimated 7-10 million persons affected worldwide. Its main neuropathological feature is the aggregation of the phosphorylated form of the protein α-Synuclein (α-Syn) creating characteristic formations called Lewy bodies in the soma and Lewy neurites in neuronal processes. This aggregation is considered the major cause of the neurodegeneration of Tyrosine Hydroxylase (TH) enzyme containing central neurons belonging to the Noradrenergic and Dopaminergic system in the *Substantia Nigra* and in the *Locus coeruleus* nuclei, respectively.

To assess possible PD-related neurodegeneration in *N. furzeri,* I first analyzed the expression of TH in *Nothobranchius furzeri* brain and realized a whole mount 3D map of the monoaminergic system in clarified brains. Secondly, I compared the amount of TH positive cells between young- and old-animals in the *Locus coeruleus* and in the hypothalamic *posterior tuberculum* (the teleost homolog to the mammalian *Substantia Nigra*) to investigate markers of neurodegeneration. I analyzed animals at 5, 12 and 37 weeks of age and found a statistically significant age-dependent reduction of TH+ neurons in the *Locus coeruleus* but not in the *posterior tuberculum*.

Immunoreactivity for phospho-Synuclein (pSyn) in the soma of *Locus coeruleus* neurons was detected already at 5 weeks of age, indicating initial aggregation early in life, with the signal increasing in older samples. No signs of immunoreactivity for phospho-Synuclein were detected in the somata of TH+ hypothalamic neurons at any age. This observation supports the link between the accumulation of somatic phospho-Synuclein and neurodegeneration that is restricted to *Locus coeruleus* neurons. This observation is also in line with Braak's staging of human PD development according to α-Syn immunoreactivity: Braak hypothesizes a caudo-rostral spreading of aggregation and neurodegeneration starting in the vagal nuclei, then spreading to the *Locus coeruleus* and only in later stages involving the *Substantia nigra.*

Staining for aggregated proteins in *Locus coeruleus* cells also revealed presence of aggresomes localized mainly in vacuolized areas of cytoplasm devoid of TH staining in old samples.

Overall, this data point to *N. furzeri* showing a pre-symptomatic like form of PD-related neurodegeneration during normal ageing.
FTD is a neurodegenerative disease involving aggregation and mislocalization of TDP-43. TDP-43 is normally localized into neuronal nuclei, but in FTD patients it localizes in the cytoplasm near the nuclear envelope forming aggregates.
To assess TDP-43 localization in *N. furzeri* brain during ageing, I performed immunofluorescence labelling on both sections and whole mount brains for TDP-43 in young and old animals and I detected abnormal TDP-43 localization in old brains: the protein concentrated in proximity of the nuclear envelope. I was also able to detect protein aggregates stained by aggresome dye associated with cells showing an abnormal TDP-43 staining, supporting the idea of the correlation between abnormal TDP-43 localization and protein aggregation. Moreover, I was also able to observe localization of TDP-43 staining overlapping with G3BP in stress granules (SG) in accordance with the known role of TDP-43 in regulating SG formation.
Finally, I also developed organotypic slice culture of *Nothobranchius furzeri* to exploit the fast ageing of this model for *in vitro* studies. I report culturing of thick brain slices for at least five weeks. I could also demonstrate persistence of adult neurogenesis and survival of TH+ cells in these cultures.

Index

1. Introduction

1.1 Impact of dementia and neurodegenerative diseases at socio-economical level

Neurodegenerative diseases are the prevalent cause of dementia and are currently regarded as cerebral proteopathies, in which the accumulation of particular, disease-specific, misfolded proteins is a key pathological mechanism (e.g., Cox et al., 2020; Vaquer-Alicea & Diamond, 2019) Dementia is defined by the World Health Organization (WHO) as a syndrome characterized by deterioration in cognitive function beyond what might be expected from normal ageing, and it is usually of a chronic or progressive nature. Dementia is one of the major causes of disability and dependency among older people worldwide: even if ageing is the major risk factor for developing dementia, this it is not a normal consequence of ageing itself, but instead it derives from a variety of traumas and pathologies affecting the brain. The primary causes of dementia are neurodegenerative diseases, Alzheimer's disease being the most common accounting for about 60-70% of cases, followed by dementias of vascular origin which are thought to account for 15-20% of cases in North America and Europe (Wolters & Arfan Ikram, 2019). Other frequent neurodegenerative diseases include Lewy bodies pathologies (e.g., Parkinson's disease) and Fronto-Temporal Dementias (FTDs) (WHO, 2019).
In 2019, approximately 50 million people are affected by dementia and this number is projected to increase greatly in the next few years reaching 82 million in 2030 (WHO, 2019).
At present, no effective treatments have been found for these diseases. Due to the slow and progressive nature of these pathologies, combined with the worldwide human median lifespan increase, it is evident how dementias pose a significant challenge to society (i.e., the families and caregivers of the patients) and to the health system, both economically and in terms of quality of life. In fact, in 2015, the total global societal cost of dementia was estimated to be 818 billion dollars, equivalent to 1.1% of the global gross domestic product (WHO, 2019), and this cost is certain to increase significantly. Thus, finding a cure for neurodegenerative diseases is an important goal for biomedical research, leading in recent years to a greatly increased effort in terms of public funding invested and studies performed in this field (Cummings et al., 2021; Pickett & Brayne, 2019). Conversely, the lack of results in terms of successful treatments discovered in the last decades lead the pharmaceutical companies to reduce their effort in terms of research investments(Cummings et al., 2021).

1.2 Protein aggregation

Protein aggregation is a process by which proteins lose their functional native conformation and undergo insoluble aggregate formation and deposition via initial self-assembly (Merlini et al., 2001). The process of aggregation is composed of various stages, the first of which is the spontaneous dimerization of partially unfolded proteins. These dimers then form more complex structures (oligomers) by beta structures annealing, leading in the end at the formation of tight polymer stack referred as 'amyloid fibrils' (Merlini et al., 2001; Patel & Kuyucak, 2017). This fibrillary formations are resistant to denaturation by chemical agents, proteases and heat, and cells are not able to remove them, thus they become toxic if their amount surpass a certain threshold and they ultimately lead to cell death (Dovidchenko et al., 2014). Protein aggregation can lead to effects other than the simple formation of insoluble particles: once aggregation has initiated the misfolded protein can interact with heterologous proteins, leading to the sequestration of other important cell components (e.g. ribosomal proteins, Kelmer Sacramento et al., 2020; S. Banerjee et al., 2020; Gruber et al., 2018) and to an overall remodeling of the cellular proteome (Hosp et al., 2017), providing an additional source of toxicity besides the simple aggregation.

The initiation of the formation of the amyloid state can be due to exposition of amide and carbonyl groups of the polypeptide backbone chain, allowing for H bonds formation with other polypeptide chains. Exposition of these groups can be caused by denaturation of normally folded protein, protein overexpression such as to reach the saturation point, peptide cleavage (e.g. Aβ) or production of native disordered protein. This process can be initiated also by post-translational modifications such as phosphorylation (Eisenberg & Jucker, 2012; Yang et al., 2016).

Study on the Prion protein revealed that the acquisition of the amyloid conformation leads to the toxicity of the misfolded protein. In particular, that the presence of a specific region of the PrP protein called Prion-Like Region (PLR) is sufficient for proteins to acquire the same characteristics of a self-perpetuation typical of prions (Falsone & Falsone, 2015; Prusiner et al., 1983). This is due to the ability of the PRL to fold spontaneously into amyloid-like conformations. The PRL domain can be found in various proteins, usually in a modular architecture (Kato et al., 2012).

Amyloid folding and prion-like behavior is tightly linked to toxicity (Aguzzi & Rajendran, 2009), but can also modulate protein function in physiological condition through reversible assembly of protein particles and various organisms, ranging from prokaryotes to higher level mammals have evolved controlled protein aggregation. Several proteins have been discovered in neurons that gain a new, unique and physiologically relevant function through aggregation (e.g. ARC for synaptic inverse tagging or FUS for RNA binging functions) (Bailey et al., 2004; Chernova et al., 2014; Falsone & Falsone, 2015; Gilks et al., 2004; Nikolaienko et al., 2018; Shelkovnikova et al., 2013).

It has been speculated that toxicity of protein aggregation can be avoided if it is reversible as well as spatially and temporally controlled. It seems that this control can be achieved by a strict regulation of transcript abundance for aggregation-prone proteins and by effective surveillance for protein quality control and clearance, thanks to molecular chaperones and different degradation machineries (Gsponer & Babu, 2012; Hipp et al., 2014).

A striking example of prion-like proteins involved directly in important biological functions are proteins involved in Stress Granules (SG) formation. SGs are membrane-less organelles that form transiently in the cytosol by liquid phase separation upon different forms of cellular insults, contributing to the arrest of mRNA translation (Anderson & Kedersha, 2008; Balagopal & Parker, 2009). When homeostasis is restored, these granules dissolve rapidly and completely (Falsone & Falsone, 2015; Kedersha et al., 2013). In physiological conditions, these assemblies are reversibly decomposable into monomers. Their conformational rearrangement occurs, however, in a fashion typical of prions: the prion conformer displays structural and physical features of amyloids (self-organization, cross beta structure), catalyzes its own template-driven conversion and can be non-genetically transmitted, maintaining at the same time reversibility and a minimal toxic hazard (Falsone & Falsone, 2015; Kedersha et al., 2000, 2013; Malinovska et al., 2013).
This observation is incredibly relevant in a pathophysiological context since alterations in SG integrity correlate to the prevalence of organic disorders (Aulas & Velde, 2015; Fan & Leung, 2016).

1.3 Neurodegeneration and aggregation

Notably, all neurodegenerative diseases are characterized by protein aggregation and consequent neuronal death and every neurodegenerative disease is characterized by massive aggregation of a specific protein (or combination of proteins) and preferential death of a specific subtype of neurons (Merlini et al., 2001; Ross & Poirier, 2004; Saxena & Caroni, 2011; Vaquer-Alicea & Diamond, 2019). Aggregation is thought to be one of the main pathophysiological mechanisms leading to neurodegeneration, due to the consequent proteostasis collapse and to dysregulation of metabolic, signaling and repair pathways, all of which are implicated in cellular maintenance, ageing and lifespan control (Cox et al., 2020; Francisco et al., 2020; Kelmer Sacramento et al., 2020).

It was discovered that amyloidogenic proteins such as α-Synunclein (α-Syn), Tau, Amyloid-beta (Aβ) and TDP-43, the proteins whose aggregation is observed in the most common neurodegenerative diseases (AD, PD and FTD), do not have particularly stable three dimensional structures in physiological conditions. They tend to assume a more stable form only upon binding to other proteins that are their specific interactors (Aguzzi & Calella, 2009; Frost & Diamond, 2010; Perutz et al., 2002; Vaquer-Alicea & Diamond, 2019). The misfolded form of these proteins, on the other hand, has exposed beta sheet stretches that are prone to bind other proteins with low specificity. Therefore, their amyloid folding can act as cross nucleation seed that initiate secondary misfolding of a host of other proteins. Disease-associated proteins can also cross-seed their aggregation. It has been shown, for example, that α-Syn can initiate Tau deposition in mice (J. L. Guo et al., 2013) and that TDP-43, the main protein found in ALS aggregates and involved in FTDs, can act as seed for Aβ fibril growth (Fang et al., 2014). In addition, unbiased proteomic analysis of protein aggregates has revealed a complex, heterogeneous composition suggesting that sequestration of important proteins may result in loss of function (Cox et al., 2020; Furukawa et al., 2011; Hipp et al., 2014; Hosp et al., 2017; Radwan et al., 2017; Yang et al., 2016).

In cases of amyloid folding, these particles can propagate between cells like prion-like particles, spreading through axonal projections and leading to specific patterns of dissemination through interconnected systems (Desplats et al., 2009; Frost & Diamond, 2010; Nonaka & Hasegawa, 2018; Vaquer-Alicea & Diamond, 2019; Volpicelli-Daley et al., 2011).

Furthermore, indications suggest that Synuclein-based deposits accumulate according to a complex pattern, involving intestinal, olfactory, and medullar circuits, before targeting midbrain nigral neurons, and this could in principle involve an axonal spreading mechanism, in the same manner that injection of α-Syn seeds in healthy mouse brains triggers polymerization of endogenous α-Syn and its self-propagation, along with PD symptoms (Hawkes et al., 2007; Luk et al., 2012)

These observations led to the proposition of Braak's hypothesis of staged evolution of both Parkinson's and Alzheimer's diseases (for more detail about Braak's hypothesis see paragraph 1.5)

Each neurodegenerative disease is characterized by a principal protein aggregate and results in a typical progression of neurodegeneration across specific neuronal subpopulation. As disease-causing proteins tend to be broadly distributed, it appears that certain types of neurons are more

vulnerable due to variations in the gene expression and physiological properties (review by Freer et al., 2016; Fu et al., 2018; Kundra et al., 2020).
An interesting theory trying to explain this phenomenon has been proposed by Saxena and Caironi (2011), who called this theory the Stressor Threshold Model. A central principle of this hypothesis is that misfolding-prone proteins may accumulate upon cell stress in or near the vulnerable neurons, to then interfere with neuronal function selectively and cause more neuronal stress, due to vulnerability of those neurons. This occurrence of events would thus favor proteostasis instability through vicious cycles involving cell stress and misfolding protein targets (Saxena and Caironi, 2011).

1.4 Ageing as major risk factor for neurodegenerative diseases

Neurodegenerative diseases are caused by a combination of protein aggregation and failure of cellular stress response pathways. It is well known that the ability of cells to maintain the integrity of their homeostasis pathways diminishes with advancing age, and this likely explains that prominent role of age as a risk factor for neurodegenerative diseases (Hou et al., 2019; Kaushik & Cuervo, 2015; Mattson & Magnus, 2006; Tran & Reddy, 2021)

To conceptualize the multifaceted aspects of aging, Lopéz-Otín et al. (López-Otín et al., 2013) have proposed nine hallmarks of ageing (i.e., genomic instability, telomere attrition, epigenetic alterations, mitochondrial dysfunction, deregulated nutrient sensing, loss of proteostasis, cellular senescence, stem cell exhaustion and altered intercellular communication). All these hallmarks were observed in neurodegenerative diseases (as reviewed in Hou et al., 2019) .

Mitochondrial dysfunction seems to have a particularly prominent role. Aggregation of α-Synuclein and mitochondrial dysfunction seems to have a synergistic relation (Poewe et al., 2017; Rocha et al., 2018).

It is also important to note that the genes identified as causative of familial forms of PD (i.e., Pink1, DJ-1, LRRK2, Parkin) are also linked to mitochondrial function and stability (R. Banerjee et al., 2009; Bogaerts et al., 2008)., It remains to be determined whether these mutations cause Parkinson's disease directly via the impairment of mitochondrial function or through other pleiotropic mechanisms. α-Syn is physiologically involved in the vesicle releasing mechanism at synapses and its dysfunction may cause deficits through possible alteration of SNARE complex formation; the mechanistic relationship between α-Synuclein mutations and PD may thus involve also synaptic transmission and excitability (Bridi & Hirth, 2018).

Likewise, DJ-1 has a role as oxidative stress sensor, and Parkin also has a role in stress protection, suggesting that the relationship between these genes and PD may also involve cellular stress pathways in addition to mitochondrial stress (R. Banerjee et al., 2009).

Similarly, it has been observed that an age-related decline in the protein PGC1α, which is involved in the promotion of cellular plasticity, mitochondrial biogenesis and energy production, has a causal relationship to the increase of aggregated proteins, augmented ER stress and faster progression of disease in animal models of neurodegenerative diseases and it has also been directly linked to α-Synuclein aggregation (Cui et al., 2006; Eschbach et al., 2015).

Ageing is also strictly associated with progressive loss of proteostasis and its relation with protein aggregation has been extensively studied (Alavez et al., 2011; Balch et al., 2008; Kaushik & Cuervo, 2015; Ray, 2017). Wide proteome remodeling has also been observed in the ageing model organisms *C. elegans* and *Nothobranchius furzeri*, together with an increase of aggregation (Kelmer Sacramento et al., 2020; Walther et al., 2015). Among the many pathways affected by ageing, two systems can be identified as key factors in proteostasis dysfunction: proteasome and ribosome.

The proteasome machinery (UPS, Ubiquitin-Proteasome System) plays an important role in preventing misfolded protein aggregation, especially in neurons (Falsone & Falsone, 2015) and its pharmacological inhibition can lead to aggregation and neurodegeneration in different model organisms (Matsui et al., 2010; Romero-Granados et al., 2011). Also genetic impairments of UPS

system can lead to neurodegeneration and inclusion formation reminding of Lewy bodies (Bedford et al., 2008). Deletion of a single proteasomal subunit is, strikingly, sufficient to drive mislocalization and precipitation of TDP-43 and FUS in motor neurons evoking ALS (Amyotrophic Lateral Sclerosis) symptoms in mice (Tashiro et al., 2012). Lastly, it has been demonstrated that proteasome inhibition leads to protein synthesis inhibition (Ding et al., 2006).
Ribosomes constitute the major protein component in the cytoplasm (Beck et al., 2011) and they obviously have a major role in the control and maintenance of proteostasis via their role pf protein translation. Thus, their dysregulation and aggregation have a significant impact on the loss of proteostasis. It has indeed been shown how ribosomes can be found in aggregates of proteins involved in neurodegenerative diseases (S. Banerjee et al., 2020; Gruber et al., 2018), creating a link between neurodegenerative diseases, proteostasis imbalance and ribosome sequestration. Both proteasome and ribosome show loss of stoichiometry and down-regulation during aging of *N. furzeri* (Kelmer et al., 2020)
Given the wealth of experimental data and the evident correlation of ageing and neurodegenerative diseases in humans, it is safe to assume that there are links between ageing-related signaling pathways, ER stress, mitochondrial dysfunction and protein misfolding, leading all together to greater neuronal vulnerability and neurodegeneration risk.
The Stressor Threshold Model states that the disease can remain for extended periods at an overall sub-threshold level to escalate into full blown pathology only later in life (Saxena & Caroni, 2011).
Thus, the initiation of neurodegenerative diseases could be initiated at any ages by chronic alteration of cellular homeostasis pathways, and then the convergence of other stressors can lead to dysfunction and degeneration of more vulnerable neurons. Supra-threshold dysfunction and progressive neurodegeneration would become evident only when age-related stressor tolerance decreases.
This hypothesis is concordant with the observation that accumulation of misfolded proteins is often not sufficient to cause disease. Studies conducted in human populations suggest how additional factors must combine with the age-related accumulation of misfolded proteins for disease to develop. Indeed, the presence of characteristic macroscopic protein aggregates in the same neurons can be observed in brains of some aged but functionally preserved subjects and do not represent sufficient evidence to assume the presence of the pathology, if other signs of major disease manifestations are not present as well (Dickson et al., 2008; Forno, 1969; Hedden et al., 2009).

1.5 Parkinson's disease principal features

Parkinson's disease is the second most common age-related neurodegenerative disorder after Alzheimer's disease. An estimated 7-10 million people worldwide suffer from Parkinson's disease. Clinically, this pathology is characterized by motor and non-motor symptoms. The four main motor symptoms are tremor at rest, rigidity, bradykinesia and postural instability. In addition, flexed posture and freezing is observed in most patients. Some of the non-motor symptoms are, among the others, cognitive impairment, depression, sleep disorders and fatigue (Jankovic, 2008; Poewe et al., 2017).

The main histopathological hallmarks are the formation of Lewy neurites within axons and dendrites, Lewy's bodies in cells' soma, and neurodegeneration of Tyrosine Hydroxylase expressing neurons, especially in the *Substantia Nigra pars compacta* (SNpc), and in the *Locus coeruleus* (Del Tredici & Braak, 2012; Schneider & Obeso, 2014; Zarow et al., 2003).

Lewy's bodies and neurites are composed primarily of α-Synuclein aggregates carrying a specific phosphorylation at the aminoacid residue Serine 129. Up to 90% of the aggregated form of α-Synuclein carries this specific post-translational modification (Samuel et al., 2016).

Having observed the elevated presence of this protein into the aggregates, Braak and colleagues linked the spatial progression of the pathology to the diffusion of α-Syn stained aggregates. They formulated the hypothesis that the aggregates spread in a prion-like manner and follow an ordered path, starting from the vagal nerve, progressing to the *Locus coeruleus*, then to the *Substantia Nigra,* and eventually reaching limbic and neocortical brain regions. Based on such observations, they divided the progression of PD into standardized stages (Braak et al., 2002, 2003).

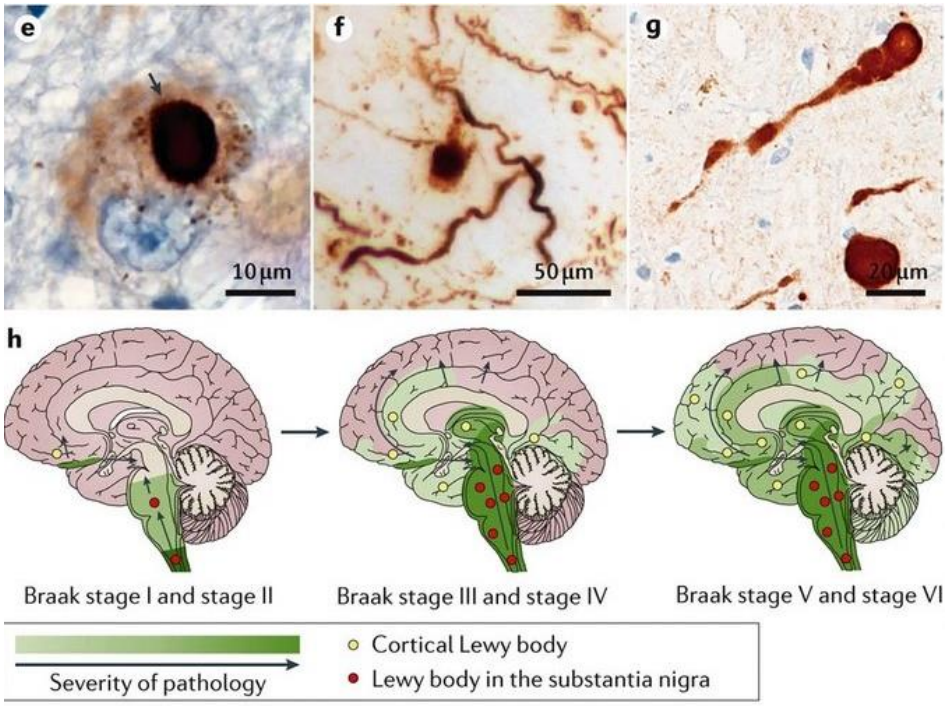

Fig 1: Principal characteristics of Parkinson's disease. Aggregation of the protein α-Synuclein leads to the formation of Lewy bodies and Lewy neurites. Initial preclinical stages of Parkinson's disease are identified by the presence of Lewy's bodies and neurites in

the dorsal nucleus of the vagal nerve and into the *Locus Coeruleus*. The following stage involves the *Substantia Nigra* and the appearance of the firsts motor symptoms, then the aggregates reach more frontal areas involving the cortex and leading eventually to the appearance of the non-motor symptoms. Modified from Poewe et al., 2017.

One of the most affected areas in Parkinson's disease is the *Substantia Nigra pars compacta*, formed primarily by dopaminergic neurons, whose dysfunctions account for the major clinical manifestations of PD (Alexander, 2004). These neurons are particularly vulnerable to mitochondrial stress, and various studies have been conducted with the aim of linking ageing, mitochondrial dysfunction, and ROS production to Parkinson's. In particular, it was discovered that deficits of the complex I of the respiratory chain have a link to sporadic cases of PD, and animals treated systemically with rotenone (a complex I inhibitor) showed an enhanced ROS production in the *Substantia nigra*, dopaminergic neuron loss and Lewy bodies formation(Keeney et al., 2006; Sherer et al., 2003; Thomas et al., 2012). This and other observations show a clear association between Parkinson's disease and protein aggregation and a mitochondrial dysfunction, but the actual causal relationship is still to be determined.
Mitochondrial vulnerability might be a first hit target, predisposing *Substantia nigra* neurons to PD possible development or the mitochondrial respiratory chain dysfunctions may be an aggravating consequence, rather than a cause of disease (Saxena & Caroni, 2011).
The etiology of PD may thus require overburdening of stress pathways, also involving mitochondria, which are particularly sensitive in dopaminergic neurons of the *Substantia nigra.*
Locus coeruleus is another nucleus highly affected by neurodegeneration during Parkinson's disease (Del Tredici & Braak, 2013; McMillan et al., 2011; Zarow et al., 2003). *Locus coeruleus* is located in the pons and is the main source of noradrenaline in the brain (Szabadi, 2013). During Parkinson's disease, Lewy bodies formation in the *Locus coeruleus* cells is an early event (stage 2 of Braak's stadiation, Braak et al., 2002) that precedes onset of motor symptoms and degeneration of the *Substantia nigra* (Rommelfanger & Weinshenker, 2007; Zarow et al., 2003).
The *Locus coeruleus* contains a relatively small amount of neurons that sends diffuse projections with neuromodulatory action to the entire brain (Szabadi, 2013) and it is involved in a number of functions ranging from arousal and attention to learning, autonomous system regulation and others (Bari et al., 2020; Szabadi, 2013). In particular, *Locus coeruleus* is of extreme importance in maximizing task -oriented performance, especially under stress or novel circumstances (Benarroch, 2009; Del Tredici & Braak, 2013).
In Parkinson's disease, loss of noradrenergic neurons is associated with cognitive decline (Cash et al., 1987; Peterson & Li, 2018). As the *Locus coeruleus* projects heavily to the hippocampus and parahippocampal formation (Szabadi, 2013; S. Zhang et al., 2016), loss of noradrenergic signaling may lead to hippocampal dysfunction and memory deficits.
It is thus important to also consider neurodegeneration of this area as critical during Parkinson's disease development, even if the derived symptoms may be less evident than those deriving from *Substantia nigra* neuron loss.

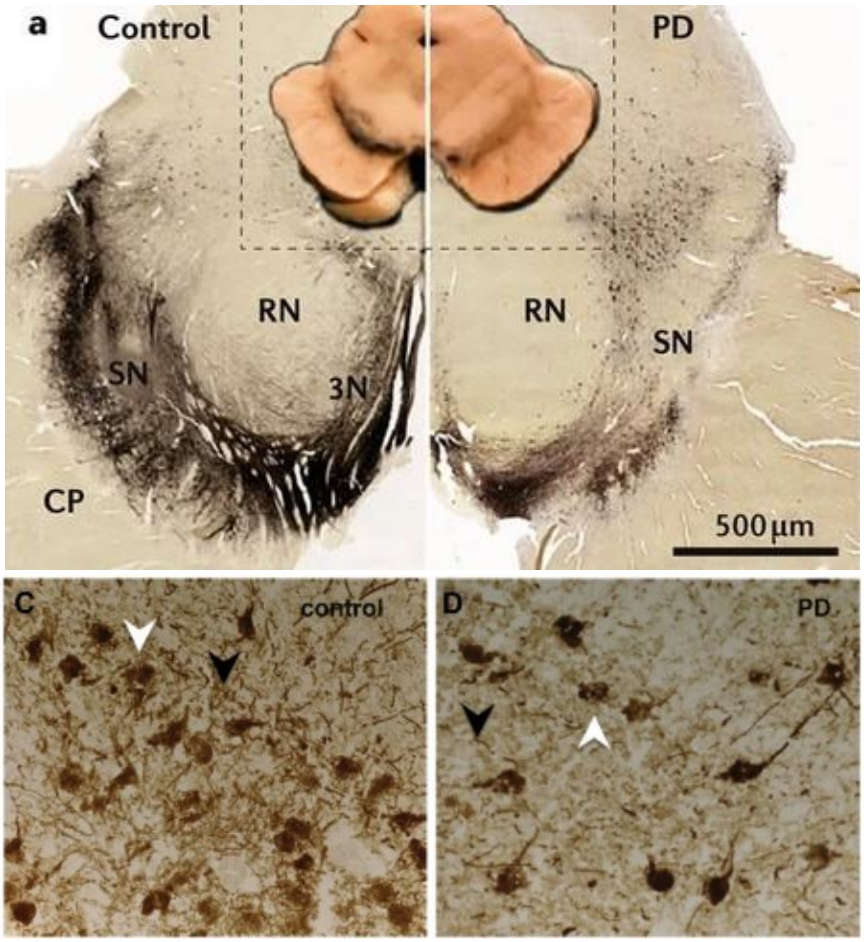

Fig 2: Main areas affected by neurodegeneration in Parkinson's disease in post-mortem human brain samples. Neurodegeneration in the *Substantia nigra* (upper panel) and *Locus coeruleus* (lower panel) Showed as TH immunoreactivity. Modified from Poewe et al., 2017 and McMillan 2011.

Notably, presence of phospho-Synuclien (pSyn) immunoreactivity and Lewy bodies are not an exclusive feature of PD. They are found in ~10% of clinically unimpaired subjects over the age of 60 with a distribution similar to PD, but showing lesser density of inclusions and a lesser degree of Tyrosine Hydroxylase (TH) reduction, as compared to what observed in PD, suggesting that pSyn immunoreactivity and LB formation are already detectable at preclinical stages, before the onset of motor symptoms (Dickson et al., 2008; Forno, 1969; Fumimura et al., 2007).
Several approaches were undertaken to model PD in animal models. Dopaminergic loss and the associated motor symptoms can be induced in rodents and primates by acute pharmacological treatments (for reviews see Johnson & Bobrovskaya, 2015; Meredith & Rademacher, 2011). These models are useful to test acute neuroprotection of therapeutical interventions, but fail to model the progressive and age-associated nature of PD. An alternative approach envisages the genetic manipulation of either α-Syn or other PD-associated genes like LRRK2, PINK1, Parkin, or DJ-1 (Jagmag et al., 2016). Some of these models show a more progressive onset of the neurodegeneration but, in most cases, the disease is modelled in young or, at best, in young adult animals. It should also be noted that the majority of PD cases do not have a clear genetic origin but are classified as idiopathic. Teleost fishes like Medaka and Zebrafish have also been utilized to

model PD with similar approaches (L. J. Flinn et al., 2013; Matsui, 2017; Matsui et al., 2009, 2012; Uemura et al., 2015).
MTPT (1-methyl-4-phenyl-1,2,3,6-tetrahydropyridine) is a commonly used toxin to mimic PD via induction of midbrain dopaminergic neuron loss. Its use in zebrafish leads to the same type of neurodegeneration observed in mammals (Lam et al., 2005; McKinley et al., 2005; Sallinen et al., 2009; Wen et al., 2008) causing motor deficits (Robea et al., 2020; Sarath Babu et al., 2016). Effects of MPTP can be prevented by inhibition of monoamine oxidase-B (MAO-B) or the dopamine transporter (DAT), indicating a conservation in the mechanisms (McKinley et al., 2005).
Alternatively, various zebrafish transgenic lines have been created in attempt to induce PD. A *Pink1* KO line shows reduction of TH neurons but not behavioral deficits (Bandmann et al., 2010), while a Parkin KD lead also to a reduction of dopaminergic neurons and mitochondrial disfunction but not to an alteration of swimming behavior (L. Flinn et al., 2009). KD or mutation of LRRK2 in zebrafish leads to dopaminergic neuron loss, aggregation and swimming deficits (Prabhudesai et al., 2016; Sheng et al., 2010)
These models offer a cost-effective alternative to study PD but suffer from the same limitations of the rodent models, failing in reproducing the progressive staging of PD and ignoring the aging context in which PD arises, being realized in young adult fish at best.
For a more precise modelling of the disease, it would be crucial to carry such studies in the context of aging animals, which is the natural environment for neurodegenerative diseases, and therefore the use of animals such as *Nothobranchius furzeri* could provide the right platform in which to recreate age-dependent modelling of PD.

1.6 TDP-43 and its role in Fronto-Temporal Dementia (FTD)

TAR DNA-binding protein 43 kDa (TDP-43) is an RNA-binding protein involved in RNA metabolism (Alami et al., 2014; Buratti & Baralle, 2001; Ishiguro et al., 2016; Kim et al., 2010). It was first described in 1995 as a protein associated with HIV transcription (Ou et al., 1995) and reconsidered later on as an important component of splicing (Buratti & Baralle, 2001; Polymenidou et al., 2011), mRNA transport and translation (Chu et al., 2019; Ishiguro et al., 2016; Neelagandan et al., 2019). TDP-43 It is prone to aggregation (B. S. Johnson et al., 2009) due to the presence of an inherently disordered domain at the C-terminus of the protein showing prion properties involved in functional protein aggregation (Louka et al., 2020; Udan & Baloh, 2011). Recently, TDP-43 has been found to be the major component of insoluble intracellular inclusions in motor neurons affected by ALS and in 90% of patients suffering from the α-Synuclein, Tau negative Ubiquitin subtype of Fronto-Temporal Dementia (FTD) (Mackenzie & Rademakers, 2008; Neumann et al., 2006).

Hallmarks of these diseases are the presence of aberrant, polyubiquitinated and hyperphosphorylated cytosolic aggregates of TDP-43 in different areas of the central nervous system (Neumann et al., 2006; Prasad et al., 2019). An increasing consensus is building on the notion that TDP-43 aggregation is not only a marker, but represents the pathological mechanism of these diseases (Hergesheimer et al., 2019).

Stress granule formation is one of the many cellular protective mechanisms as a response to cellular stress (Anderson & Kedersha, 2009). Their formation is initiated by the oligomerization of the core proteins Ras GTPase-activating protein-binding protein 1 (G3BP) and Cytotoxic Granule Associated RNA Binding Protein (TIA1) whose expression is regulated by TDP-43 (Gilks et al., 2004; McDonald et al., 2011; Tourrière et al., 2003). TDP-43 can be found in stress granules under cellular stress conditions and TDP-43 positive pathological inclusions in post-mortem tissues from ALS patients are positive for stress granule markers (Liu-Yesucevitz et al., 2010; Parker et al., 2012).

As already discussed, functional prion-like aggregates and stress granules seem to organize themselves and assemble/disassemble, depending on the cellular state, exploiting the aggregation properties of the PRL domain of the protein composing the granules themselves.

It has also been discussed how these organelles must preserve reversibility as a prerequisite for physiological function. Processes interfering with the assembly/disassembly, and thereby the steady-state integrity of SG, have been associated to misfolding, mislocalisation, or sequestration of various SG components, such as TDP-43, FUS, and hnRNPA isoforms, which are all major regulators of inclusion body neuropathologies (Dudman & Qi, 2020; Iguchi et al., 2013; Shelkovnikova et al., 2013).

TDP-43 is not a primary nucleator of SGs but influences size, morphology and formation kinetic of this organelle. Mutations in TDP-43 reducing its ability to incorporate into SGs or its complete deletion leads cells to a delayed formation of SGs that show also irregular shape when present (Besnard-Guérin, 2020; Khalfallah et al., 2018; McDonald et al., 2011).

In the event of a persistent cellular stress, TDP-43 localizes initially to SGs, then detaches and forms insoluble cytoplasmic inclusions (Parker et al., 2012). Inclusion formation has been observed

upon overexpression of mutated forms of TDP-43 with increased cytosolic/SG localization or increased aggregation propensity (Besnard-Guérin, 2020; Cohen et al., 2011; W. Guo et al., 2011). Moreover, aggregation-prone TDP-43 mutants induce aggregation of SGs, suggesting that TDP-43 can favor the transition from physiological to pathological conformation (Cohen et al., 2011). Several animal models based on overexpression were developed to model TDP-43-mediated diseases (Liu et al., 2013), including zebrafish models (Asakawa et al., 2020; Bose et al., 2019; Svahn et al., 2018).

1.7 The turquoise killifish *Nothobranchius furzeri* as a possible model for the study of idiopathic neurodegenerative diseases

Ageing is a complex process that affects all organs and should be studied in the entire organism. The relatively long median lifespan of vertebrates makes the use of these animal models expensive, and researchers utilize mostly invertebrate animals or *in vitro* models to perform the majority of ageing studies. This approach, although useful, entails several limitations, including the great differences in physiology and body organization between mammals and invertebrates.
On the other hand, to avoid the cost, in terms of money and time, of waiting for the animals to age researchers have developed genetic approaches to overexpress pathologically-mutated proteins or to use toxins in order to induce a pathological phenotype in relatively young or young adult animals as a models of age-related neurodegenerative diseases. This approach has led to useful information regarding the downstream molecular players involved in neurodegenerative diseases, but it has proven to be, in the end, not accurate enough to recapitulate the state of pathology observed in humans to allow for the development of a successful cure. Moreover, as discussed extensively in the previous paragraphs, ageing entails progressive changes in the brain both at cellular and molecular level, and those changes are tightly related to neurodegenerative diseases and aggregation. Thus discarding completely the study of the pathology in the correct ageing context, leads unavoidably to a partial recapitulation of the human condition.
A model representing an equilibrium between the technical needs of research (low costs, short time, and ease of manipulation) and the right characteristics needed to conduct a study that recapitulates in the most accurate way possible what is observed in humans is therefore needed.
The turquoise killifish *Nothobranchius furzeri* has emerged in the last decade as a valuable new model for ageing studies. *N. furzeri* belongs to the group of the African annual killifishes that are all characterized by a lifespan of the duration inferior of one year (Cellerino et al., 2016). This trait is a natural consequence of the evolutionary processes that enables survival in their temporary habitat. *N. furzeri* originates from Eastern African savannah and lives in temporary ponds that appear during the brief rain season and last only few months (Cellerino et al., 2016). In that short period of time, the fish need to go through their entire life cycle of hatching, growing, and reproducing. At the end of rain season, the ponds desiccate and all adult fish die. Survival of the species is warranted by the ability of the embryos to enter diapause; a state of metabolic dormancy that blocks the development in order to survive the hostile desiccation conditions (Dolfi et al., 2019). Interestingly, the short lifespan is maintained also in the laboratory in constant presence of water (Baumgart, Cicco, et al., 2014; Valdesalici & Cellerino, 2003). In particular, *N. furzeri* has, to date, the record for the shortest median lifespan for a vertebrate that has been raised in a laboratory; the shortest living strain of this species being GRZ, which has a lifespan of only 14 weeks (Terzibasi et al., 2008), while longer-lived strains can show a maximum lifespan (defined as 10% of population survivorship) up to 40 weeks of age (Terzibasi Tozzini et al., 2013). .
Increasing evidence has shown that *N. furzeri* shares molecular, histopathological and behavioral ageing-related signatures with mammals (Cellerino et al., 2016)
N. furzeri exhibits all the most common phenotypes linked to mammalian ageing, such as lipofuscin accumulation (Terzibasi Tozzini et al., 2013), skin depigmentation, muscle atrophy and

spinal curvature (Fig 3) (Cellerino et al., 2016), along with behavioral deficits including reduced spontaneous locomotor and exploratory activity, suggesting a decline in both cognitive and motor functions (Genade et al., 2005).

Examining brain ageing more specifically, *N. furzeri* shows extensive gliosis, lipofuscin, iron accumulation and reduction of neurogenesis (Ripa et al., 2017; Terzibasi Tozzini et al., 2013; Tozzini et al., 2012). Moreover, high-throughput expression profiling approaches have detected uncoupling of protein and transcript regulation, loss of stoichiometry in several protein complexes, reduced proteasome function and ribosome aggregation (Kelmer Sacramento et al., 2020). These same mechanisms were previously observed during ageing in *C. elegans* (David et al., 2010; Walther et al., 2015) and are known to be linked to aggregation and neurodegeneration (Falsone & Falsone, 2015; Gruber et al., 2018; Matsui et al., 2010; Romero-Granados et al., 2011; Tashiro et al., 2012).

Lastly, the possibility to insert human pathogenic mutations in the *N. furzeri* ortholog gene using CRISPR/Cas9 and homologous recombination expands the possibility of applications for this model (Harel et al., 2015).

The general anatomical organization of the central nervous system is conserved between fish and mammals and some specific homologous cell populations (such as cathecolaminergic neurons) making teleost fishes valuable models for neurobiological investigations with translational potential.

In 2019, Matsui and colleagues (Matsui et al., 2019) utilized *Nothobranchius furzeri* to study Parkinson-like neurodegeneration and observed an age dependent accumulation of αSyn. They report age-dependent neuronal loss in both noradrenergic neurons located into the *locus coeruleus* and in the dopaminergic population forming the hypothalamic *posterior tuberculum,* the putative teleost homolog of the *substantia nigra* (Kaslin & Panula, 2001; Rink & Wullimann, 2001) as identified by Tyrosine Hydroxylase (TH) immunoreactivity. This result was supported also by a reduction of TH expression both at protein and RNA level as verified by Western blotting and qPCR. Moreover, knock-out of α-Syn using CRISPR/Cas9 was sufficient to abolish degeneration of TH positive cells.

This unique asset of characteristics makes of *N. furzeri* a model that recapitulates both the advantages of vertebrates (similarity with mammals in terms of anatomy and genetic homology) and invertebrates (short lifespan, fast ageing, easy transgenesis). Moreover, recent evidence pointing to age-related aggregation and neurodegeneration in *N. furzeri* via mechanisms similar to those observed in mammals strengthens further the potential of this organism as a model enable faster and more affordable investigations into ageing and ageing-related diseases.

Fig 3 : Ageing of the fish *Nothobranchius furzeri* from (Platzer & Englert, 2016). The same male of MZM-04/03 strain exhibiting a maximum lifespan of one year has been photographed at different moments during its lifespan.

1.8 Organotypic cultures for the study of Parkinson's disease and TDP-43

In vitro dissociated cell cultures are widely used in any field of biology and medical research. They enable the study of a great variety of cell types in an isolated, defined and easily manipulated environment, maintaining at the same time the basic morphological and physiological characteristics of the cells under study. Moreover, this *in vitro* technique is in concordance with the principle of the three R (Replacement, Refinement, Reduction) by reducing the number of animals utilized for experiments and transferring the treatments phase (and associated suffering) to the *in vitro* condition. However, one of the major disadvantages of this technique is the lack of a 3D structure and cell-to-cell contacts. This disadvantage is particularly pertinent in the case of CNS structures whose connections are destroyed upon dissociation. Organotypic culture maintain the overall structure of the area of interest as well as the local patterns of synaptic connectivity and local interactions with the surrounding cells, representing a much better model of the *in vivo* situation.

Organotypic cultures of hippocampus from rat pups was first established by Gähwiler, 1984 and then extended to many other CNS structures such as retina (Gancharova et al., 2013), hypothalamus, cerebellum and others (Eun et al., 2007; Wolf, 1970). The method consists primarily in cultivation of thick brain slices (ranging from 100µm to 500µm) cultured over semipermeable membranes (Stoppini et al., 1991) that maintain the tissue at the interface between medium and atmosphere in order to allow oxygen and nutrient exchange (Humpel, 2015; Stoppini et al., 1991).

The advantages of culturing tissue slices, typically obtained from very young animals, for prolonged periods of time *ex vivo* are numerous and consist primarily in the maintenance of the overall *in vivo* architecture of the isolated sample, the lack of hematoenchephalic barrier and the extreme ease of experimental interventions.

Organotypic culture have been extensively utilized for the study of both *Substantia nigra* and *Locus coeruleus*. Culturing of these nuclei has been performed for decades (Jaeger et al., 1989; Knöpfel et al., 1989) and the maintenance of their morphological and physiological characteristics have been proved (Rohrbacher et al., 2000). Treatment with toxins to induce Parkinson-like neurodegeneration has been tested (McCaughey-Chapman & Connor, 2017; Stahl et al., 2009; Testa et al., 2005) as well as neurodegeneration via rescission of nigro-strialtal pathway (Daviaud et al., 2014).

Organotypic slices were utilized also to study TDP-43-realted neuropathologies; treatment of mouse brain slices with tunicamycin lead to cytoplasmic TDP-43 inclusion (Hicks et al., 2020; Leggett et al., 2012) and organotypic cultures from rat expressing a human mutated form of TDP-43 has been shown to develop astrogliosis and microgliosis and have enabled the study of secreted factors which induce selective neuronal death (Bi et al., 2013).

This technique is well-developed and widely used for mammalian models, but only few attempts have been performed in teleost, mainly using retina (Kustermann et al., 2008; Lahne et al., 2017) whole embryo (Langenberg et al., 2003) and one attempt at whole brain culturing for one week (Tomizawa et al., 2001). To the best of my knowledge, there are no reports of long-term brain

organotypic cultures in teleosts. Long-term organotypic cultures in *N. furzeri* could provide a unique system to study brain aging *ex-vivo*.

1.9 Aim of the study

Considering the advantages that a model organism such as *Nothobranchius furzeri* offers to the field of ageing-related pathology, I assessed if *N. furzeri* could be utilized as a model to study neurodegenerative diseases, focusing on Parkinson's disease and TDP-43 related pathologies.
First, I investigated whether accumulation of protein aggregates is a general feature of *N. furzeri* ageing.
Secondly, I investigated the neurodegeneration of the nuclei majorly affected during Parkinson's disease (i.e., the *locus coeruleus* and the area homologous to the *substantia nigra*).
Thirdly, I specifically investigated the subcellular localization of TDP-43 in young and old animals.
Lastly, I developed a protocol to realize long-term organotypic cultures of *N. furzeri* brain slices with the prospect of utilizing this technique, in the future, to study brain ageing *in vitro* and to test drug treatments for reducing neurodegeneration and protein aggregation.

2. Materials and Methods

2.1 Fish maintenance and sampling

The MZM-222 strain fish were hatched and housed locally in a Tecniplast system with automatized water flow and pH and salinity control. All the animals were hatched, fed and maintained as described in detail in (Terzibasi et al., 2008).
The protocols of fish maintenance were carried out in accordance with all animal use practices approved by the Italian Ministry of Health (Number 96/2003a) and the local animal welfare committee of the University of Pisa.
Eggs were maintained on wet peat moss at room temperature in sealed Petri dishes. When embryos had developed, eggs were hatched by flushing the peat with tap water at 16–18 °C. Embryos were scooped with a cut plastic pipette and transferred to system tank. Fry were fed with newly hatched Artemia nauplii for the first 2 weeks and then weaned with finely chopped Chironomus larvae. The system water temperature was set at a constant 27 °C.
At the desired age, fish were sacrificed via anesthetic overdose (Tricaine, MS-222), in accordance with the prescription of the European (Directive 2010/63/UE) and Italian law (DL 26/04-03-2014), and the brain was immediately extracted under a stereomicroscope and fixed overnight in a solution of PFA 4% in PBS.
Samples used for Sca/eS procedure were then gradually dehydrated by sequential steps of incubation in solutions with growing EtOH concentration (25%, 50%, 75%) and finally stored at -20° in EtOH 90% until use.
Samples used for immunofluorescence were instead incubated overnight in sucrose 30% at 4°C and the day after were included in cryo-embedding medium (Tissue-Tek® O.C.T., Sakura Finetek). Serial slices of 25 µm of thickness were then cut using a Leica cryostat and collected on Superfrost plus slides® (Thermo scientific).

2.2 AbSca/e procedure

Sca/eS technique is a clarification technique (Hama et al., 2015) and was an improvement of the first Sca/e technique (Hama et al., 2011) which was slower and had the drawbacks of removing the lipids and increase the sample size of approximately 1.25 times.
We followed the principal steps of the AbSca/e technique, which is a subtype of Sca/eS thought especially to combine immunofluorescence and tissue cleraing, adapting some of the steps to the considerably smaller size of *Nothobranchius furzeri* brains. All the steps and the solutions used for this procedure are summarized in tables 1 and 2.
Briefly, the samples were re-hydrated via incubation in solutions containing decreasing concentrations of ethanol (90%->75%->50%->25%->PBS) and adapted with the S0 solution for 18h at 37°C. Then the samples were permeabilized with sequential incubations in A2-B4(0)-A2 solutions at 37°C. After permeabilization the samples were de-Sca/ed trough incubation in PBS for 6h at RT followed by incubation with primary antibody in AbSca/e solution for 3 days at 4°C, rinse twice in AbSca/e for two hours each and incubation with secondary antibody for 18h at 4°C. The samples were then rinsed for 6h in AbSca/e and subsequently in AbRinse solution twice for 2 hours. After a re-fixation step in PFA4% for 1 h and a rinse in PBS for another hour the samples were finally cleared in Sca/e S4 for 18h at 37° and maintained in Sca/eS40 at 4° until imaging. The Sca/eS4 solution was used also as imaging medium.

Step	Procedure		
	Solution	Timing(approx)	Temp
Fixation	4% PFA	ON	4°C
Adaptation	Sca/e S0	18h	37°C
Permeabilization	Sca/eA2	36h	37°C
	Sca/eB4(0)	24h	37°C
	Sca/eA2	12h	37°C
DeScaling	PBS	6h	RT
Immunostaining	AbSca/e+ primary antibody	3d	4°C
	AbSca/e	2h (x2)	RT
	AbSca/e+ secondary antibody	18h	4°C
Wash	AbSca/e	6h	RT
Rinse	AbRinse	2h (x2)	RT
Refixation	4%PFA	1h	RT
Wash	PBS	1-2h	RT
Clearing	Sca/eS4	18h	37°C
Mounting	Sca/eS4		4°C

Table 1. AbSca/e protocol. In this table are listed all the steps of the AbSca/e protocol that I used to clear and stain *Nothobranchius furzeri* brains. The principal difference with the original AbSca/e procedure consists in the steps of incubation with the antibodies; the original article suggested to perform both incubations at 37° for two days but, in

our case, this led to an high background staining, therefore we decided to perform a longer incubation at a lower temperature (4°) to allow more specific interaction of the antibodies with their antigens. ON: overnight, RT: room temperature.

Ingredients	Sca/eA2	Sca/e B4(0)	Sca/eS0	Sca/eS4	AbSca/e	AbRinse
D-(-)-sorbitol (w/v)%	-	-	20	40	-	-
Glycerol (w/v)%	10	-	5	10	-	-
Urea (M)	4	8	-	4	0.33	-
Triton X-100 (w/v)%	0.1	-	-	0.2	0.5	0.05
Methyl-ß-cyclodextrin (mM)	-	-	1	-	-	-
ɣ- Cyclodextrin (mM)	-	-	1	-	-	-
N-acetyl-L-hydroxyproline (w/v)%	-	-	1	-	-	-
DMSO (v/v)%	-	-	3	25	-	-
PBS	-	-	1x	-	-	0.1x
BSA (w/v)%	-	-	-	-	-	2.5

Table 2. AbSca/e solutions. In this table are listed the compositions of each solution used to perform AbSca/e. No modification to the original solutions was applied.

2.3 Immmunofluorescence and Proteostat™ Aggresome staining

We performed immunofluorescence experiments on cryo-sections of 25 microns and proceeded as previously described (Tozzini et al., 2012). Briefly we washed the sections in PBS to remove the cryo-embedding medium; then we performed an acid antigen retrieval step (Tri-sodium citrate dehydrate 10mM, tween 0,05%, pH6). Afterwards, we stained the section with aggresome (ProteoStat™ Aggresome Detection Kit, Enzo Life Sciences Inc.; for more details see Shen et al. 2011) as follows: we applied a solution 1:2000 of aggresome dye in PBS for 3 minutes, rinsed in PBS and left the sections immersed in 1% acetic acid 40 minutes for de-staining. We applied blocking solution (5%BSA, 0,3% Triton-X in PBS) for 2 hours, then the primary antibody at proper dilution in a solution of 1% BSA, 0,1% triton in PBS, and incubated the samples overnight at 4°C. After rinsing in PBS, the following day secondary antibody was applied at a 1:400 dilution in the same solution used for the primary antibody. After 2 hours, slides were rinsed 3 times with PBS and mounted with a specific mounting medium added with nuclear staining (Fluoroshield DAPI mounting, Sigma-Aldrich). List of the antibodies utilized, and their working dilutions can be found in table 3.

Tab. 3 List of antibodies utilized in the immunofluorescence experiments.

Antibody	**Product type**	**Working dilution**	**Company (Cat N.)**
TDP-43	Rabbit Polyclonal	1:1200	Proteintech (10782-2-AP)
TDP-43	Rabbit Monoclonal	1:500	AbCam (ab190963)
G3BP	Mouse Monoclonal	1:500	AbCam (Ab56574)
TH	Rabbit Monoclonal	1:500	AbCAm (ab75875)
pS129	Mouse Monoclonal	1:500	BioLegend (825702)
PCNA	Mouse Monoclonal	1:500	Dako (M0879)
LAMP1	Rabbit Polyclonal	1:500	AbCam (Ab24170)

2.4 AbSca/e samples images acquisition and processing

To analyze the AbSca/e treated samples we acquired images on a Leica Ire2 confocal microscope using a 20x objective, exciting with an Ar-laser (488 nm).
We acquired 1024x1024 pixel sequential focal planes along the z axis, at a distance of 1.5 µm each, of the regions of interest and then processed the 3D reconstruction utilizing the Bitplane Imaris™ software. First, we applied median filtering to reduce background, then we adjusted the tone curve accordingly to the characteristics of the imaged sample.
To count the TH+ cells in the *locus coeruleus* and the hypothalamus of Nothobranchius furzeri brain we utilized the Imaris™ 'Ortho Slicer' function to optically isolate portions of the z-stack and the function 'Spots' to manually count every TH positive cell.
We analyzed a total of 4 animals per age.

2.5 Immunofluorescence images acquisition and processing

Images were acquired using a Zeiss Axiovision microscope equipped with Apotome slide and subsequently processed using the suite Zen Blue.
Single area images were acquired using two different magnifications (objectives 40x and 63x both oil immersion) as z-stacks formed by multiple focal planes at a distance of 0.5 µm each.

2.6 Whole brain pSyn quantification

To perform a statistical quantification of pSyn staining in whole *N. furzeri* brain, we cut 25µm thick cryo-slices in series of three, processing only one whole series per animal (i.e. 25µm every 75µm of tissue) for pSyn and TH staining as described in the Immunofluorescence and Proteostat™ Aggresome staining section. We analyzed six animal per age (5w and 37w). We then acquired tiles at 20x using an AxioScan Zeiss microscope to obtain images of whole sections, using constant exposure time and applying the 'Best Fit' algorithm in ZenBlue.
The whole section images were then exported as .tif files and analyzed using Adobe Photoshop as described as follows:
Two copies of the image were created:
To the first copy a blur filter was applied (Filter -> Blur Gallery -> Field Blur, applied 80px level). This image was applied to a second copy (Image -> Apply Image -> fusion option subtract) as a first background subtraction method. A threshold (value 40) was then applied to isolate the staining. The staining was then selected (Selection -> Color interval) and analyzed (Image -> Analysis -> Record Measurements) and the summary result containing the total pixel of staining per section was exported.
The area of the staining was registered for each animal in an Excel file and the total stain pixels per brain were calculated.

2.7 Central telencephalon pSyn analysis

We used images collected with the same methodology used for the whole brain pSyn quantification. We analyzed six animals per age (5w and 37w). We selected the four sections corresponding to the most central portion of the telencephalon along the dorso-ventral axis, and we isolated a square of 300px x 300px (A) into the central region on each section. The images were analyzed with the same methodology utilized for the whole sections and the percentage of stained area was calculated as follows (R=ratio, S=px of staining, A=area, i=section):

$$R = \frac{\sum_{i=1}^{4} S_i}{4A}$$

2.8 pSyn and Aggresome analysis into the *Locus coeruleus*

We analyzed images of *locus coeruleus* acquired at a Zeiss AxioScan microscope with Apotome slide on a 40x magnification, all with the same exposure time and to which we applied the 'Best Fit' option in ZenBlue. We analyzed five animals per age for pSyn and four animals per age for Aggresome. We acquired a z-stack of the area and then analyzed the single focal plane presenting the majority of TH staining. We used the open license software Icy (http://icy.bioimageanalysis.org/) for spot analysis. To the selected z-plane we applied the algorithm 'Best Thresholder' (method 'Otsu') on the TH channel to isolate the locus coeruleus cells. Since TH is not distributed homogeneously into the cytoplasm but presents vacuolization containing aggregates, we adjusted manually the selected ROI to include areas containing aggregates. We then used the algorithm 'Spot Detector' imposing to perform the analysis only in the selected ROI with the following parameters:
Preprocessing: red channel
Detector: Detect bright spots over dark BG, scale 1 (for pSyn) or scale 2 (for Aggresome)
Region of interest: ROIFixedFromSequence
Output: export to ROI
The ROIs created (containing the data of both the area of TH and each single spot detected) were exported in an excel file and the following parameters were calculated:

- Percentage of stained area: spots area/ TH area
- Mean spots abundance: number of spots / TH area
- Mean spot dimension: spots area / number of spots

2.9 Western blot

We performed western blot experiments to quantify the expression of Thyroxine Hydroxylase in the brains of MZ-222 Nothobranchius furzeri at various ages. The brains were extracted, immediately stored at -80° and then homogenized for 30 seconds using GelD2 buffer with addition of protease (cOmplete Mini, Roche) and phosphatases (PhosSTOP, Roche) inhibitors at 1x concentration. After centrifugation for 10 minutes at 16000 rpm, supernatant was taken, quantified using the BCA kit (Thermofisher) and stored at -80° for further use.
To perform the western blot, we run 20µg of pulled protein extract derived from four samples per age and run them in precast gels (AnyKD Mini-Protean TGX Gels, Biorad) for 35 minutes at 100V. Afterwards the samples were blotted on a nitrocellulose membrane for 35 minutes at 150V. The membranes were then imaged with a Chemidoc XRS scanner using the Quantity one Biorad software and band intensity quantification was performed using the opensource ImageJ software. We analyzed four animals for each age (5,8,12,27,37 weeks).

2.10 RNA-seq and proteomics data analysis

To assess TH expression, I realized graphics of RNA expression starting from RNA-seq data derived from public cross-sectional experiments (Baumgart, Groth, et al., 2014; Kelmer Sacramento et al., 2020). We combined two RNA-seq datasets of brain aging in *N. furzeri*: a dataset covering five time points (5, 12, 20, 27, and 39 weeks) and 5 biological replicates for each age and the second containing 4 replicates per ages: 5,12 and 39 weeks. These ages correspond to sexual maturity, young adult, adult (as defined by a decrease in growth rate), median lifespan and old (~30% survivorship) (Baumgart et al., 2014). In total, these represent 37 different samples spanning five different ages. We first normalized the samples using the Deseq2 package in the suite R and then divided the counts of the two datasets for the average expression of their respective 5w samples to be able to combine the datasets.
We also analyzed publicly available proteomic data (Kelmer Sacramento et al., 2020). The dataset contains five replicates for age (5, 12, 39 weeks) and is a combination of two separate experiments performed utilizing tandem mass tag and analyzing the same 12w animals twice in two different contrasts: 39w vs 12w and 5w vs 12w. Therefore, we combined the data normalizing the protein expression dividing them for the mean value of the 12w animals.
For both transcriptomics and proteomics data we performed statistical analysis calculating the Spearman correlation value, the pValue adjusted and the FDR to assess the statistical significance of the observed expression variability.
All the analysis were performed utilizing the R software.

2.11 Establishment of organotypic cultures and immunofluorescence

The following procedure was performed under a horizontal flux hood and all the instruments were placed under UV light for 30mins before starting the experiment.
To perform organotypic cell culture we sacrificed 5 weeks old *Nothobranchius furzeri* animals by anesthetic overdose (Tricaine). We then immersed the whole body in 0,05% NaOH for 30s and in EtOH 70% for 30s to sterilize the body prior to brain extraction to reduce the probability of bacterial contamination of the tissue.
Afterwards we cut the head from the body and proceeded to extract the brain under a stereomicroscope in a solution of Hank's salt added with 1% Penicille-Streptomicine mixture (Penstrep). The extraction of the brain was performed as quickly as possible to minimize the time between animal death and placing of the tissue over the porous membrane; this is a critical step in order to reduce the death of the tissue.
After extracting the brain, this was placed onto a micrometric slide where, with the aid of a microblade, coronal sections of approximatively 500 µm were cut. To obtain *Locus coeruleus* containing slices we used as anatomical reference the cerebellum and cut in front and behind it.
After the cut the slices were gently taken with forceps and quickly immersed in three consecutive baths of 1% penstrep to reduce the risk of contamination and then placed on semi porous membrane into six well plates containing 1 ml of culture medium and kept on ice.
We placed three brain slices onto each membrane.
After completion of slice gathering the 6-wells were placed in an incubator at 28° and 5% CO2 and the medium was changed after three hours.
In the following days the medium was changed every second day.
Medium composition was the following:
DMEM/F12 (Cat. 21331020, Thermofisher, USA)
FCS 10% (Cat. ECS5000L, Euroclone, Italy)
Sterile milliQ water 10%
Insulin 0.033% (Cat. L9278, Merk Life SCIENCE, Germany)
Ascorbic acid 511 µM
PenStrep 1% (Cat. ECB3001D, Euroclone, Italy)
Glucose to adjust the solution at 0,4%(Cat. A2494001, Thermofisher, USA)For EdU staining the sections were given 5µg EdU for three days starting from day one *in vitro*.
After one, three or five weeks the slices were fixed in 4% PFA for 10 minutes (1ml over the membrane 1ml under the membrane) and then treated for immunofluorescence.
The sections were washed in PBT (PBS plus triton 0.5%) three times and then incubated overnight at 4° in PBT for permeabilization.
The following day the sections were incubated four hours in blocking solution (5%BSA, 0,5% triton, PBS). Afterward, the sections were gently detached from the membrane and transferred in a 12 well to reduce the amount of primary antibody used. The slices were then incubated overnight at 4° in primary antibody diluted in a solution of 1%BSA, 0,5%Triton in PBS.

The third day sections were washed three times in PBT and the incubated four hours in secondary antibody at RT. Sections were then rinsed and, if needed treated for EdU revelation for 30 minutes using the Click-it Edu Staining kit (C10337, Thermofisher Scientific, USA) and rinsed again. Sections were then incubated ON in Sca/e A2 solution to clear them and then in Sca/e S4 until imaging.

3. Results

Note: Part of the following results are modified, extended and adapted from the following publications (complete citations for published articles and preprints are listed in the references):
Results 3.1 (Kelmer Sacramento et al., 2020)
Results 3.2 (Bagnoli et al., 2021), currently under review in Aging Cell
Results 3.3 (Louka *, Bagnoli * et al., 2021) * authors have contributed equally to the paper, revised version ready for submission to Aging Cell

3.*1 Nothobranchius furzeri* shows signs of protein aggregation during ageing

As described in detail in our publication (Kelmer Sacramento et al., 2020), we observed an unbalance in mRNA and corresponding proteins level in *Nothobranchius furzeri* brain during ageing, leading to a loss of protein stoichiometry for many protein complexes which particularly affected the ribosome.
Using biochemical fractionation techniques in combination with mass spectrometry in mice, we also observed an increase of protein aggregates SDS insoluble fractions that were also enriched in ribosomal proteins (Fig.1). The small dimension of the *N. furzeri* brains prevented us from performing a biochemical analysis of aggregates. To investigate age-dependent aggregation in *N. furzeri* of ribosomal proteins in killifish, I performed staining of young (7-10 weeks post hatching) and old (27-30 weeks post hatching) brain slices using Proteostat, an amyloid-specific dye (Shen et al., 2011), and LAMP1 as lysosomal marker. I detected abundant intracellular aggregates in old brains, but only in occasional cells in young brains. These aggregates were large in size and typically placed near the nucleus. Double labelling with LAPM1 revealed that these aggregates correspond to apparently enlarged lysosomes. The aggregates also appeared to contain the ribosomal protein RPS6 (Fig.1). Taken together, these data demonstrate that an age-dependent aggregation of ribosomal proteins observed in mice is also conserved in old fish.

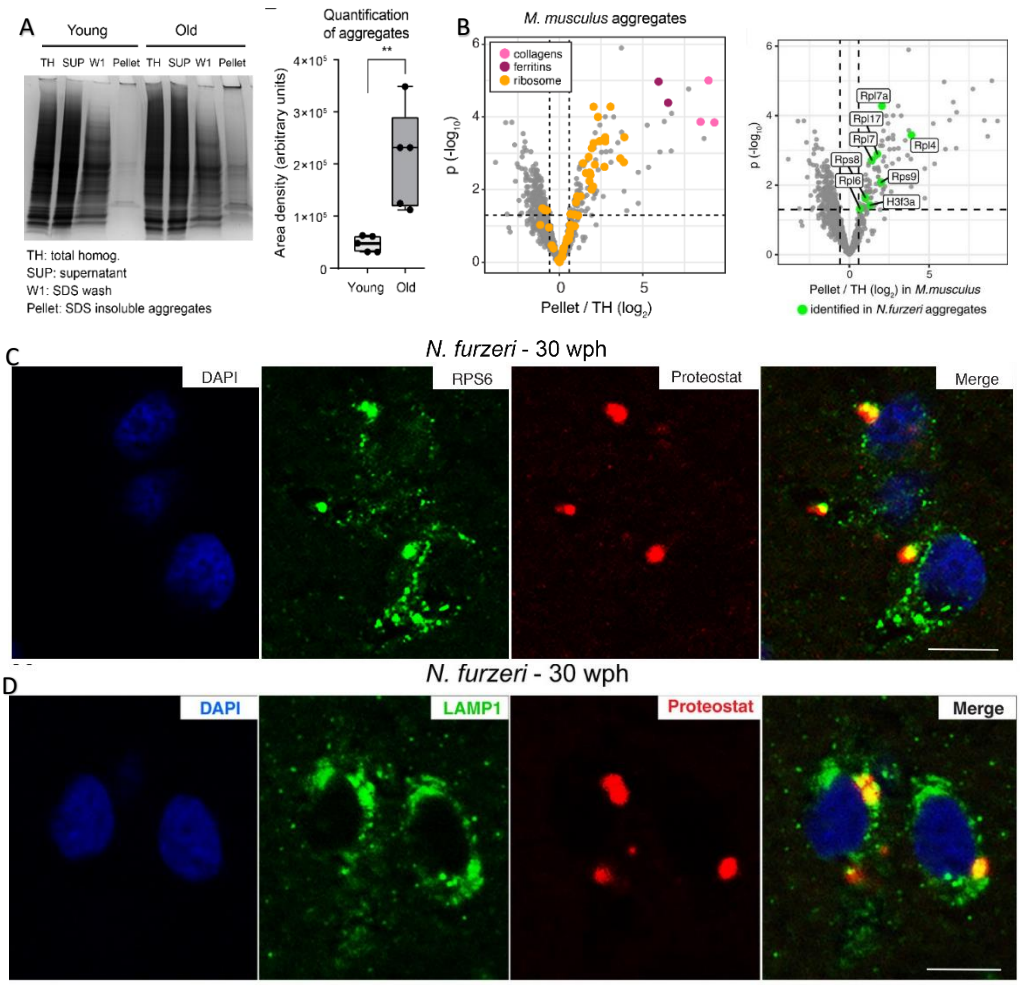

Fig. 1 A) Representative Coomassie-stained SDS–PAGE gel showing the isolation of SDS-insoluble aggregates from mouse brain lysates and quantification of the yield of SDS-insoluble aggregates from young and old brain lysates based on densitometry analysis of Coomassie-stained gel bands obtained from different animals, n = 5 per age group. SUP = supernatant, TH = total homogenate, W1 = SDS-soluble fraction, Pellet = formic acid soluble fraction. **P < 0.01, unpaired t-test. In boxplots, the horizontal line represents the median, the bottom, and top of the box the 25th and 75th percentile, respectively, and the whiskers extend 1.5-fold the interquartile range. B) Volcano plot based on protein quantification by label-free mass spectrometry depicting the enrichment of specific proteins in protein aggregates. The x-axis indicates the log2 ratio between protein abundance in aggregates (Pellet) and starting total homogenate (TH). The horizontal dashed line indicates a P value cut-off of 0.05 and vertical lines a log2 fold change cut-off of ± 0.5. Selected proteins are highlighted as colored dots as indicated in the figure legend. Same volcano plot with ribosomal proteins enriched in mouse aggregates identified in *N. furzeri* aggregates highlighted in green dots. C) Double labeling of telencephalic sections of *Nothobranchius furzeri* with anti-RPS6 (green) as ribosomal marker and Proteostat as a marker for aggregated proteins (red). Nuclear counterstaining was performed with DAPI (blue). Scale bar corresponds to10 µm. D: Magnification showing a detail of the co-localization between lysosomal structures (green) and protein aggregates (red) in the old telencephalon. Scale bar = 10µm.

3.2 Aging is associated with a degeneration of noradrenergic-, but not dopaminergic-neurons, in *Nothobranchius furzeri*

In order to investigate the possible use of *Nothobranchius furzeri* as a valid model to study neurodegeneration linked to Parkinson's disease, I analyzed individuals from the *N. furzeri* population MZCS-222 that belongs to the same genetic clade of the population MZCS-24 studied by Matsui and the population MZM-0410 that has been extensively used in our group previous studies. This population was collected in Africa later than MZM-0410 and is therefore likely to be more genetically heterogeneous and closer to the wild population. The median lifespan of this strain in captivity is around 6 months (Žák & Reichard, 2020).
I set out to quantify the total number of Tyrosine hydroxylase positive (TH+) cells in the *Locus Coeruleus* (LC) and in the *posterior tuberculum* (hypothalamus) in young (5 weeks), adult (12 weeks) and old (37 weeks) animals to assess the presence of possible neurodegeneration. These age groups were chosen in order to have a clear idea of the amount of cells in the *Locus coeruleus* and *posterior tuberculum* throughout the life of the fish. The size of the brain increases during this period and the spatial distribution of cells may vary between animals of different ages (Fig. 2, 3A). Since at 5 weeks of age in the brain there is still a high rate of neurogenesis (Tozzini et al., 2012, Fig. 2), we wanted to exclude that any eventual neurodegeneration observed between young (5w) and old samples (37w) was due to analysis between a not fully developed nucleus and a nucleus with age-dependent cell reduction. Thus, we analyzed also samples from 12w of age, age in which the neurogenesis potential is reduced (Tozzini et al., 2012, Fig.2) and the number of cells in the nuclei should be definitive, at least in some brain areas.

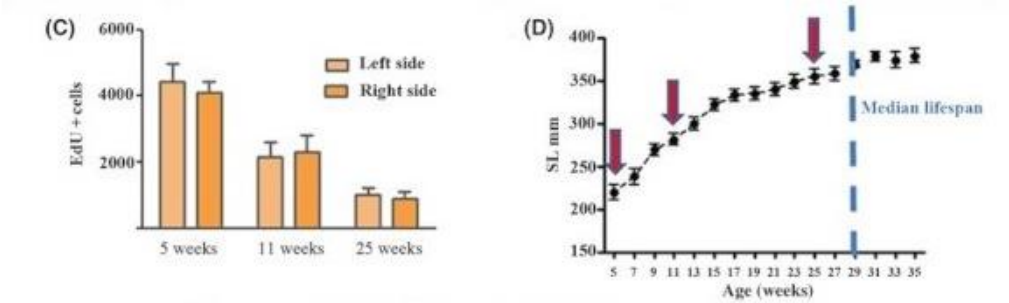

Fig. 2, from Tozzini et al., 2012. Panel on the left is an histogram reporting unbiased estimation of EdU+ cells into the tectal germinal layer at three different age-steps. Estimates for left and right *tecta* are reported separately. Five animals per time point were analyzed, and error bars represent standard deviations. The panel on the right represents the growth curve of *N. furzeri* males. The analyzed age-steps for the quantification are marked by red arrows. Forty-five animals were measured to produce this curve. Error bars represent standard errors of means.

In order to visualize and count all TH+ cells in the region of interest, we cleared the brain using the Sca/eS procedure (Hama et al., 2015) and reconstructed all the different TH+ nuclei of the *N. furzeri* in their entire 3D extent by scanning through the transparent brain (Fig. 3, 4).
The *N. furzeri posterior tuberculum* contains two clearly separated populations of TH+ cells (Fig.5, panel A), one comprised of larger and more anteriorly- and dorsally located cells and one comprised of smaller and more posteriorly- and ventrally-located cells. These two nuclei are very similar to the nuclei 12 and 13 described in the zebrafish *posterior tuberculum* using TH immunofluorescence (Sallinen et al., 2009) and are proposed as homologous to the A-9 A-10 mammalian dopaminergic cluster comprising the substantia nigra (Kaslin & Panula, 2001; Rink & Wullimann, 2001). I counted all cells in these two populations and could not detect a significant difference in their numbers between young, adult, and old animals (Fig. 5C), as opposed to the

remarkable ~ 50% reduction reported by Matsui et al. Notably, the number of TH+ cells we detected was larger than the number reported by Matsui et al.: average 77 (range 59-86) vs.~ 30.

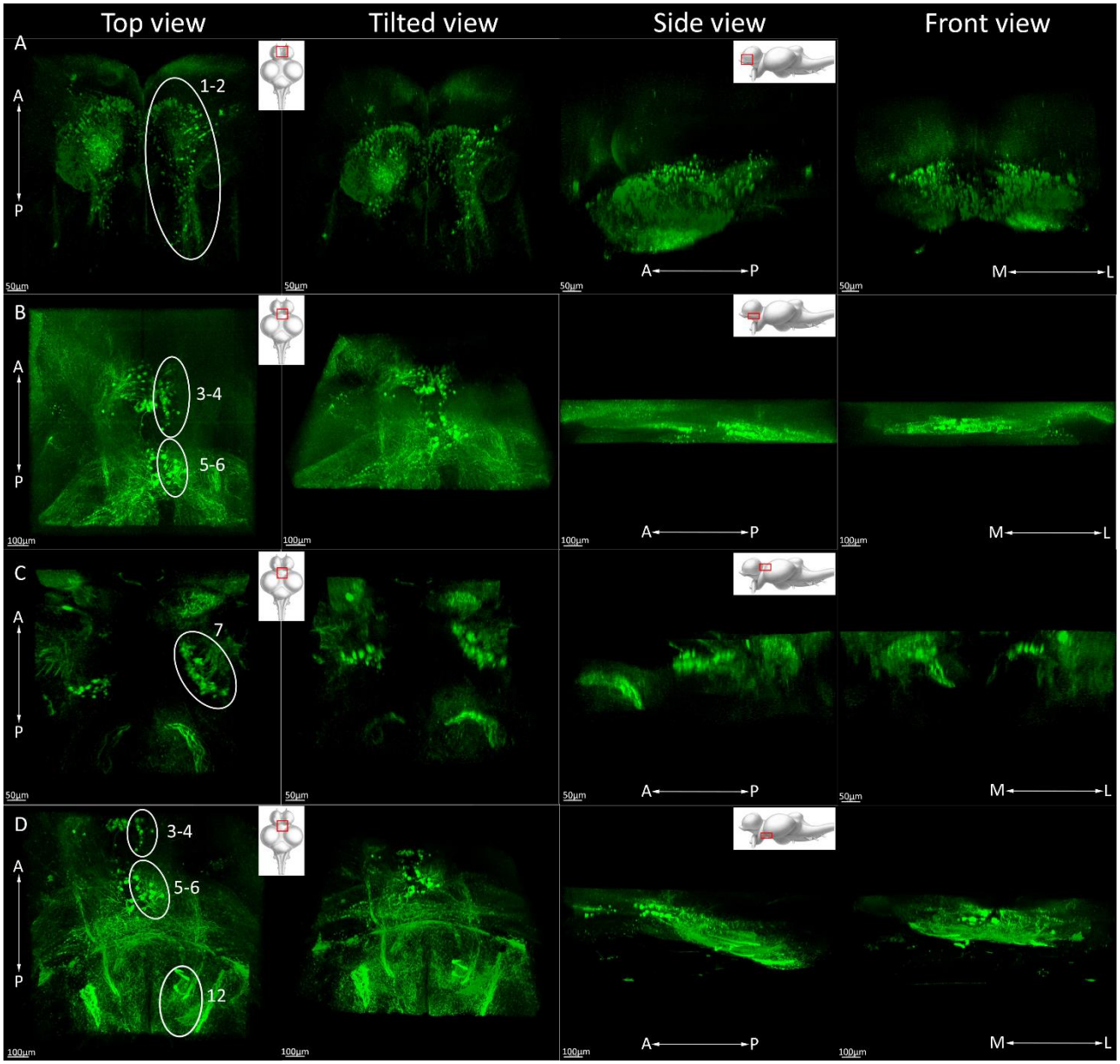

Fig.3 Localization of the TH+ nuclei in the brain of *Nothobranchius furzeri*, anterior. As the main reference for nuclei identification a Zebrafish map from Sallinen et al. was used. Panel A: main nuclei of the olfactory bulbs and ventral telencephalon (homolog to nuclei 1-2 from Sallinen et al., 2009). Panel B: caudal telencephalic nuclei and rostral diencephalic nuclei (homolog to nuclei 3-4 and 5-6 from Sallinen et al., 2009). Panel C: periventricular pretectal nuclei (homolog to nuclei 7 from Sallinen et al., 2009). Panel D: caudal telencephalic nuclei, rostral diencephalic nuclei and beginning of periventricular organ, Posterior tuberculum (homolog to nuclei 3-4, 5-6 and 12 from Sallinen et al., 2009). A=anterior, P=posterior, M=medial, L=lateral. Scale bars indicate 100 µm.

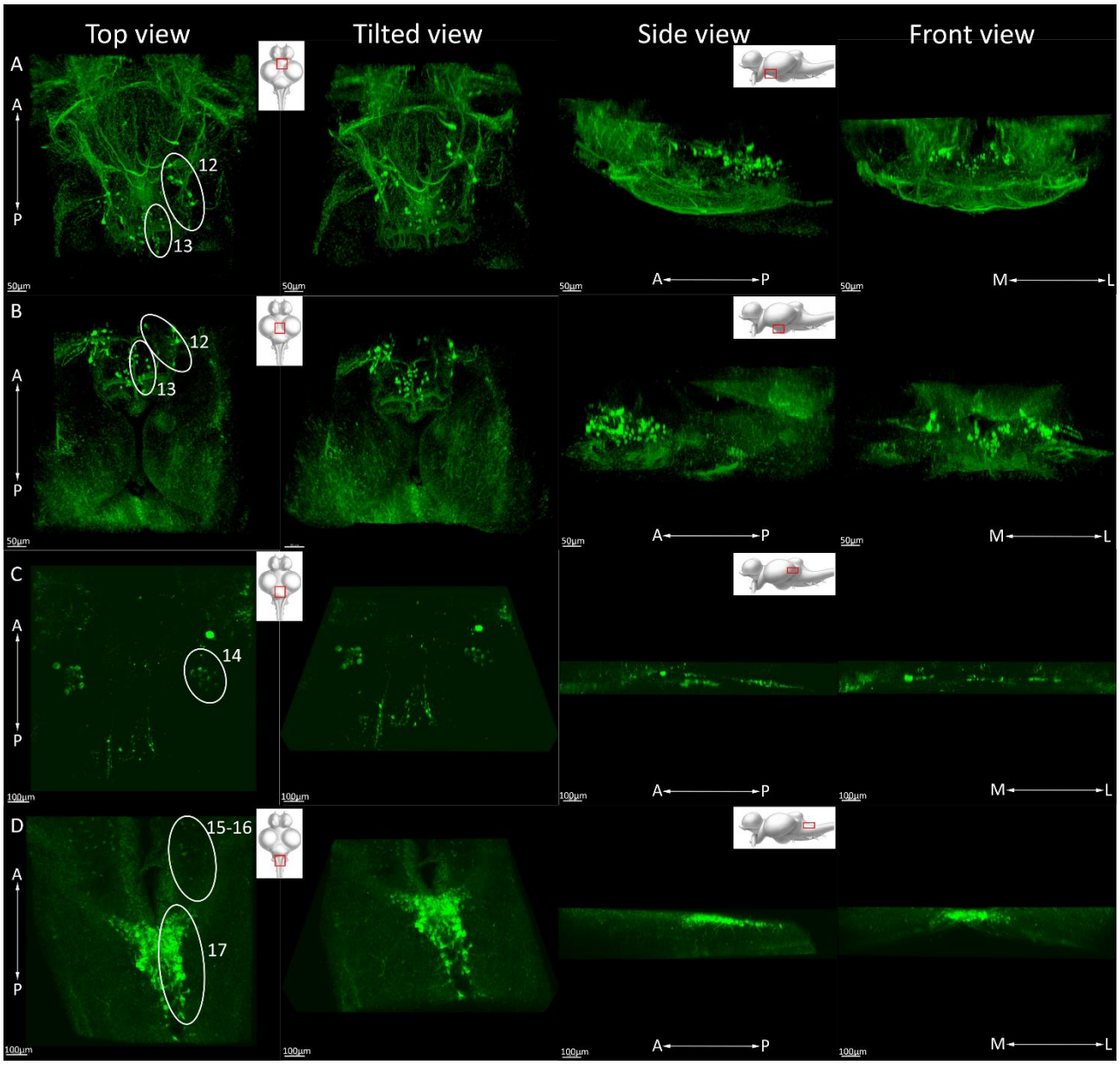

Fig.4 Localization of the TH+ nuclei in the brain of *Nothobranchius furzeri*, posterior. As the main reference for nuclei identification a Zebrafish map from Sallinen et al. was used. Panel A: main diencephalic nuclei of the *posterior tuberculum*: periventricular organ and periventricular hypothalamus (homolog to nuclei 12-13 from Sallinen et al., 2009). Panel B: more caudal view of main diencephalic nuclei of the *posterior tuberculum*: periventricular organ and periventricular hypothalamus (homolog to nuclei 12-13 from Sallinen et al., 2009). Panel C: *Locus coerule*us nuclei (homolog to nuclei 14 from Sallinen et al., 2009). Panel D: Vagal nuclei (homolog to nuclei 15-17 from Sallinen et al., 2009). Scale bars indicate 100 µm.

As opposed to hypothalamic nuclei, a modest but significant decrease in the number of LC neurons between young and old animals (Fig. 5B, D) was detected. The reduction was not evident between animals at 5 weeks and 12 weeks (conversely to what observed by Matsui et al.) but seems to be an event occurring strictly between adulthood and old age. Also in this case, the number of labelled cells we detected is larger than what reported by Matsui et al.: 33 (range 37-27) vs. ~ 20 and the amplitude of the cell loss much smaller (27% vs ~ 75%).

Matsui et al. also reported a down-regulation of TH protein and transcript in the whole brain by Western blot and qPCR. I interrogated two independent public databases of RNA-seq (Fig. 5E) and one database of mass-spectrometry based proteomics of *N. furzeri* brain aging (Fig. 5F) and I could not find any support for a down-regulation of TH neither at the transcript- nor at the protein-level. I repeated Western blot analysis, both animals singularly and pooled, and also in this case I could not detect a down-regulation of TH; instead from the pulled experiment emerged a significant increase of whole brain TH content between 5 and 8 weeks of age. This increase is visible also from the single animal experiment but it did not reach statistical significancy in that setup (Fig. 5 G, H). The increase is reflected also in the proteomic graph (Fig. 5F) although not statistically significant. The proteomic data seems to suggest also a reduction of the expression between 12w and 37w, not reflected by the western blot experiment: seen the general high variance of the samples at 37 weeks (shown by the errors bars in the western blot and the plot of single animals in the proteomic graph) and the reduced number of samples used for proteomics data (3 animals per age), we think that this reflects the high variability in neurodegeneration state of different individuals in the overall monoaminergic system.

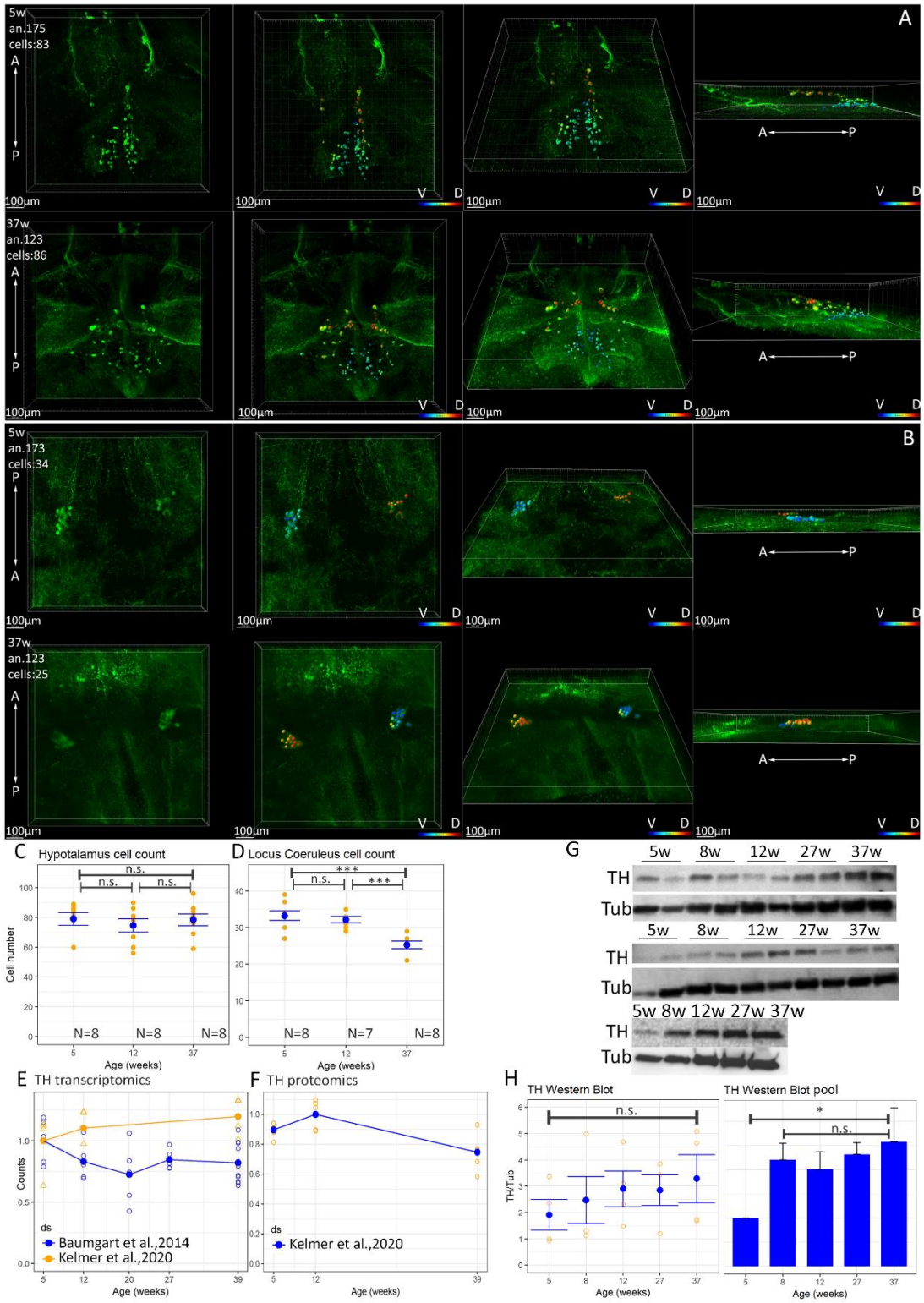

Fig.5 Assessment of neurodegeneration in LC and posterior tuberculum and quantification of TH expression during ageing. A) Representative images of 3D reconstruction and cell counting in the *posterior tuberculum* nuclei of a young (5 weeks old) and old (37 weeks old) N. furzeri. V=ventral, D=dorsal, A=anterior, P=posterior. The color code indicates the depth of the cells in the reconstructed volume. B) Representative images of a 3D reconstruction and cell counting of LC of a young (5 weeks old) and old (37 weeks old) *N. furzeri*. V=ventral, D=dorsal, A=anterior, P=posterior. The color code indicates the depth of the cells in the reconstructed volume. C) cell counts of *posterior tuberculum* nuclei in young and old animals. Each open dot represents a single animal and the solid dot the mean of the group and the error bar the SEM. D) cell counts of LC nuclei in young and old animals. Statistically significant difference was assessed by unpaired Student's t-test, n.s. indicates $p > 0.05$, *** indicates $p < 0.001$. E) Quantification of TH mRNA expression.

Two independent RNA-seq datasets (from Baumgart et al., 2014, and Kelmer et al., 2020) were analyzed. F) Analysis of TH protein expression by mass spectrometry. We assessed a proteomic dataset (from Kelmer et al., 2020). Each open dot represents a single animal and the solid dot the mean of the group and the error bar the SEM. To assess the statistical significance of age-dependent regulation, we calculated Spearman correlation with age. In both cases p > 0.05. G) Images of TH protein expression by Western blot, A total of four animals per each age were analyzed, independently or pulled. H) Quantification of TH Western blot. The intensity of TH band was normalized with respect to the tubulin band. To assess statistical significance, we calculated Pearson's correlation coefficient of the expression with age and respective pValue, the data are expressed as mean ±SEM.

To assess pathological post-translational modifications of α-Syn, I used an antibody directed against phosphorylated S129 (pS129) in double-labelling with TH.
N. furzeri α-Synuclein aminoacid sequence presents a substitution of the serine located at the residue 129, involved in phosphorylation, with a threonine (Fig.6). Since threonine is a phosphorylable aminoacid, and the vast majority of kinases present in the cell are serine-threonine kinase (included the ones responsible for α-Syn phosphorilation, Waxman & Giasson, 2011), coupled with the fact that the immediately adjacent amminoacids to the Tre129 of *N. furzeri* are conserved with the human sequence, we assume that Tre129 can be phosphorylated and that antibodies able to recognize pSer129 are able to work in our model as well.

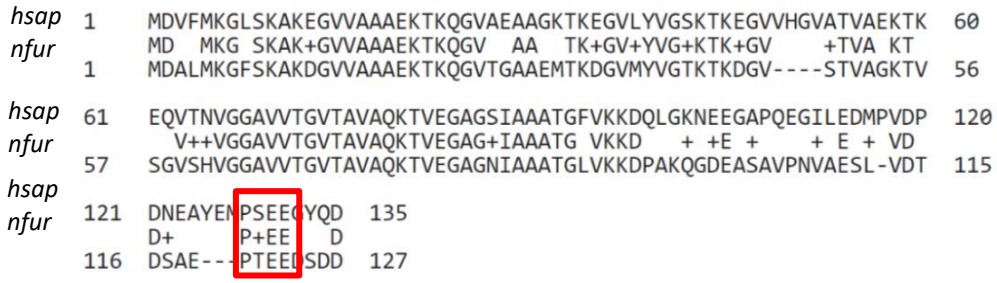

Fig 6. Alignment of human and *N. furzeri* α-Syn. Highlighted is the Ser129Tre aminoacid substitution with the adjacent aminoacids conserved.

Labelling of *posterior tuberculum* neurons did not reveal any somatic staining for pS129 in either young (5 weeks) or old (37 weeks) samples (Figure 8A). On the contrary, a punctate labelling of pS129 was readily detected in the LC neurons from old fish (Fig.7B). Remarkably, LC TH+ neurons contained punctate labelling of pS129 already at young age (Fig.7A). The only other cells showing early somatic labelling in the brain were TH+ cells in the vagal nuclei (Figure 8B). Quantitative analysis of the staining revealed that the size of pS129+ puncta increased between young and old animals (Fig.7C-E), while their number does not increase in a statistically significant way. It should be noted that the cytoplasm of LC neurons in old animals shows a clear vacuolization, apparent as spherules devoid of TH immunoreactivity (Fig. 7Bb). Interestingly, pS129+ puncta are not present in the vacuoles but seem to be associated with- or in proximity of- their external surface (Fig.7Bb).

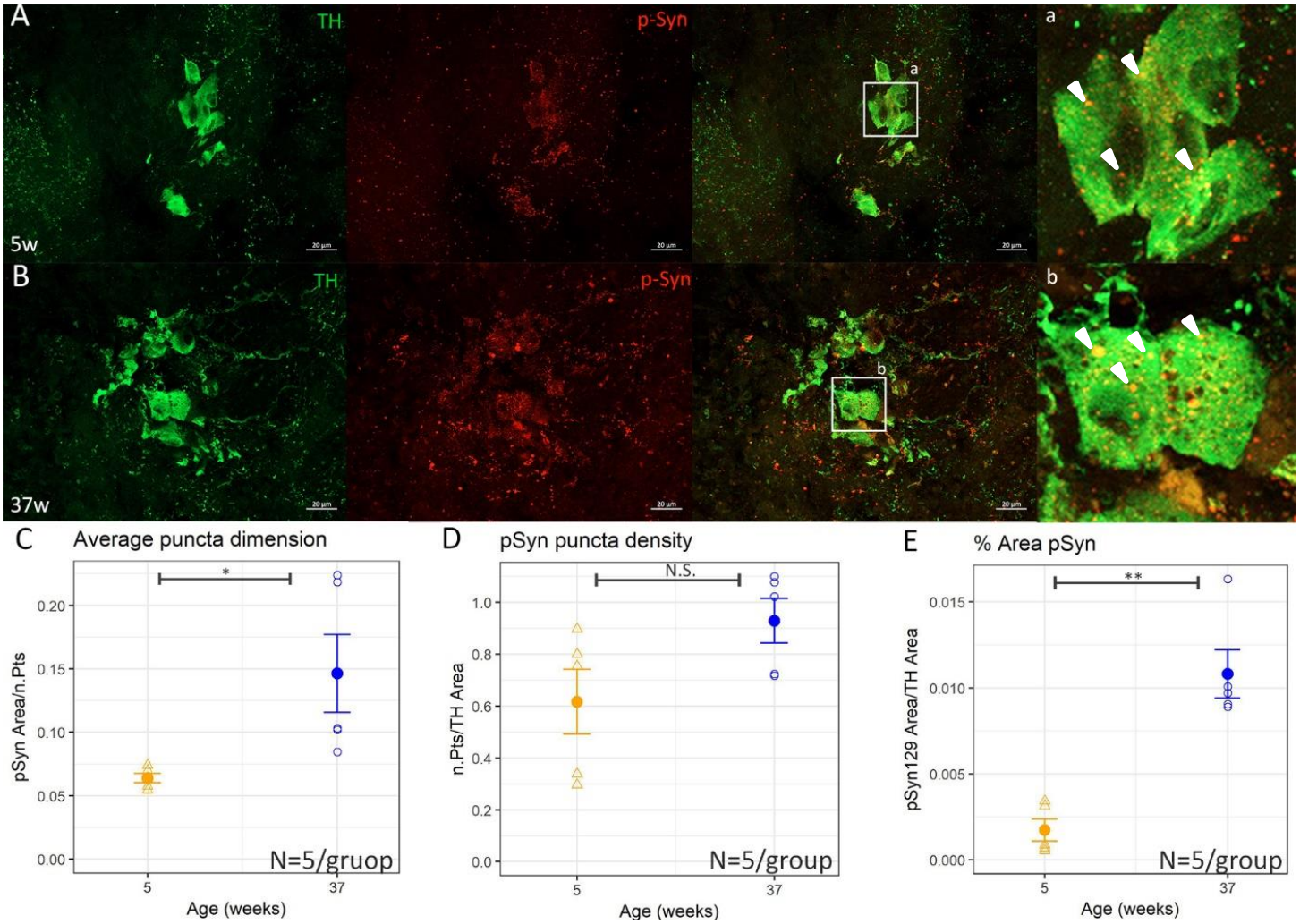

Fig.7 Double immunofluorescence for TH (green) and phospho-Synuclein (red) in *locus coeruleus* cells. A diffuse, punctate staining (white harrowheads) is visible in both young (5w, panel A,a) and old (37w, panel B,b) animals. Please note in the magnification shown in panel b the presence of cytoplasmic vacuoles. The dimension (panel C) and the area (Panel E) of the puncta increases significantly with age. To test significance two tailed unpaired t-test was used, n.s. indicates $p > 0.05$ * = $p < 0.05$, ** = $p < 0.01$ the data are expressed as mean ±SEM. Scale bars correspond to 20 µm.

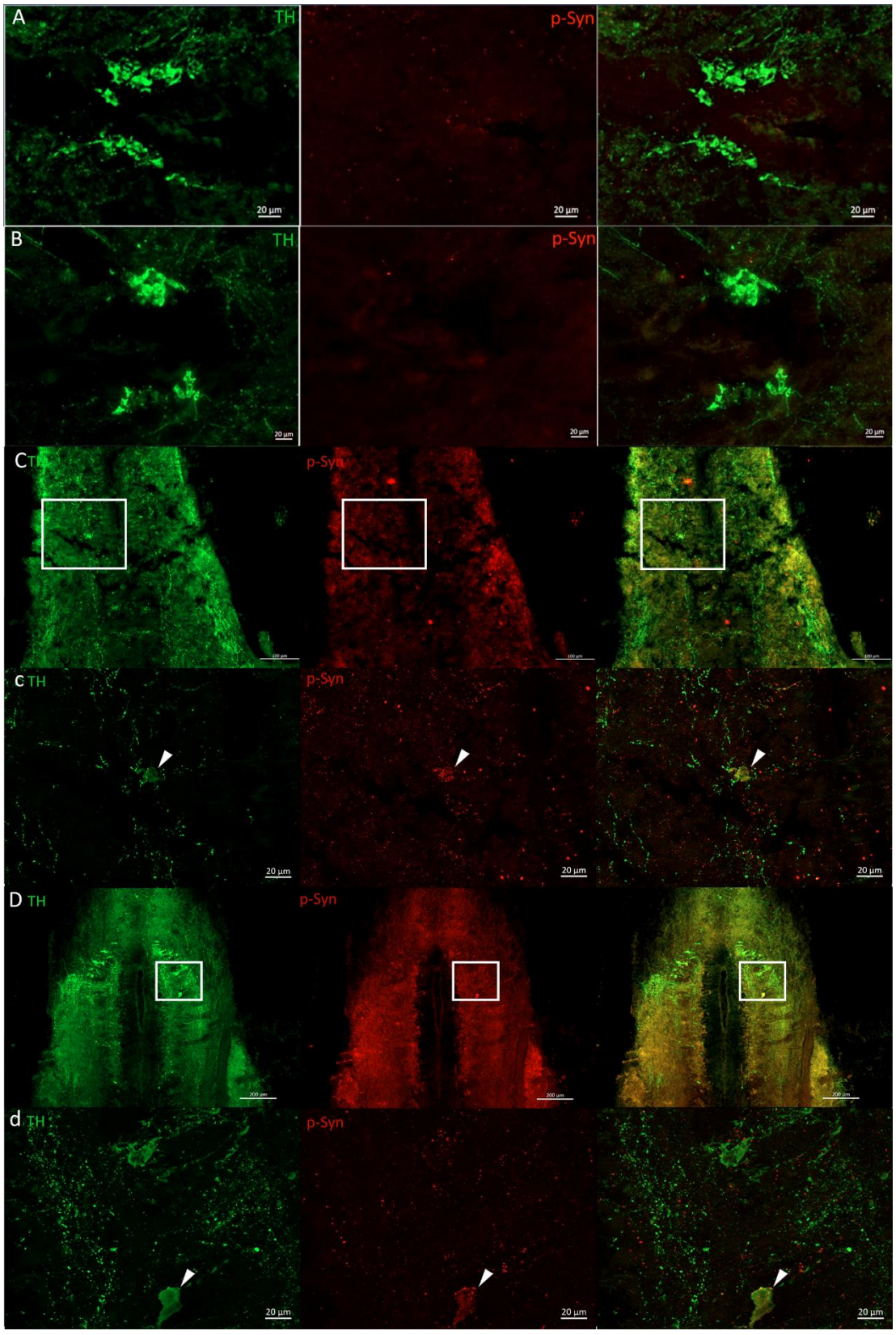

Fig.8 TH (green) and phospho-Synuclein (red) staining in *posterior tuberculum* (hypothalamus) and vagal nuclei. Phospho-Synuclein staining was absent from hypothalamic cell bodies both at young (5w, panel A) and old age (37w, panel B), while a somatic, punctate staining was present already at young age (5w, panels C,c) in cell bodies located in the vagal nuclei and remained evident also in old animals (37w, panels D,d). In panel C scale bar corresponds to 100 µm and in panel D to 200 µm.

I also assessed a general increase of pS129 staining in the whole brain and in the central telencephalon specifically (Fig. 9A, B), this region was chosen because age-dependent appearance of protein aggregates was previously demonstrated by us (Kelmer et al., 2020). Labelling outside of the LC was observed mostly in the form of labelled processes and, unlike in the LC and vagal nuclei, clearly labelled somata with punctuate labelling could not be detected. Both the total brain area covered by pS129 labelling and the density of labelling in the telencephalon were increased in old animals (Fig.9C, D). Remarkably, pS129 in the telencephalon appeared to be associated, albeit not exclusively, to TH+ positive axonal fibers (Fig.9E). These dystrophic axons may originate from the LC, but I have no definitive proof of their identity.

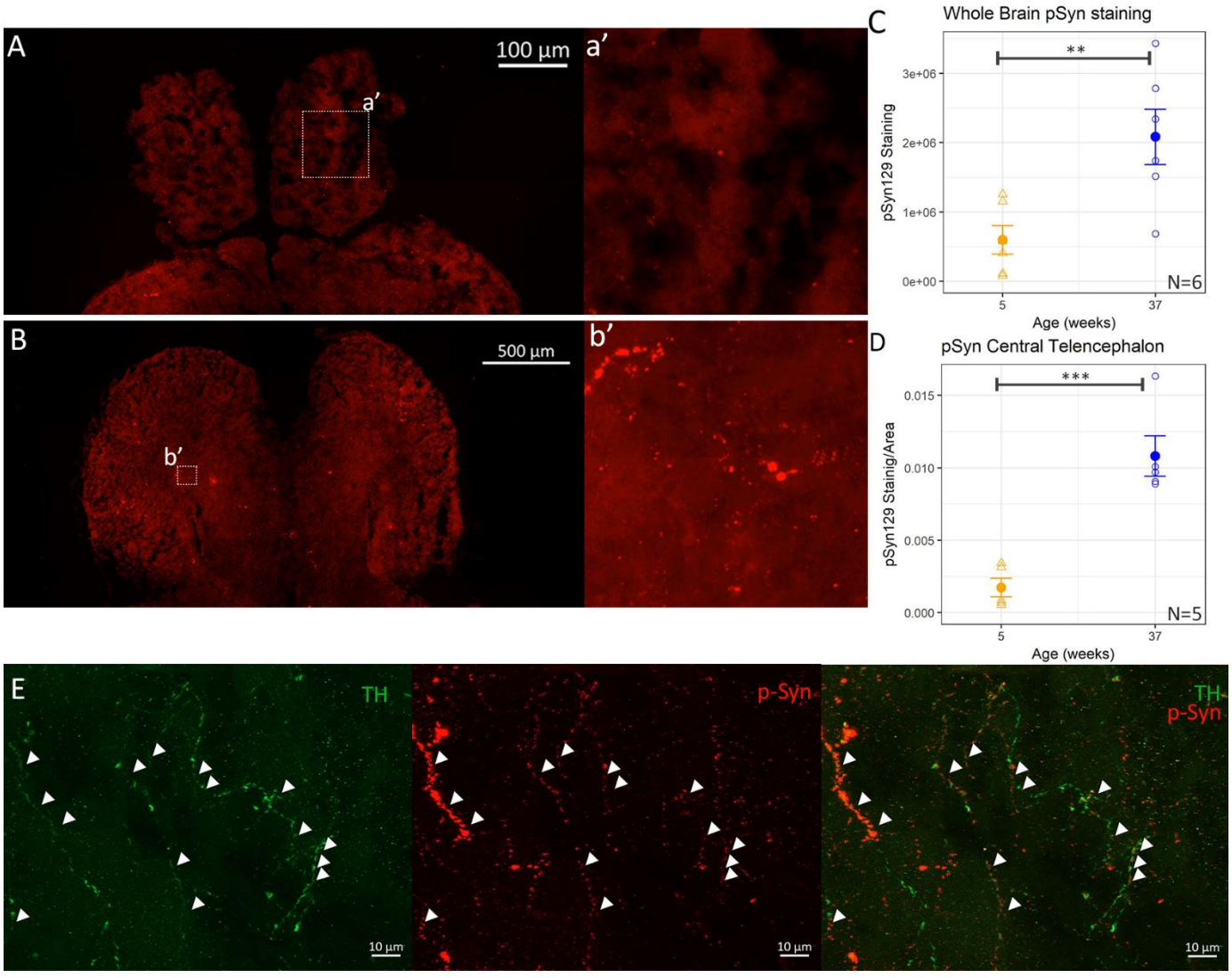

Fig.9 Phospho-Synuclein staining in other brain areas. I quantified the amount of phospho-Synuclein staining in the whole brain of young (5w panel A) and old (37w panel B) animals and we found a significant increase with ageing (panel C). I also focalized the analysis in the central telencephalon (panels a', b'). Also in this area we found a statistical significant increase of phospho-Synuclein staining (panel D). To test significance two tailed t-test was used, ** = $p<0.01$ and *** = $p<0.001$, the data are expressed as mean ±SEM.
Apart from locus coeruleus and vagal cells, the staining of phospho-Synuclein is localized in processes, not exclusively colocalizing with TH positive fibers. We were able to find such staining associated with TH positive processes especially in old animals (37w) telencephalic areas (panel E).

In addition, I investigated the presence of protein aggregates (aggresomes) in LC neurons from old fish. The Proteostat dye revealed a punctate staining in TH+ neurons from old, but not young fish (Fig. 10 A, B). This difference was apparent and was also confirmed by quantitative analysis (Fig.10 C-E). The localization of aggresomes in LC neurons was distinct from that of pS129 puncta, as protein aggregates were clearly contained within the cytoplasmic vacuoles (Fig. 10B, b'-b'''').

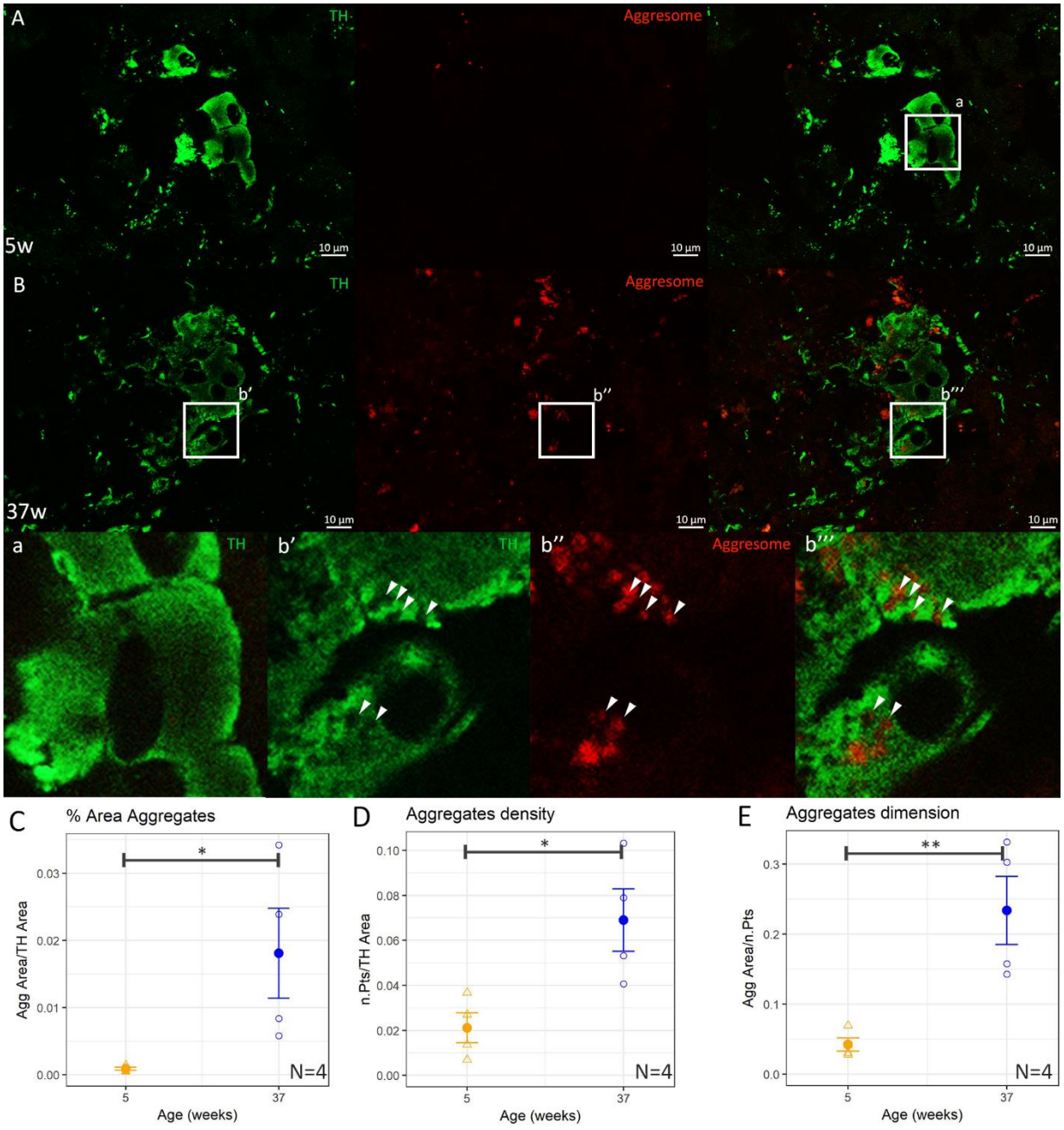

Fig.10 Double immunofluorescence for TH (green) and Aggregates (Proteostat Aggresome Dye, red) in *locus coeruleus* cells. Aggresome staining is absent in young animals (5w, panel A) and becomes visible in old animals (37w, panel B). In particular, aggregates are mainly located in vacuolized areas of cytoplasm devoid of TH staining (panels, b', b'', b''') that are not present in young animals (panel a). The area (panel C), the number (panel D) and the dimension (panel E) of the aggregates all increased significantly with ageing. To test significance two tailed t-test was used, * = $p<0.05$ and ** = $p<0.01$, the data are expressed as mean ±SEM. Scale bars correspond to 10 µm.

3.3 TDP-43 undergoes a change of distribution during ageing in *Nothobranchius furzeri*

Since TDP-43 is another protein associated with neurodegeneration and age-dependent neurodegenerative diseases, we decided to check its cellular distribution and possible aggregation during ageing in *Nothobranchius furzeri.* In our work realized in collaboration with the group of prof. Annalisa Pastore at the King's college in London, we describe how the *N. furzeri* TDP-43 protein shows aggregation characteristics similar to the human isoform *in vitro* (Louka et al., 2021).
Seen these interesting first observations, I probed the localization of the protein distribution throughout the principal areas of the fish brain, such as telencephalon and optic tectum performing immunofluorescence experiments on 25 mm cryo-sections of *N. furzeri* MZM-04010 brains, to assess *N. furzeri* TDP-43 localization during ageing *in vivo*. I compared animals at 5 weeks, the age at which the animal reaches maturity, with animals at 27 weeks, when age-dependent mortality starts (Terzibasi et al., 2008). To verify the robustness of the staining pattern, we used two different antibodies raised against the human protein with different epitope specificities: a monoclonal (Abcam) and a polyclonal (Proteintech) rabbit antibody, respectively. The two different antibodies showed comparable staining patterns (Figure 11) but the monoclonal antibody showed an overall cleaner signal, which was also more stable over prolonged storage. The staining associated with the polyclonal antibody was instead labile and decayed in a few days. For this reason, we decided to use the monoclonal antibody in all further experiments.
TDP-43 staining showed a variable level of diffuse expression in the cell nuclei of young animals (Fig. 11A, B), presenting cells with brighter signal (white arrowheads), and others with a less intense TDP-43 positivity (white arrows). Staining in old tissues was characterized by the presence of cells with a peculiar endo-perinuclear concentration of protein labelling (Fig. 11C, D, doughnut-like stained cells, red arrowheads). Doughnut-like stained cells were sporadically present in the young animals (data not shown). This fact, together with the presence of cells with diffuse labelling in the old tissue, suggested that the altered protein distribution has a progressive evolution over time.

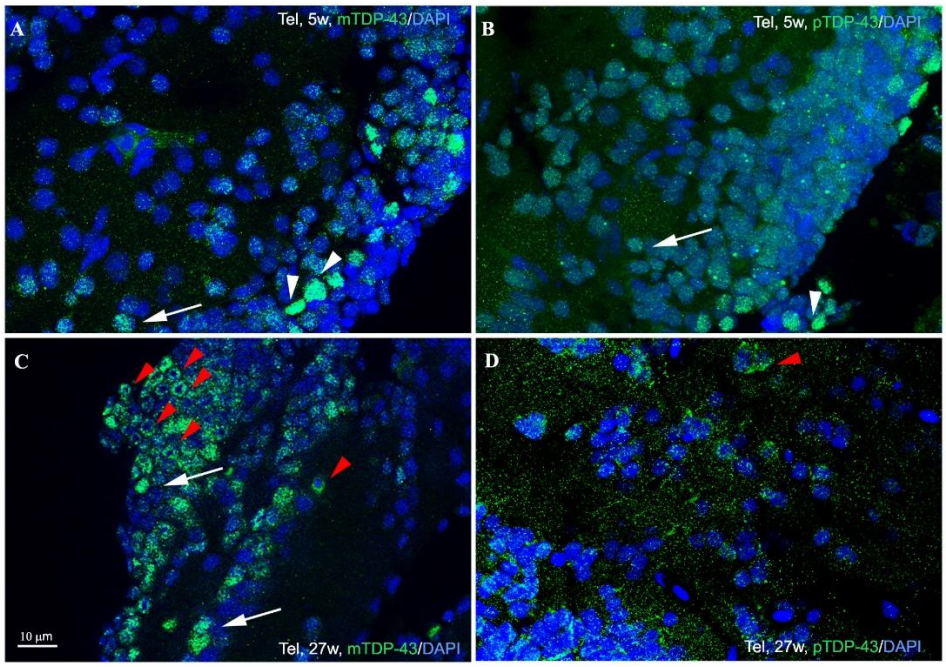

Fig. 11: Immunostaining of TDP-43 with monoclonal (A/C) and polyclonal antibody (B/D). The staining resulted quite comparable in both cases with the presence of cells showing a more intense labelling (white arrowheads) and other

with a less strong signal (white arrows). Both staining highlighted the presence of doughnut-like cells especially in old samples (panels C/D, red arrowheads). Sale bar indicates 10 µm.

To better appreciate the doughnut-like TDP-43 distribution in old animals, I performed whole mount brain staining (Fig.12): I cleared and stained whole *N. furzeri* brains, by using a Sca/eS immunofluorescence-optimized methodology (AbSca/e) (Hama et al., 2015), and registered 3D brain reconstructions by acquiring confocal serial stack images and processing them through the IMARIS Software. By comparison of the 3D representations of the tissues from young (Fig.12 Aa) and old (Fig.12 Bb) animals, we observed an apparently higher proportion of doughnut-like cells (red arrowheads) in the telencephalic area of the old fishes as compared to that of the young ones. Diffuse stained nuclei were detectable in both tissues.

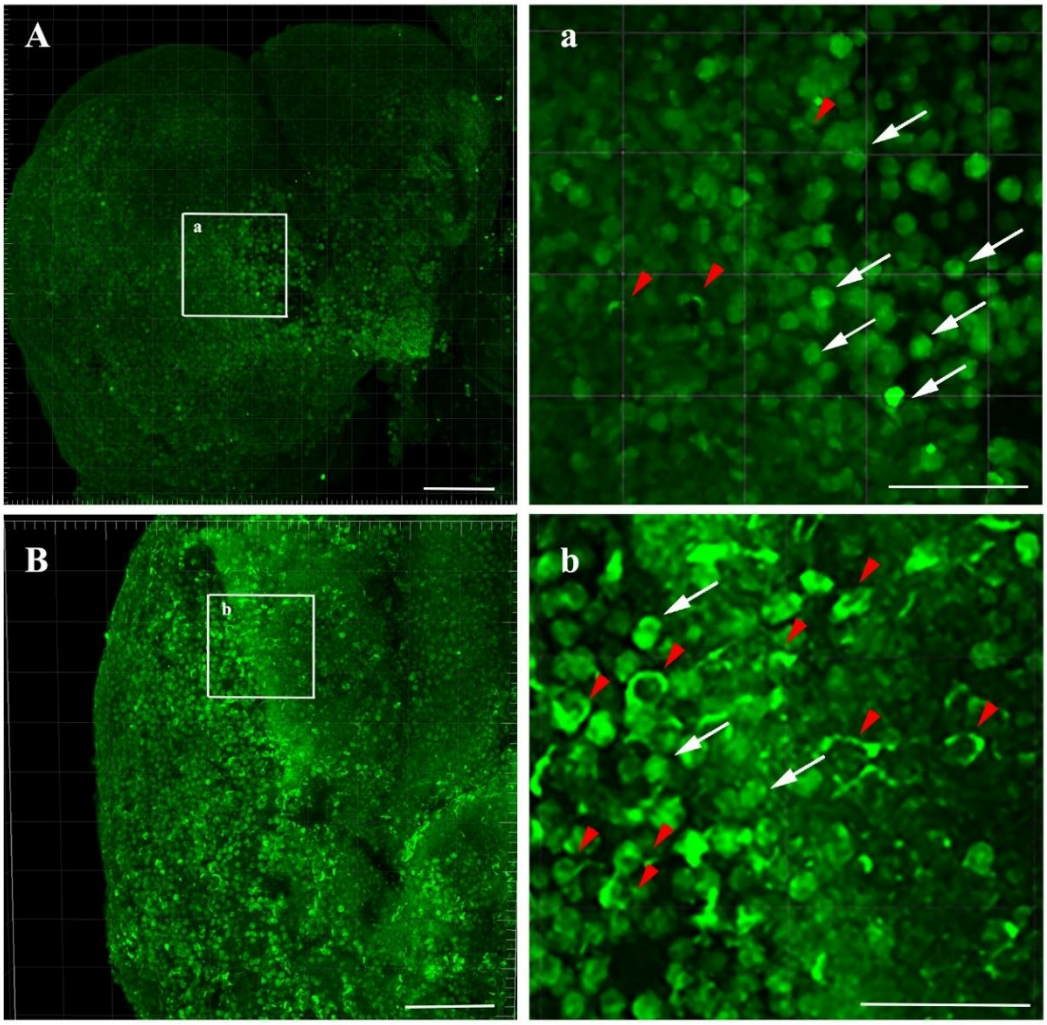

Fig. 12: Whole mount staining of TDP-43 in *Nothobranchius furzeri* brains. Using AbSca/e clarification protocol we were able to observe TDP-43 expression in whole mount brains of young and old *Nothobranchius furzeri*. In this images telencephalic regions are shown and it is clear how the number of doughnut-like cells (red arrowheads) is greater in old telencephalon (panel B) compared to the young sample (panel A). Scale bars correspond to 50 µm in each panel.

To assess the precise subcellular localization of TDP-43, I run a double immunofluorescence with Nup, an antibody against the nucleoporin complex (Fig.13). I was able to identify doughnut-like cells in all brain major areas (telencephalon, optic tectum, cerebellum and rhombencephalon). The localization of TDP-43 appears mainly intranuclear, with the rest cytoplasmatic in close proximity to the nuclear envelope.

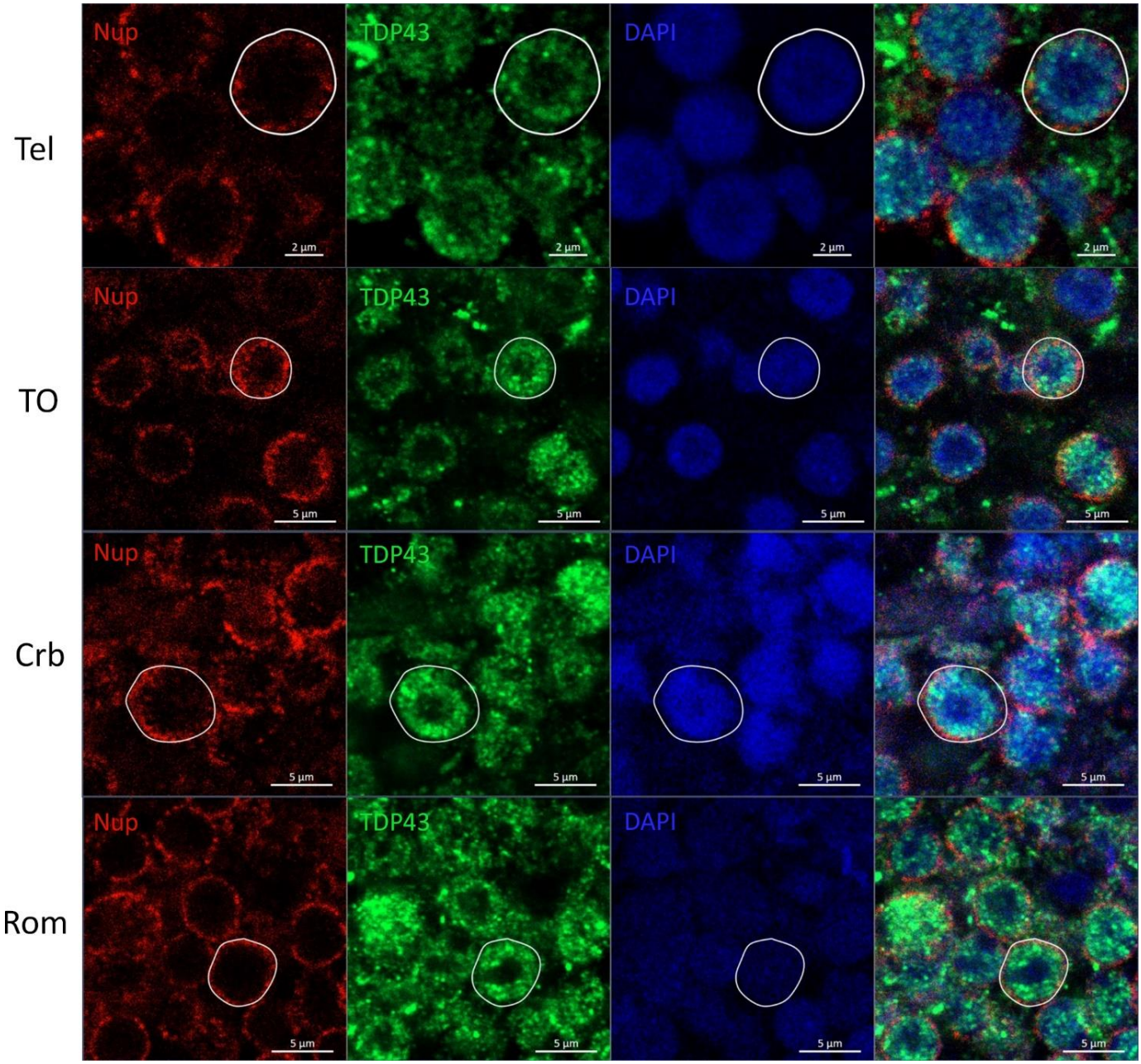

Fig. 13 : Subcellular localization of TDP-43 in doughnut-like cells. We were able to find presence of doughnut-like cell in all major brain areas of old animals. The majority of TDP-43 stain in these cells is located internally to the nuclear envelope as highlighted by the white circle drawn around Nup (Nucleoporin) staining. The rest of TDP-43 staining is cytoplasmatic, partially located in close proximity to the nuclear envelope. Tel= telencephalon, TO= optic tectum, Crb= cerebellum, Rom= rhombencephalon. Scalebars indicates 2 µm in the first row and 5 µm in all the others.

I then performed a double staining, by combining TDP-43 immunofluorescence (Fig. 14, 15 green) with the Aggresome dye (Fig. 14, 15 red), to discriminate between generic protein aggregates and specific TDP-43 aggregates, visualized as co-localized green-red fluorescent dots. Comparison of sections from young and old brain tissues showed the presence of several double stained TDP-43 granules in the old tissue (Fig. 14B, b red arrowheads). Some of the granules were strictly associated to doughnut-like cells. In contrast, consistent with our previous results (Kelmer Sacramento et al., 2020) we were unable to detect aggregates in the young brain tissue, either with or without TDP-43 staining (Fig.14 A). The red fluorescent signal detectable in the young tissue was not a specific Aggresome staining, but it was to ascribe to auto-fluorescent blood vessels and erythrocyte cells as it is evident in all fluorescent channels.
These results demonstrate that it is possible to follow ageing-related aggregation of TDP-43 in *N. furzeri* mimicking the neuronal alterations typical of ALS/FTD and supported the killifish as a convenient model of TDP-43 aggregation in vertebrates with compressed lifespan.

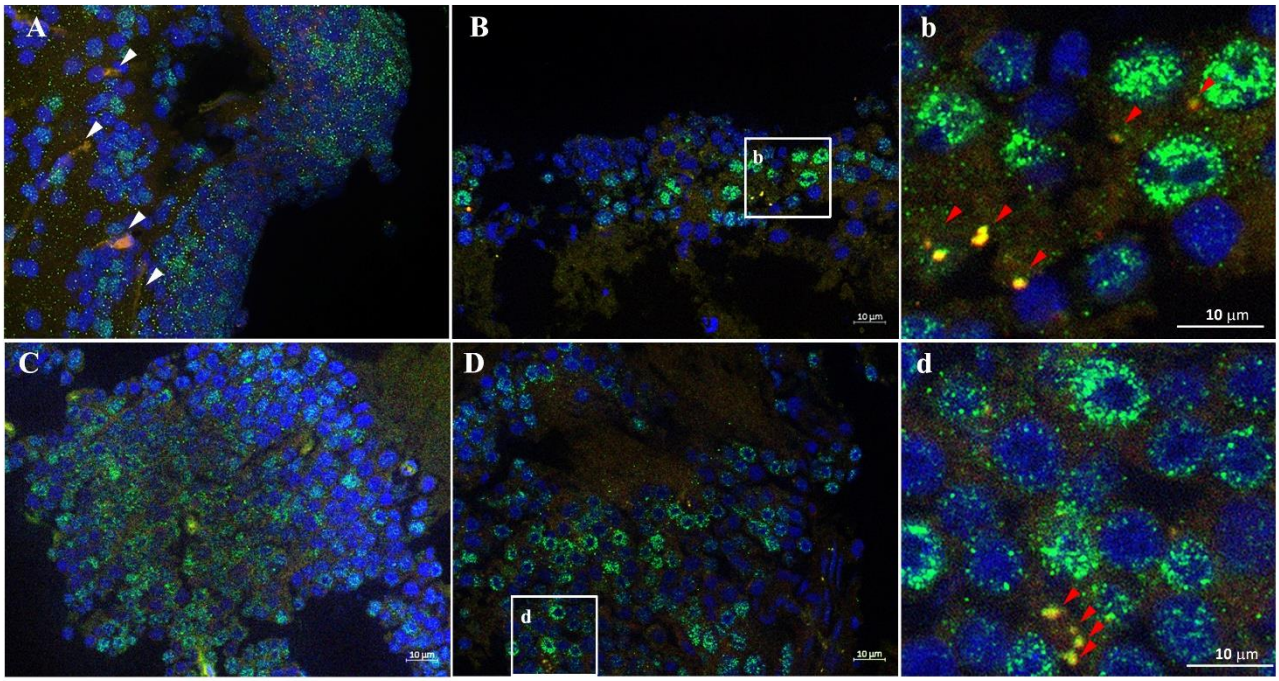

Fig. 14: Immunostaining of TDP-43 and colocalization with protein aggregates in old versus young *Nothobranchius furzeri* brains. Protein aggregates were stained using aggresome dye (red), while TDP-43 was labelled with the monoclonal antibody (green). Both in telencephalon (panels A/B) and optic tectum (panels C/D) we were able to observe aggregates presence in old brains only (panels B/D) while no trace of aggregation was detectable in young samples (panels A/C). Moreover, TDP-43 staining often colocalize with aggregates signaling, and such aggregates appear to be localized mainly near doughnut-like cells (b/d magnifications, red arrowheads). White arrowheads in panel A indicates blood cells autofluorescence. Scale bars indicate 10 µm.

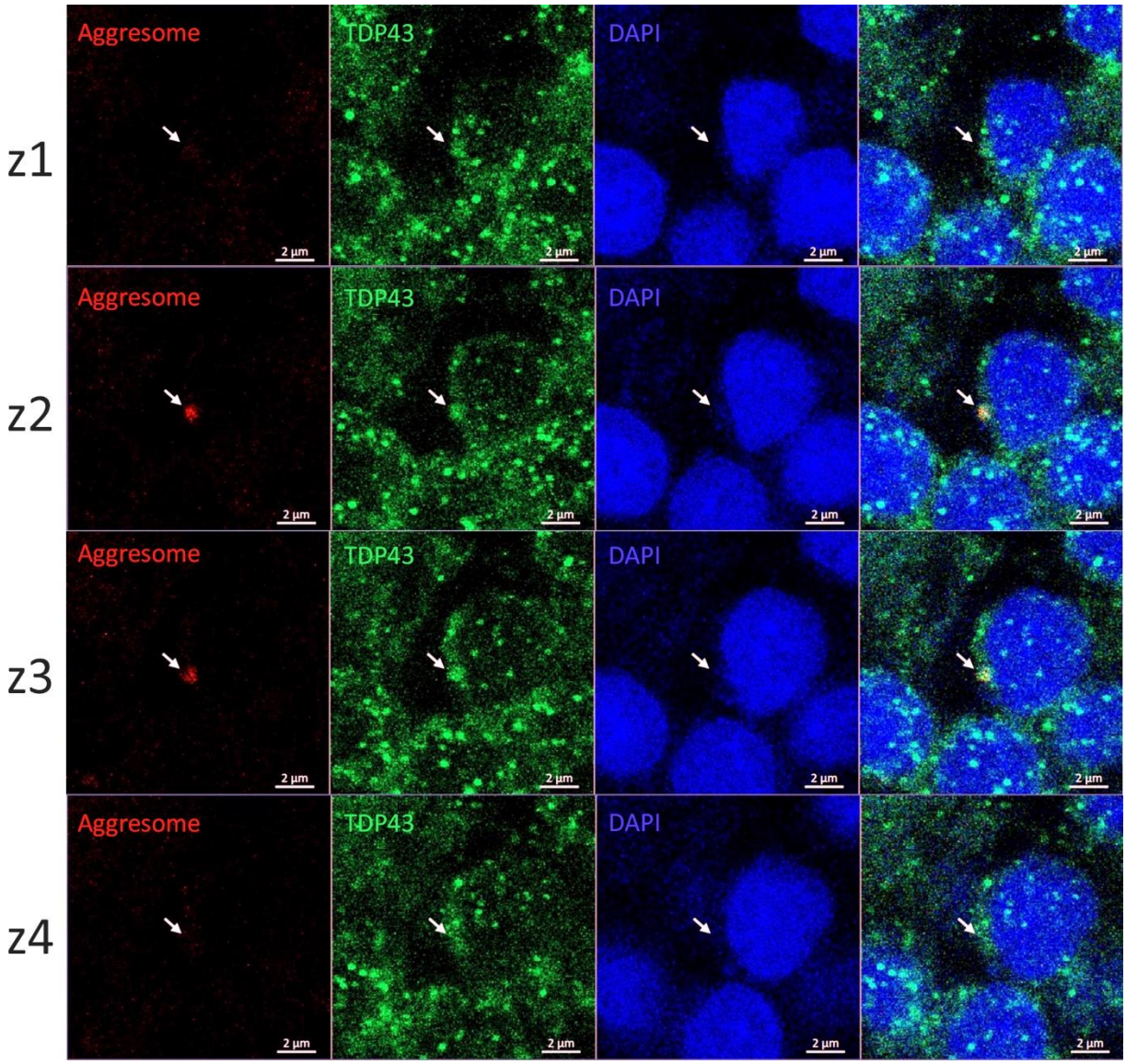

Fig.15 High resolution images of TDP-43 in aggregates. We were not able to find signs of aggregation in young animals. In old animals some aggregate colocalize with TDP-43 (white arrow). The z represents four consecutive planes acquired along the z axis, each acquired at 1µm step from the previous. Scale bars indicate 2 µm.

Seen the interesting relationship between TDP-43, stress granules and aggregation discussed in the introduction, I investigated the possible co-localization of TDP-43 with stress granules in *N. furzeri* tissues. To do so, I performed double immunostaining for *furzeri* TDP-43 and G3BP, a core protein of the stress granules often used as a marker (Martin & Tazi, 2014). The labelling for G3BP was more widespread than that of TDP-43 both in telencephalon and optic tectum, being the signal distributed widely in the cytoplasm of the majority of cells (Fig. 16). We were nonetheless able to observe the presence of granular structures double-labelled for G3BP and TDP-43 in samples of both young and old animals. This evidence supports the idea that a TDP-43 involvement in stress granules formation and regulation is conserved in *N. furzeri*. Even more importantly, the amount of granules containing TDP-43 inclusions seemed to be greater in the samples from old animals (Fig.16 insert, white arrowheads, Fig.17**)**. This is consistent with the idea of an increase of stressing conditions during ageing and thus an increased formation of stress granules inside the cell. Accurate quantification of this visible difference was not attempted for the time being.
These exciting results demonstrate the possibility to study granule formation in *N. furzeri*.

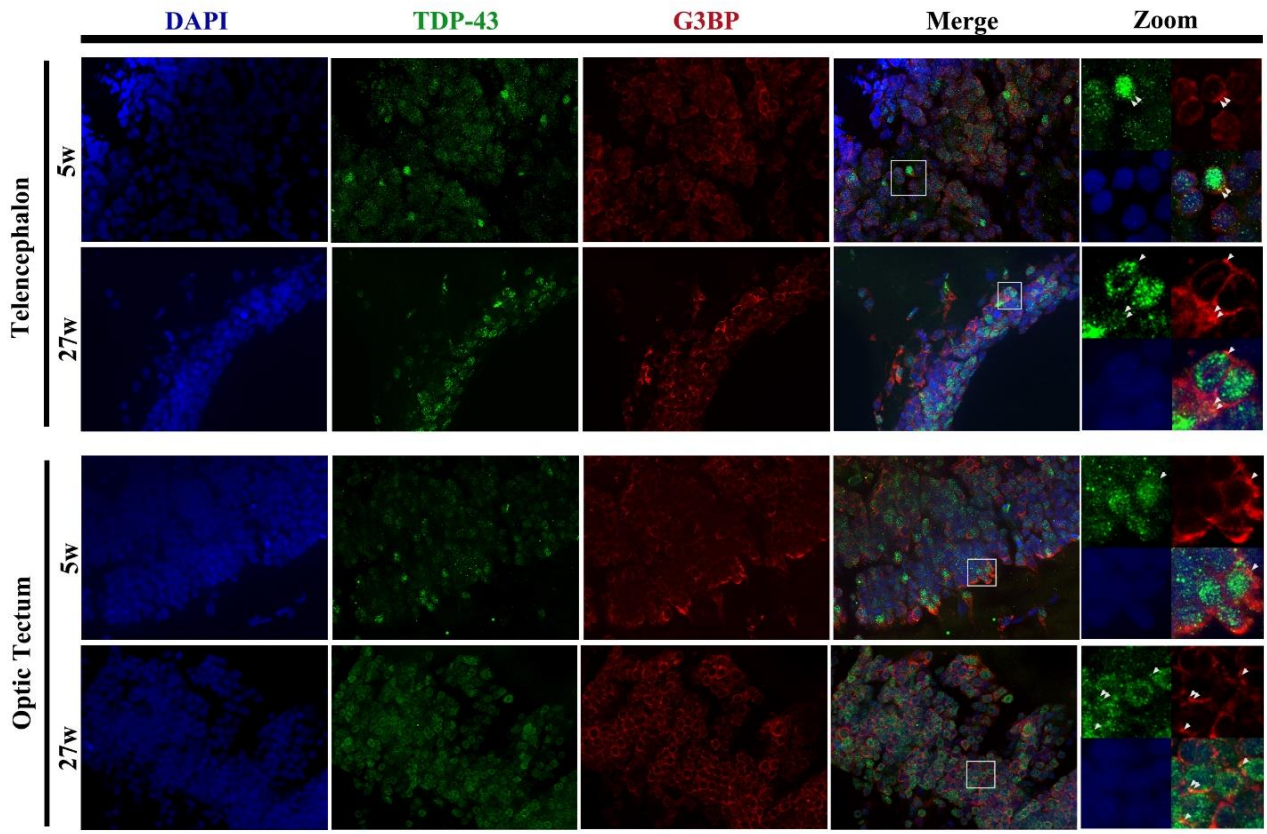

Fig. 16: Immunostaining and colocalization of TDP-43 (green) and G3BP (red). We were able to observe several cells showing partial overlapping signal between TDP-43 and G3BP (white arrowheads), used here as Stress Granules marker. SG are present both in young and old tissues and are visible in both the optic tectum and telencephalon.

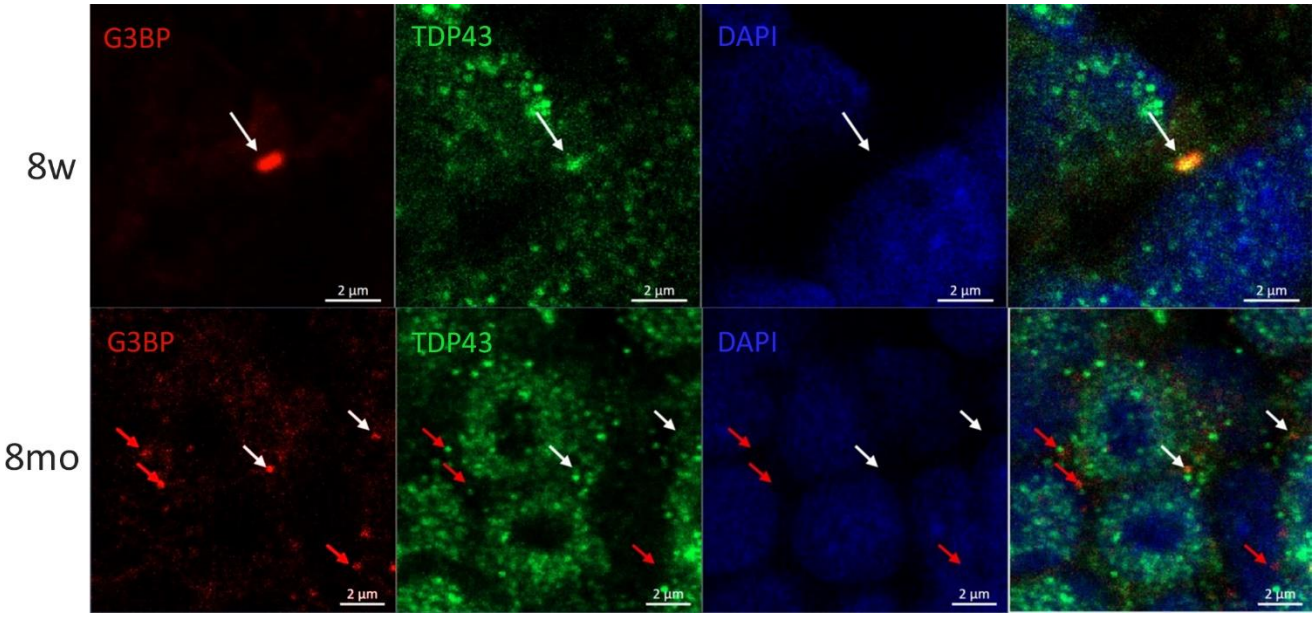

Fig.17: High resolution images of localization of TDP-43 in stress granules (SG). We found presence of SG both in young and old samples. Some SG colocalize with TDP-43 (white arrows). The ones not colocalizing (red arrows) are located in close proximity to TDP-43. Scale bars indicate 2 µm.

3.4 Establishment of *N. furzeri* brain organotypic cultures to study ageing ex-vivo

To perform long term culturing, I operated in strictly sterile conditions under a hood (Fig. 18) to extract the brain of young (5-weeks old) fish and I manually cut coronal slices of approximatively 500µm width with the aid of a micro-knife and a micrometric slide (Fig. 19). The slices were then immersed briefly (1-2s) in three consecutive wash of antibiotics (Pen-strep 1%) to maintain sterility of the tissue and gently placed onto a semipermeable membrane located into a six well plate (Fig. 19). The slices were then incubated at 27°C with a CO_2 tension of 5%, and an ad-hoc medium was changed every second day.

Fig.18: Experimental setup for organotypic slice preparation. All procedures were performed under a sterile horizontal flux hood to avoid sample contamination.

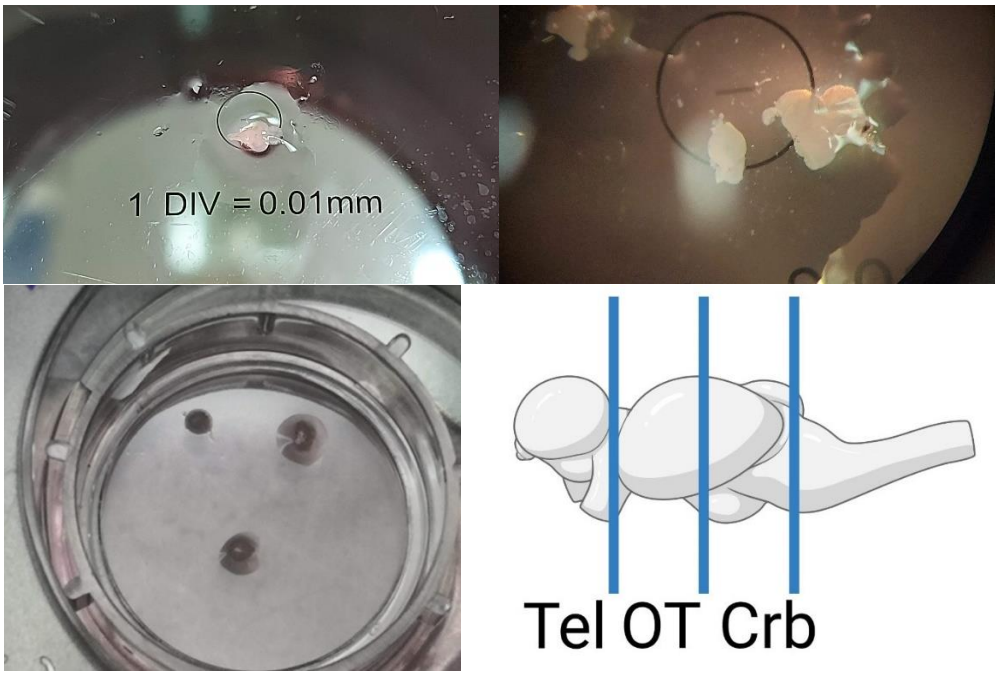

Fig.19: Organotypic slices cut and placement. Extracted *N. furzeri* brains are placed on a micrometric slide and approximately 500µm thick slices are cut. After three washes in Pen-Strep, the slices are carefully laid onto the semiporous membrane inserted into a six well plate containing the culturing medium. Slices were cut from Telencephalon (Tel), *Optic tectum* (OT), and Cerebellum (Crb).

Slices were obtained from telencephalon, mid-brain/optic tectum and hindbrain/cerebellum (Fig. 19). Viability of slices was inspected visually during regular medium changes. Healthy brain slices become thinner and spread over the surface becoming attached and more translucent after a couple of days in culture. Slices that acquire a milky-white appearance and fail to attach to the membrane were discarded. Moreover, the macroscopic structure of the tissue could be easily recognized utilizing an inverted microscope in healthy slices (Fig. 20).

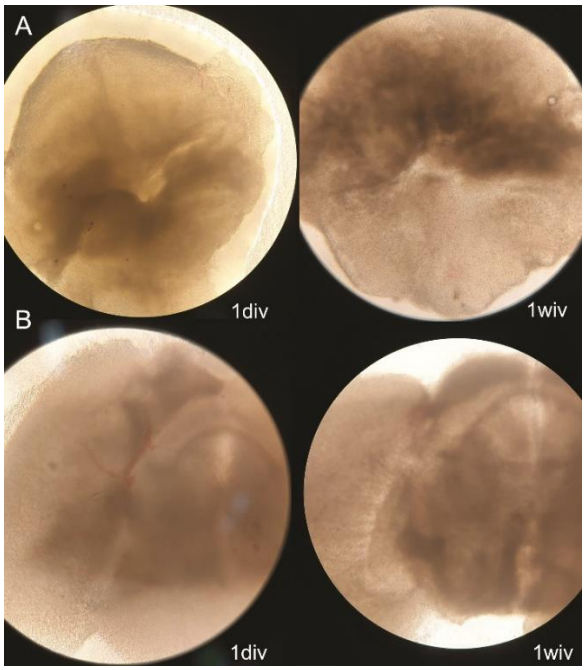

Fig.20: Examples of organotypic slices of cerebellar-pontine area (panel A) and optic tectum area (panel B) at 1 day *in vitro* and 1 week *in vitro*.

To assess neuronal survival, I performed whole-mount immunofluorescence on slices cultured for different times (wiv: weeks *in vitro*). Specifically, I decided to assess preservation of the *Locus coeruleus* in cerebellar-pontine slices, taking advantage of the ease in isolating the anatomic area containing this nucleus (i.e., taking as point of reference for the cut the anterior and posterior margins of the cerebellum) and of the already well-tested immunofluorescence procedure for TH. I observed slices at 1wiv, 3wiv and 5wiv and in all three time points I was able to observe fluorescence signal identifiable as *Locus coeruleus* cells (Fig. 21,22), demonstrating that these cells were able to survive up to 5wiv in healthy-looking slices. I initially cultured 6 slices per experimental group, unfortunately though, the number of slices that survived was too low to allow a statistical analysis of cell survival (3 slice per group).

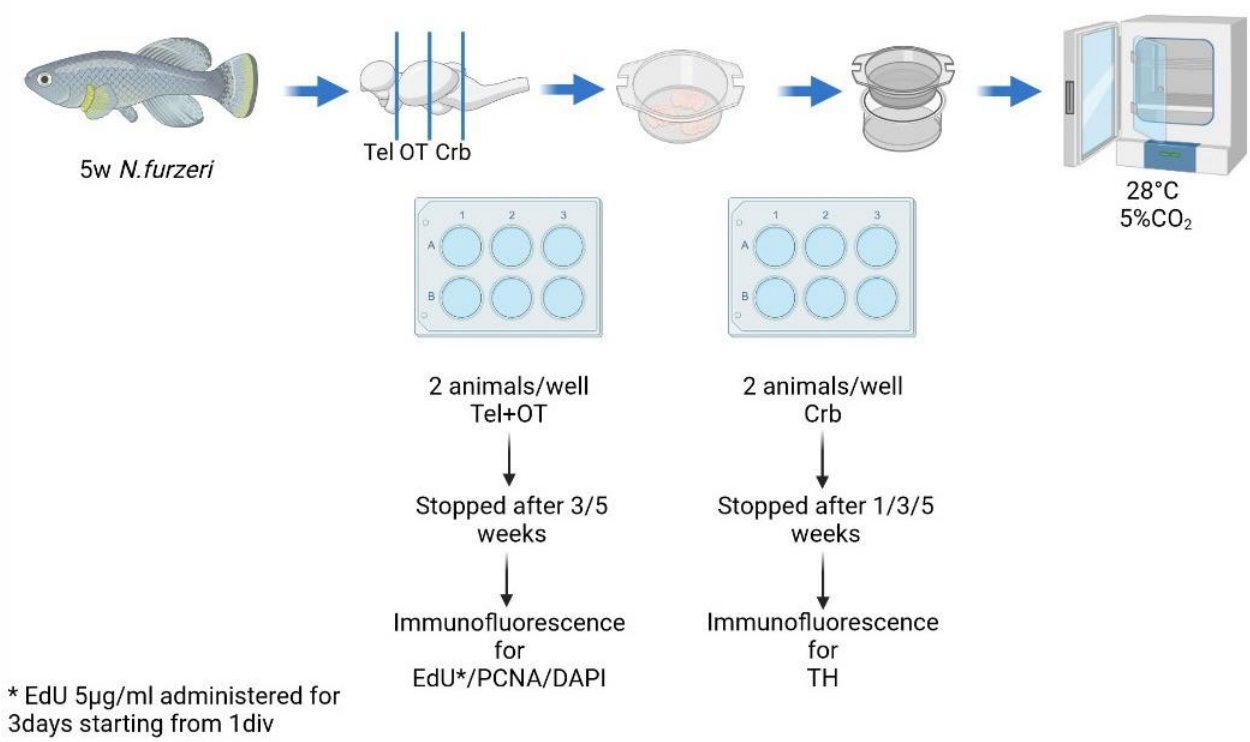

Fig.21: First experimental design of *N. furzeri* organotypic slices. Div: days *in vitro.*

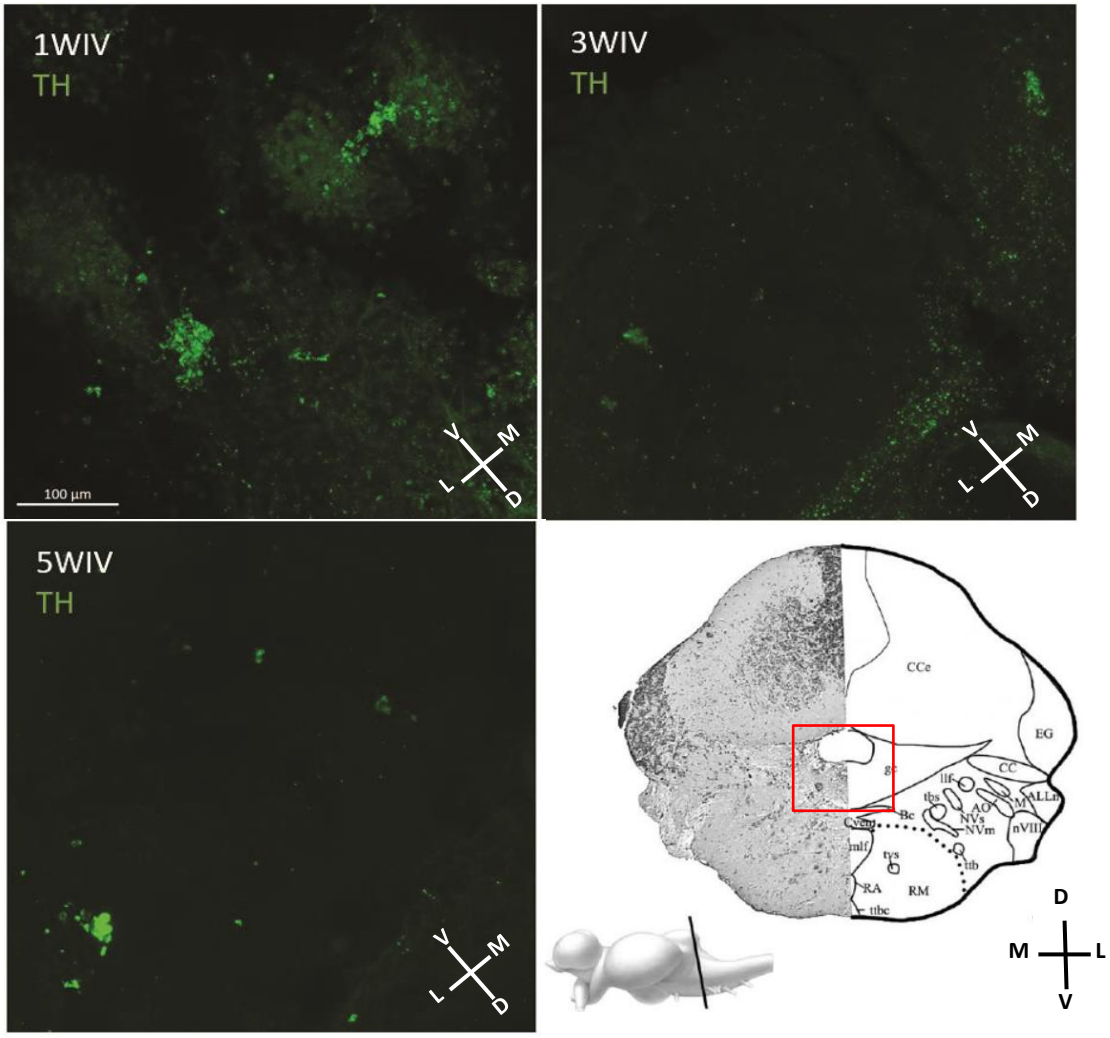

Fig.22: Examples of *Locus coeruleus* cells imaged from *N. furzeri* organotypic slices of 5w old animals after 1, 3 or 5wiv. Anatomical reference modified from D'Angelo 2013, in red highlighted the area of imaging. D=dorsal, V=ventral, L=lateral, M=medial. Scale bar indicates 100 µm.

Adult neurogenesis is widespread in the killifish brain (Tozzini et al., 2012). I decided to analyze adult neurogenesis in optic tectum and telencephalon using EdU staining. EdU is a thymine analog that is incorporated in the DNA during replication and can be easily visualized in tissue slices. EdU was previously used in my group to identify adult neurogenic niches in *N. furzeri* (Tozzini et al., 2020). In order to do so, EdU at a concentration of 5µg/ml was administered for three consecutive days starting from 1div (div: days in vitro) and then samples were analyzed at 3wiv and 5wiv (Fig. 23). In both cases, I was able to observe EdU staining. To label the neurogenic niches, I used PCNA as a marker (Tozzini et al., 2012). The EdU positive cells are displaced from the PCNA positive area; this phenomenon is also visible *in vivo* (Tozzini et al., 2012), and indicates that, after their terminal division, the EdU cells have survived for at least five weeks. This observation leads to the conclusion that also in organotypic slices, the tissue is able to grow and organize in similar fashion to what is observed *in vivo*.

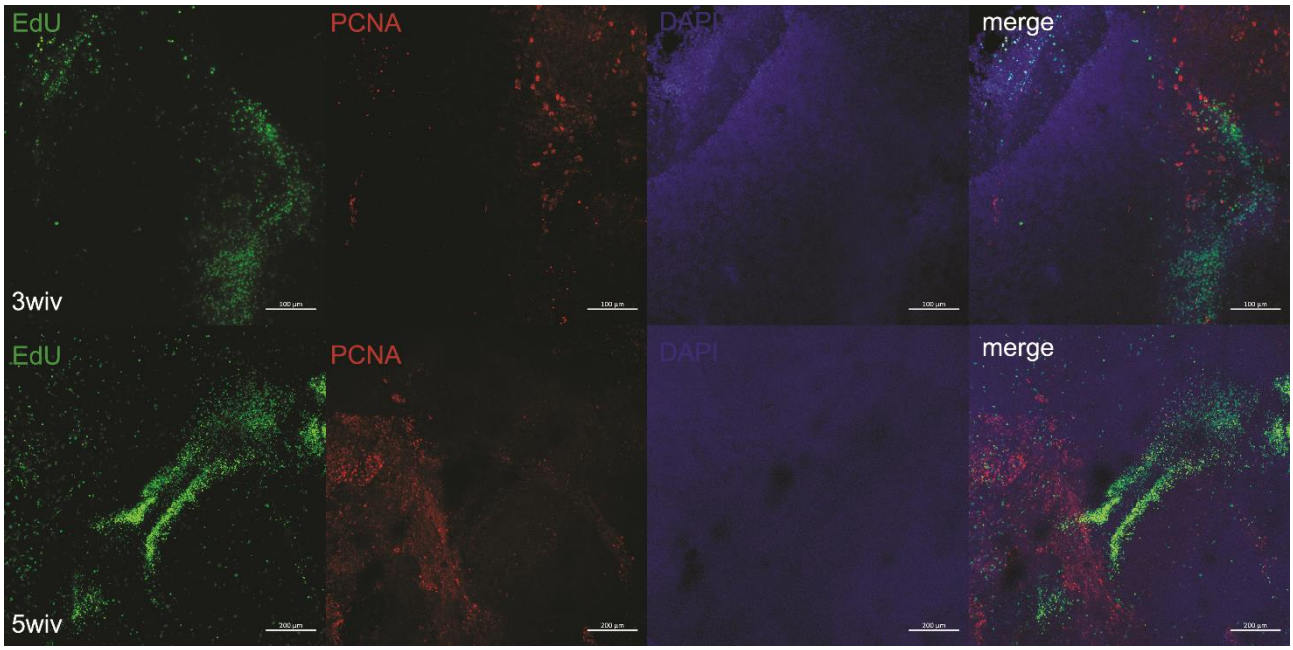

Fig.23: Optic tectum organotypic slices from 5weeks old animals at 3viw. I was able to perform PCNA and EdU staining and migration of EdU stained cells apart from the PCNA positive is clearly visible. Scale bars indicates 100 µm on the first row and 200 µm on the second row.

I also tried to perform organotypic culturing of tissues taken from old animals (30 weeks of age). Also in this case, I performed immunofluorescence for TH in cerebellar-pontine slices and EdU staining in optic tectum and telencephalic slices.
I started from 6 slice per group but, having utilized much older tissues their survival was greatly reduced; pontine-cerebellar slices lasted in culture approximately two weeks before starting to show signs of degeneration. At the end only 2 slices per group were in good enough state to be imaged.
Again, I was able to observe *Locus coeruleus* cells also in old tissues after 2wiv (Fig. 24) and I was able to observe and identify neurogenic niches as observed from in vivo tissues (Fig. 25).
The results showed in this section are obtained from my first attempt at culturing organotypic slices. Therefore, there is still the need to optimize the technique and attempt again these experimental setups prior to publication.

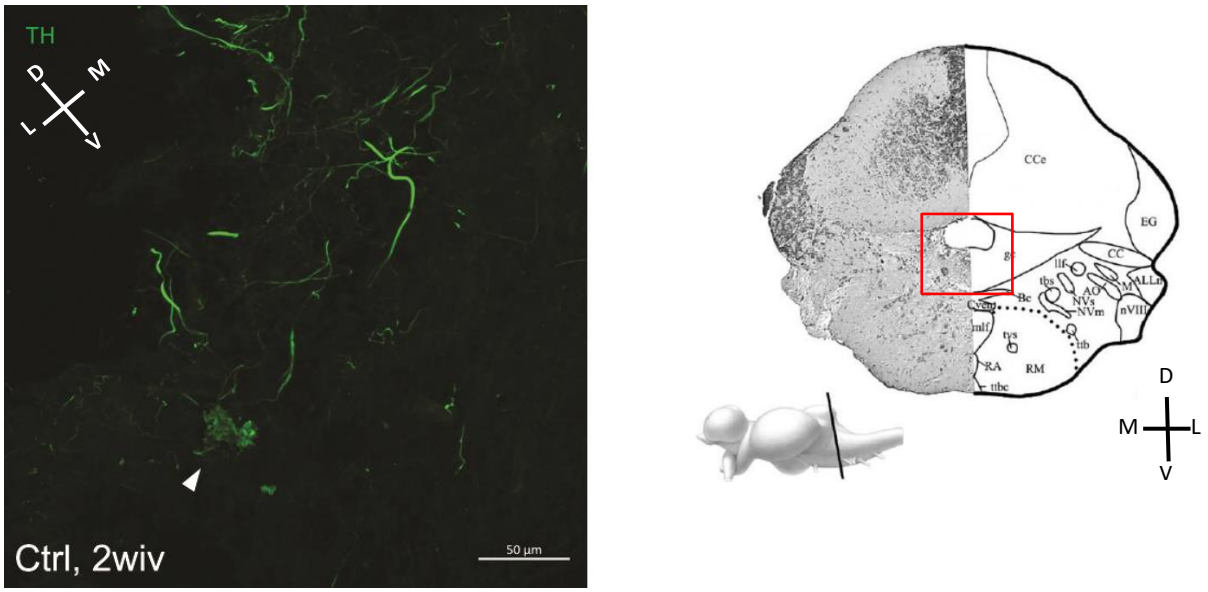

Fig.24 Example of *Locus coeruleus* cells (white arrowheads) in *N. furzeri* organotypic slices taken from 30w old individuals and imaged after 2 wiv. Anatomical reference modified from D'Angelo 2013, in red highlighted the area of imaging. D=dorsal, V=ventral, L=lateral, M=medial. Scale bar indicates 50 µm.

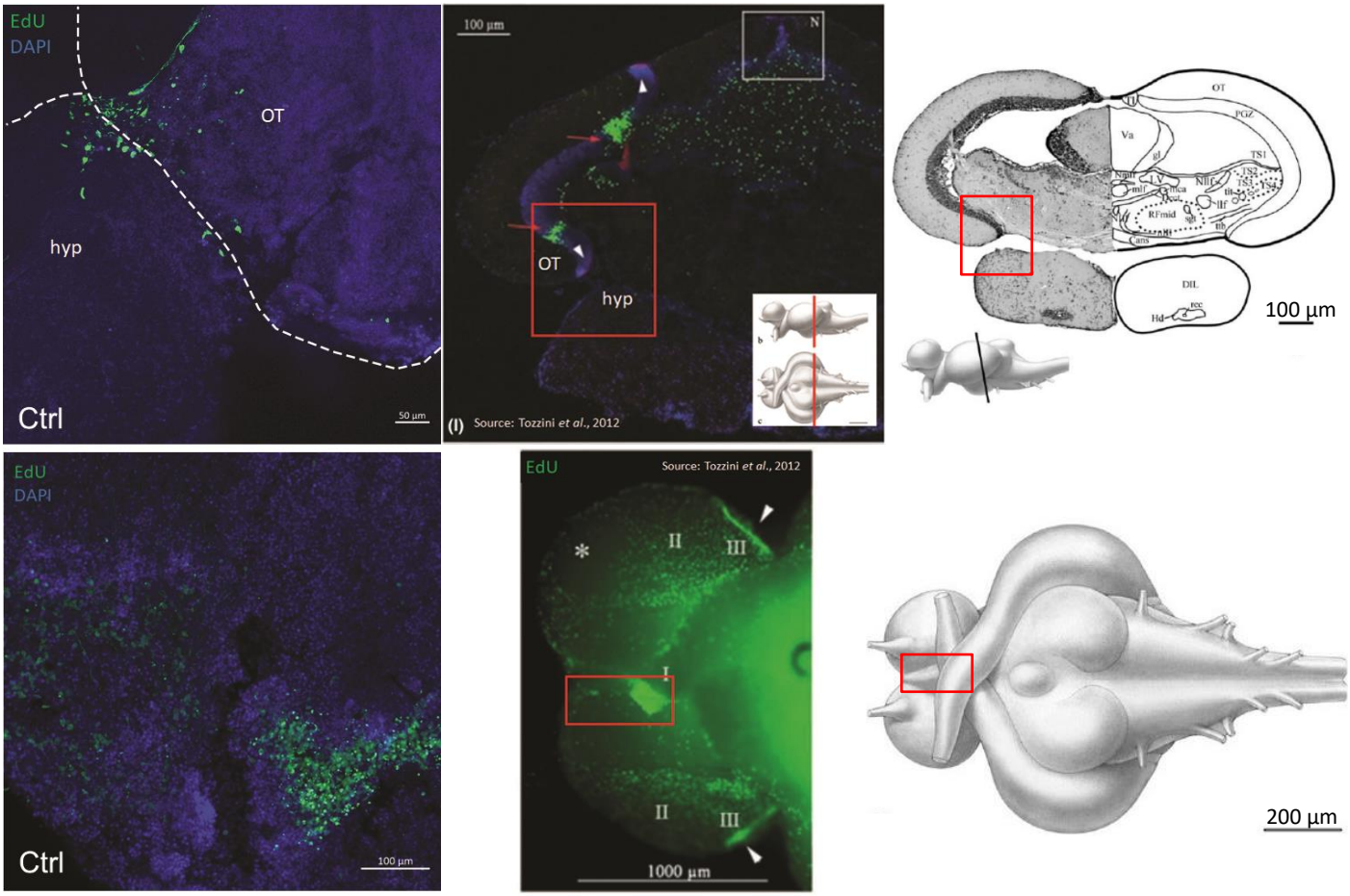

Fig.25 Optic tectum and Telencephalon organotypic slices from 30w old animals maintenance of adult neurogenic niches. On top row an optic tectum slice and comparison with neurogenic niches observed in vivo (modified from Tozzini et al., 2012, anatomical reference form D'Angelo 2013). In red is highlighted the correspondent area observed in the organotypic slices. On bottom row examples of a telencephalic organotypic slice and comparison with the corresponding neurogenic niches observed in vivo (modified from Tozzini et al., 2012, anatomical reference form D'Angelo 2013). In red is highlighted the correspondent area observed in the organotypic slices.

4. Discussion

In this thesis, I present data indicating that teleost *Nothobranchius furzeri* is a pertinent model to study physiological protein aggregation in the aging brain as well as aggregation of disease-related proteins.
I first showed that protein aggregates colocalizing with lysosomal markers accumulate with ageing in *N. furzeri* and contain ribosomal proteins. I then analyzed specific protein aggregate that are related to neurodegenerative diseases, like PD and FTD. I observed that some aspects of these diseases, that normally require genetic or toxicological interventions to be modelled in rodents or teleost, can be observed spontaneously during *N. furzeri* aging. Specifically, neurodegeneration and presence of pS129 immunoreactivity was observed in cell bodies of the *Locus coeruleus*, one of the areas that are preciously affected by PD in humans, and an increase of abnormal distribution of TDP-43 surrounding the nuclear envelop, reflecting some aspects of human pathological TDP-43 behavior. Finally, I developed an organotypic culture protocol to exploit the rapid physiological ageing of *Nothobranchius* enabling *ex vivo* studies of age-associated phenotypes in the brain.
The combination of these results clearly establishes *N. furzeri* as an experimental model of age-dependent protein aggregation.

Note: Part of the following discussion is modified, expanded and adapted from the following publications (complete citations for published articles and preprints are listed in the references):
Discussion 4.1 (Kelmer Sacramento et al., 2020)
Discussion 4.2 (Bagnoli et al., 2021), currently under review in Aging Cell
Discussion 4.3 (Louka *, Bagnoli * et al., 2021) * authors have contributed equally to the paper, revised version ready for submission to Aging Cell

4.1 Aggregates enriched in ribosomes forms during *N. furzeri* ageing

In our paper (Kelmer Sacramento et al., 2020), we showed that protein aggregates accumulate with age in mouse brain lysates as shown by biochemical fractionation and purification of SDS-insoluble precipitates. Enrichment for ribosomal proteins in aggregates was then detected using mass-spectroscopy based proteomics. I confirmed these data using staining techniques on brain sections. Firstly, I used a general fluorescent staining for aggregated proteins, and this revealed the presence of large intracellular aggregates in the telencephalon. These aggregates colocalized with lysosomal markers and therefore were likely the result of a failure of lysosomal degradation. Many different lines of evidence point to a lysosomal dysfunction in aging (Colacurcio & Nixon, 2016; Glaser et al., 1994; Nixon, 2020). Lipofuscin, an autofluorescent form of aggregates, is a universal marker of aging and it is known to accumulate in lysosomes. Up-regulation of transcripts coding for lysosomal proteins is a highly-reproducible transcriptional marker of aging (Aramillo Irizar et al., 2018; de Magalhães et al., 2009). This regulation likely represents an abortive compensatory response since lysosomal pH increases with age impairing proteolytic activity (Nixon, 2020) and we observed a stochiometric imbalance in the components of the V-type ATPase that certainly impairs its function (Kelmer et al., 2020).
To confirm that aggregation of ribosomal proteins in *N. furzeri,* I performed immunofluorescence analysis that revealed presence of aggregates in old tissues that resulted positive for RPS6 protein. It was recently shown that aggregates of disease related proteins such as Tau and Huntingtin are heterogeneous and contain ribosomal proteins (S. Banerjee et al., 2020; Gruber et al., 2018) and that ribosome aggregation can be induced also by acute injury such as ischemia (F. Zhang et al., 2006). On the other hand, impaired protein synthesis is a recognized early marker of neurodegeneration (Halliday et al., 2015; Radford et al., 2015). Therefore, ribosomal impairment and aggregation delineate yet another link between normal aging and neurodegeneration. It is already well established that loss of proteostasis is one of the main features of ageing (Alavez et al., 2011; Kaushik & Cuervo, 2015; Ray, 2017) and how this is also strictly related to neurodegenerative diseases (Cox et al., 2020; Francisco et al., 2020; Hou et al., 2019). The ribosome translational machinery is obviously a pivotal point in the production and maintenance of protein balance and therefore a loss of its stoichiometry and/or its sequestration in aggregates could lead to an inevitable imbalance of proteostasis. Moreover, ribosomal proteins are the most abundant proteins in the cytoplasm (Beck et al., 2011) and an imbalance in their synthesis and homeostasis has an impact on the entire energy state of the neurons.
The conservation of this process between mice and *Nothobranchius furzeri* could thus be used as a foundation to justify the attempt at using this novel animal model to study further aggregation and aggregation-related pathologies, taking particular advantage of the short life duration of *N. furzeri*, allowing us to analyze the relationship between ageing, aggregation and neurodegeneration in a way that is similar to what is observed during physiological ageing in humans.

4.2 Parkinson-like pathology in *N. furzeri*

In our paper (Bagnoli et al., 2021 under review), we report an age-dependent degeneration of noradrenergic neurons in the *Locus coeruleus*, but not of dopaminergic neurons in the *posterior tuberculum*, a brain region supposed to be the homolog of mammalian A8 and A9 dopaminergic populations. The results of my analysis contrasts with the results of a recent paper by Matsui et al. (Matsui et al., 2019) who report loss of noradrenergic and dopaminergic neurons in *N. furzeri* and a down-regulation of TH expression in homogenates from the whole brain. Two main factors may account for this discrepancy. In the first place, I used a different counting method and instead of counting cells in thick sections, I clarified the entire brain and reconstructed the nuclei of interest in their entire 3D extent. Since *N. furzeri* brain grows considerably during adult life and cells belonging to the *posterior tuberculum* shift and distribute along the rostro-caudal axis accordingly, it may be possible that a sampling protocol that identifies all cells in young animals may under sample the same cells in older animals. Indeed, my 3D reconstructions show that dopaminergic neurons of the *posterior tuberculum* are more widespread in brains from old fish. A second possibility is the existence of genetic differences between the two strains. Even if the population MZCS-222 we analyzed here and the population MZCS-24 analyzed by Matsui et al. are part of the same genetic clades and the distance between the two collection points is around 50 km (Cellerino et al., 2016), it cannot be formally excluded that the subtle genetic differences between the two stocks may have an impact on dopaminergic neuron maintenance. Lacking access to the population MZCS-24, I cannot exclude this possibility. Yet, our results exclude that degeneration of dopaminergic neurons is a general trait of wild-type *N. furzeri*.
To assess whole brain TH abundance Matsui et al. showed Western Blot data from pooled animals, while in our study I report both the results of individual and pooled samples and the results are supported also by non-targeted approaches such as RNA-seq and Mass-spectrometry based proteomics. I did not find any evidence for a down-regulation of TH expression, instead I found indications of an increase of TH abundance concentrated between 5 and 8 weeks of age. This can be explained with the growth of the body and brain size of the fish, together with the still high rate of neurogenesis present in this timeframe (Tozzini et al., 2012 and Results Fig. 2); it is thus reasonable to think that areas containing a very high number of TH+ cells such as olfactory bulb (Results, Fig. 3) and vagal nuclei (Results, Fig. 4) are still susceptible to an increase during this growth phase. Conversely areas containing a relatively low quantity of TH+ cells such as LC and *posterior tuberculum* seem to have already reached their full growth in terms of TH+ cell abundance at 5 weeks of age as indicated by absence of increase of cell number of such areas between 5 and 12 weeks of age (results, figure 5C). The lack of statistically significant reduction of TH protein expression in old age can be explained with the same reasoning: the presence of a large number of TH+ cells in other brain regions would make the impact of a specific loss of LC and *posterior tuberculum* neurons negligible on the abundance of TH in the whole brain.
Neurodegeneration is associated with accumulation of the pathogenic post-translational modification pS129 (Samuel et al., 2016). The condition we describe, with accumulation of pS129 is reminiscent of the prodromic, pre-symptomatic stages of PD as described by (Forno et al., 1969, Braak et al., 2003, Dickson et al., 2008) that show staining with α-Syn in the vagal nuclei and *Locus coeruleus* that precedes the degeneration of dopaminergic neurons and the onset of motor symptoms. Recently, it has been proposed that liquid-liquid phase separation could be the initial mechanism of α-Syn nucleation, and it has been demonstrated in vitro how a phosphomimetic mutation (S129E) increases the rate of liquid-droplet formation and reduces the critical concentration of protein required for the beginning of the phase separation (Ray et al., 2020), in accordance with the notion that phosphorylation of Serine 129 site is critical for aggregation of α-

Syn (Samuel et al., 2016). In our case, I was not able to observe the canonical Lewy body formations inside *Locus coeruleus* cell bodies, but what I observed is reminiscent of what is described in phase liquid-liquid separation studies; the pS129 staining is indeed punctuate and very disperse in all cytoplasm, moreover its staining does not overlap with aggresome staining, supporting further the hypothesis that this state may correspond to an initial conformation change that precedes the formation of aggregates.
In summary, from my observations, *N. furzeri* shows a condition that is more reminiscent of the presymptomatic stage of PD than the full blown out pathology. This is somewhat expected since the animal I have used are 'normal ageing' animals and have not been selected based on particular phenotypic evidence. This reflects also what is observed in humans; not all humans showing Lewy body or α-Syn aggregation are affected by PD (Dickson et al., 2008; Forno, 1969; Fumimura et al., 2007), and this suggests that indeed for PD, but reasonably for most neurodegenerative diseases, the definition of pathology is strictly related to symptoms appearance and those become evident only after a certain threshold of damage/aggregation/neurodegeneration has already occurred in the brain. We therefore should be very careful on defining pathology based only on histopathological signs, and we should take in great consideration also eventual behavioral signs. However, these considerations should not refrain us to study early stages of aggregation and neurodegeneration. Even if these signs are not sufficient to be considered pathological without the presence of other functional symptoms, is indeed undeniable that those are the first steps toward the development of the pathology itself. Moreover, the initial phases leading to neurodegenerative diseases are the less known since, in humans, studies are performed only after the emergence of the symptoms or on *postmortem* samples, when the disease is already established, and animal models often use toxic agents or uncontrolled overexpression of mutated genes to achieve pathological or behavioral signs somewhat reminiscent of human pathology. Therefore, analyzing how aggregation begins, how it worsens and become pathological is of extreme relevance. In this aspect, *N. furzeri* could represent the perfect model to study the emergence of aggregation and neurodegeneration, and to identify modifying factors responsible for pathological transition, being short-lived, having an ageing process highly conserved with that of mammals and being at the interface between ageing-related pathology development and normal ageing.

4.3 TDP-43 age-dependent aggregation in *Nothobranchius furzeri*

In our manuscript (Louka, Bagnoli et al., 2021 under review), we laid the foundations for the use of *N. furzeri* as a new animal model to follow the age-dependent aggregation of TDP-43.
In silico and *in vitro* analysis conducted on the purified *N. furzeri* TDP-43 showed and supported that the properties of nucleocytoplasmic transport, RNA and DNA binding and phase separation should be conserved. We also observed that the C-terminus has a strong tendency to aggregate in agreement with what has been observed for the human protein (Capitini et al., 2020; Vega et al., 2019).
If proteins from organisms as far apart as human and killifish retain a similar tendency to aggregate and misfold, the property must be inherent to the protein and its function.
In parallel to these *in silico* and *in vitro* studies conducted by our collaborators, I carried out an *ex vivo* investigation in animal tissues to test whether TDP-43 can form aggregates also in the animal and/or behaves differently in young and old fishes. Using immunofluorescence experiments, I proved that *furzeri* cells may show an abnormal distribution of nuclear TDP-43 (doughnut-like cells) that increases markedly during ageing. This could be interpreted as a sign of impaired nucleocytoplasmic transport, which does not come as a surprise since dysfunction of nucleocytoplasmic transport is often associated to neurodegenerative diseases and is also observed in physiological ageing (Hutten & Dormann, 2020). TDP-43 neurotoxicity in neurodegenerative disorders could thus be linked to a loss of function of nuclear TDP-43 (Xu, 2012) and, more in general, to dysfunction of nucleocytoplasmic transport.
I was then able to observe protein aggregates exclusively in old brain tissues as expected from our previous results (Kelmer Sacramento et al., 2020). Some of these aggregates were positive to TDP-43 staining and strictly associated to doughnut-like cells. This behavior, summed to my other observations, allows me to conclude that *N. furzeri* is indeed able to form intracellular pathological aggregates *in vivo* and strengthened the interpretation of doughnut-like cells as a pathological condition that can, in the future, be used as a marker to identify aged animals.
I also demonstrated co-localization of TDP-43 and G3BP, both in young and old animals, confirming that the interaction between TDP-43 and stress granules is a common feature also in *N. furzeri*. It has been shown that stress granules impair nucleocytoplasmic transport and that suppression of stress granules prevents neurodegeneration in a ALS/FTD model based on C9ORF72 gene mutation(K. Zhang et al., 2018). This observation suggests that, by preventing access of TDP-43 to the nucleus, stress granule formation may be central to the pathogenic mechanisms of ALS. It will thus be of great interest to study such interactions further in this animal model and find ways to link stress granule dynamics dysregulation with TDP-43 related neurodegenerative diseases.
In conclusion, our results clearly demonstrate the feasibility of using *N. furzeri* as a powerful model for TDP-43-related diseases, exploiting the advantages of the short lifespan of this organism, within the limitations intrinsic in any model. Further studies will be needed to observe the TDP-43-related ageing process in *N. furzeri* in a more temporally and spatially defined manner and especially to identify possible modifiers of the process.

4.4 Establishment of organotypic cultures in *Nothobranchius furzeri*

Organotypic culture is an undoubtedly useful technique that recollects the advantages of both *in vitro* and *in vivo* experiments. This has been extensively used to study rodents and also partially to perform studies regarding the central nervous system (retina) in zebrafish. But adapting this technique in *Nothobranchius furzeri* could lead to advantages unthinkable in other species. Seen the considerable short life of this model, it is reasonable that even a relatively short time of culturing as long as 5 weeks could lead to an '*in vitro* ageing' process similar to what is observed *in vivo* between 5 weeks and 10 weeks of age. This prospect, if correct, can lead to a whole new set of experiments and analysis that can be easily performed *ex vivo* avoiding much of the problems and complications of performing the same procedures *in vivo,* such as, for example, drug testing.
To be able to cultivate thick brain slices long-term, I adapted mediums already present in literature, putting particular care in the osmotic balance adjustment increasing the glucose concentration of the basal MDM-F12 medium to 0,4% and diluting the complete medium by adding 10% of water. The other medium components were relatively basic, including Ascorbic acid, insulin, Fetal Calf Serum (FCS) and Pen-Strep. The main reason behind the relatively basic composition of the medium lays in the assumption that, cultivating thick portions of tissues, the slices should be able to maintain and produce a functional microenvironment without much of intervention from outside medium, thus I focused mainly on supplying nutrients. Of course, the medium and the slice viability could be further improved via testing of other components added to the basal composition but, for the scope of my thesis and for the first implementation of this technique in a new animal model, I put more of my effort in developing the correct procedure, leaving the perfectioning of the medium for future studies. In the end I was to realize slices from both young (5 weeks) and old (30 weeks) animals and to cultivate the tissues for as long as 5 weeks *in vitro.* This, although preliminary, is a very promising result. Indeed, the anatomical integrity of the slices is maintained (results, Fig. 20) and also immunofluorescence staining revealed the maintenance of cellular distribution characteristics.
I was able to perform immunofluorescence staining of *Locus coeruleus* cells in cerebellar-pontine slices extracted from 5 weeks old animals and maintained in culture up to 5wiv, showing that the tissue survived, and the cells did not degenerate completely. Moreover, I was able to perform Edu and PCNA staining and imaging with very good results in optic tectum-derived slices, identifying a shift in the EdU staining from the PCNA positive area that can be interpreted with the ability of the slices to grow and, possibly, to differentiate new neurons even if this possibility should be addressed with further experiments (e.g., staining of new neurons with EdU and HuC/D).
I also tried to cultivate slices extracted from 30 weeks old animals. The viability of these tissues was greatly reduced as expected, but I was able nonetheless to perform immunofluorescence and identify again *Locus* coeruleus cells in the cerebellar-pontine slices, while also being able to image and recognize adult neurogenic niches in optic tectum and telencephalic slices. The observed neurogenic niches showed a great resemblance with the niches observed *in vivo* (Tozzini et al., 2012, results Fig. 25) proving further that the structural architecture of the slices is maintained during the culturing time.
Even if the results presented are very preliminary and more intensive studies are going to be performed, they can be of extreme importance in recognizing the possibility of organotypic slice culturing in *Nothobranchius furzeri*. Elsewhere in this thesis I already have addressed how the short lifespan of this animal model can be crucial to advance our understanding of ageing process and ageing-related pathologies. Thus, developing also an *in vitro* protocol to combine the fast ageing of *Nothobranchius* with the easy manipulation of *in vitro* samples could represent a winning strategy to address important questions. I firmly believe that establishing organotypic

culture of this animal could represent an important step in the advancement of our knowledge of ageing and ageing-related pathologies.

5.Conclusions

With my work, I addressed whether the teleost *Nothobranchius furzeri* could be used to study age-related diseases, focusing in particular on neurodegenerative diseases. The study of these pathology is of great relevance, since their impact is so great on our society and, despite all efforts, a definitive cure to these pathologies has yet to be found. Many animal models have been employed to try to address these imposing problems but all of them have as main drawback the long lifespan that led scientist to someway push the manifestation of the disease in young animals through use of toxic agents or strong mutated genes expression. Even if these methodologies have been useful in understanding many aspects of neurodegenerative diseases, they represent a situation that is very different from the slow progressing, age-related accumulation of aggregation and other pathologic factors observed in humans. Thus, using a model that recapitulates the main signs of mammalian ageing and presents a short lifespan could improve our current understandings of age-related pathologies.
I showed with my work, and with the work of my collaborators, that *Nothobranchius furzeri* brain accumulates aggregates during ageing, and those aggregates are particularly enriched in ribosomal proteins. The sequestration of ribosome components can lead to and worsen the proteostasis unbalance that is a common characteristic of both ageing and neurodegenerative diseases, and this observation supports the use of *Nothobranchius* as a model to study age- and aggregate-related pathologies.
Analyzing more closely the signs of Parkinson's disease in *Nothobranchius* (i.e. neurodegeneration of *locus coeruleus* and *posterior tuberculum* together with pS129 immunoreactivity), I was able to detect a sort of pre-pathological state in *N. furzeri* brain, comprised of neurodegeneration and particular presence of pS129 immunoreactivity limited to *Locus coeruleus* cell bodies while no sign of such was detectable in the *posterior tuberculum* nucleus (teleost homologs to the mammalian *Substantia nigra*). Moreover, as evidenced by the vacuolar localization of aggresome staining, even if pS129 immunoreactivity was high already from a young age and worsening with age, I was not able to identify big aggregates corresponding to Lewy bodies. All this leads to the idea that *N. furzeri* could represent a good model of the initial, pre-pathological stages of PD.
Regarding TDP-43 related pathology, I was able to identify a difference in TDP-43 localization in old animals with the appearance of a 'doughnut-like' staining near the nuclear border in line with the hypothesis of an alteration of nuclear-cytoplasmic transport and of TDP-43 function in FTD. I was also able to observe presence of TTDP-43 in Stress Granules, indicating that the role of this protein in SG formation and regulation is conserved in *N. furzeri.*

It is my personal opinion that such findings could provide a turning point on the use of a powerful ageing model like *Nothobranchius furzeri* to uncover hidden mechanisms involved in aggregation-related pathologies and strictly tied to ageing that have not yet been identified by the studies conducted in mammals. Taken together, my observations lead to the conclusion that *Nothobranchius* can be used as a powerful "tool" to study aspects of neurodegenerative diseases with approaches never used before, exploiting the natural short lifespan of this animal and its tendency to show signs of aggregation and pre-pathological states. This, coupled with the development of *ex-vivo* setups like organotypic culturing in this model could open exciting new avenues for ageing-related pathologiesresearch.
For example, the use of organotypic cultures for observing ageing mechanisms *ex-vivo* and the possibility to perform drug testing to reduce ageing phenotypes could be of extreme importance for the field. For the study of neurodegenerative diseases and aggregation-related pathology there is still the need to confirm that the phenomena that I observed *in vivo* (e.g., pSyn accumulation

and neurodegeneration of LC, TDP-43 anormal distribution) occur also in long-term cultured slices. If that was the case, it would allow for specific study of the mechanism leading to such events and open the possibility of easy drug testing to try to prevent them, in a more physiological context respect to what is currently done in transgenic mice for instance.
Overall, the data I obtained with my work could lead to a whole new area of research in *Nothobranchius furzeri* that can produce novel and unprecedented discoveries in the field of neurodegenerative diseases.

6. References

Aguzzi, A., & Calella, A. M. (2009). Prions: Protein aggregation and infectious diseases. In *Physiological Reviews* (Vol. 89, Issue 4, pp. 1105–1152). American Physiological Society. https://doi.org/10.1152/physrev.00006.2009

Aguzzi, A., & Rajendran, L. (2009). The Transcellular Spread of Cytosolic Amyloids, Prions, and Prionoids. In *Neuron* (Vol. 64, Issue 6, pp. 783–790). Cell Press. https://doi.org/10.1016/j.neuron.2009.12.016

Alami, N. H., Smith, R. B., Carrasco, M. A., Williams, L. A., Winborn, C. S., Han, S. S. W., Kiskinis, E., Winborn, B., Freibaum, B. D., Kanagaraj, A., Clare, A. J., Badders, N. M., Bilican, B., Chaum, E., Chandran, S., Shaw, C. E., Eggan, K. C., Maniatis, T., & Taylor, J. P. (2014). Axonal Transport of TDP-43 mRNA Granules Is Impaired by ALS-Causing Mutations. *Neuron*, *81*(3), 536–543. https://doi.org/10.1016/j.neuron.2013.12.018

Alavez, S., Vantipalli, M. C., Zucker, D. J. S., Klang, I. M., & Lithgow, G. J. (2011). Amyloid-binding compounds maintain protein homeostasis during ageing and extend lifespan. *Nature*, *472*(7342), 226–230. https://doi.org/10.1038/nature09873

Alexander, G. E. (2004). Biology of Parkinson's disease: Pathogenesis and pathophysiology of a multisystem neurodegenerative disorder. In *Dialogues in Clinical Neuroscience* (Vol. 6, Issue 3, pp. 259–280). Les Laboratoires Servier. https://doi.org/10.31887/dcns.2004.6.3/galexander

Anderson, P., & Kedersha, N. (2008). Stress granules: the Tao of RNA triage. In *Trends in Biochemical Sciences* (Vol. 33, Issue 3, pp. 141–150). Elsevier Current Trends. https://doi.org/10.1016/j.tibs.2007.12.003

Anderson, P., & Kedersha, N. (2009). Stress granules. In *Current Biology* (Vol. 19, Issue 10). Curr Biol. https://doi.org/10.1016/j.cub.2009.03.013

Aramillo Irizar, P., Schäuble, S., Esser, D., Groth, M., Frahm, C., Priebe, S., Baumgart, M., Hartmann, N., Marthandan, S., Menzel, U., Müller, J., Schmidt, S., Ast, V., Caliebe, A., König, R., Krawczak, M., Ristow, M., Schuster, S., Cellerino, A., … Kaleta, C. (2018). Transcriptomic alterations during ageing reflect the shift from cancer to degenerative diseases in the elderly. *Nature Communications*, *9*(1), 1–11. https://doi.org/10.1038/s41467-017-02395-2

Asakawa, K., Handa, H., & Kawakami, K. (2020). Optogenetic modulation of TDP-43 oligomerization accelerates ALS-related pathologies in the spinal motor neurons. *Nature Communications*, *11*(1), 1–16. https://doi.org/10.1038/s41467-020-14815-x

Aulas, A., & Velde, C. Vande. (2015). Alterations in stress granule dynamics driven by TDP-43 and FUS: A link to pathological inclusions in ALS? *Frontiers in Cellular Neuroscience*, *9*(OCTOBER). https://doi.org/10.3389/fncel.2015.00423

Bagnoli, S., Fronte, B., Bibbiani, C., Tozzini, E. T., & Cellerino, A. (2021). Aging is associated with a degeneration of noradrenergic-, but not dopaminergic-neurons, in the short-lived killifish Nothobranchius furzeri. *BioRxiv*, 2021.03.31.437850. https://doi.org/10.1101/2021.03.31.437850

Bailey, C. H., Kandel, E. R., & Si, K. (2004). Review The Persistence of Long-Term Memory: A

Molecular Approach to Self-Sustaining Changes in Learning-Induced Synaptic Growth initiation of these learning-related structural changes and their functional contribution to the different temporal phases of long-term facilitation. Finally, we consider the role of local protein synthesis and specifically a novel molecular mechanism for the self-perpetuating activa. In *Neuron* (Vol. 44).

Balagopal, V., & Parker, R. (2009). Polysomes, P bodies and stress granules: states and fates of eukaryotic mRNAs. In *Current Opinion in Cell Biology* (Vol. 21, Issue 3, pp. 403–408). Elsevier Current Trends. https://doi.org/10.1016/j.ceb.2009.03.005

Balch, W. E., Morimoto, R. I., Dillin, A., & Kelly, J. W. (2008). Adapting proteostasis for disease intervention. In *Science* (Vol. 319, Issue 5865, pp. 916–919). Science. https://doi.org/10.1126/science.1141448

Bandmann, O., Flinn, L., & Mortiboys, H. (2010). POMD08 Zebrafish models for early onset Parkinson's disease. *Journal of Neurology, Neurosurgery & Psychiatry*, *81*(11), e59–e59. https://doi.org/10.1136/jnnp.2010.226340.168

Banerjee, R., Starkov, A. A., Beal, M. F., & Thomas, B. (2009). Mitochondrial dysfunction in the limelight of Parkinson's disease pathogenesis. In *Biochimica et Biophysica Acta - Molecular Basis of Disease* (Vol. 1792, Issue 7, pp. 651–663). https://doi.org/10.1016/j.bbadis.2008.11.007

Banerjee, S., Ferdosh, S., Ghosh, A. N., & Barat, C. (2020). Tau protein- induced sequestration of the eukaryotic ribosome: Implications in neurodegenerative disease. *Scientific Reports*, *10*(1), 1–15. https://doi.org/10.1038/s41598-020-61777-7

Bari, B. A., Chokshi, V., & Schmidt, K. (2020). Locus coeruleus-norepinephrine: Basic functions and insights into Parkinson's disease. In *Neural Regeneration Research* (Vol. 15, Issue 6, pp. 1006–1013). Wolters Kluwer Medknow Publications. https://doi.org/10.4103/1673-5374.270297

Baumgart, M., Cicco, E. Di, Rossi, G., Cellerino, A., & Tozzini, E. T. (2014). Comparison of captive lifespan, age-associated liver neoplasias and age-dependent gene expression between two annual fish species: Nothobranchius furzeri and Nothobranchius korthause. *Biogerontology 2014 16:1*, *16*(1), 63–69. https://doi.org/10.1007/S10522-014-9535-Y

Baumgart, M., Groth, M., Priebe, S., Savino, A., Testa, G., Dix, A., Ripa, R., Spallotta, F., Gaetano, C., Ori, M., Terzibasi Tozzini, E., Guthke, R., Platzer, M., & Cellerino, A. (2014). RNA-seq of the aging brain in the short-lived fish N. furzeri - conserved pathways and novel genes associated with neurogenesis. *Aging Cell*, *13*(6), 965–974. https://doi.org/10.1111/acel.12257

Beck, M., Schmidt, A., Malmstroem, J., Claassen, M., Ori, A., Szymborska, A., Herzog, F., Rinner, O., Ellenberg, J., & Aebersold, R. (2011). The quantitative proteome of a human cell line. *Molecular Systems Biology*, *7*(1), 549. https://doi.org/10.1038/msb.2011.82

Bedford, L., Hay, D., Devoy, A., Paine, S., Powe, D. G., Seth, R., Gray, T., Topham, I., Fone, K., Rezvani, N., Mee, M., Soane, T., Layfield, R., Sheppard, P. W., Ebendal, T., Usoskin, D., Lowe, J., & Mayer, R. J. (2008). Depletion of 26S proteasomes in mouse brain neurons causes neurodegeneration and lewy-like inclusions resembling human pale bodies. *Journal of Neuroscience*, *28*(33), 8189–8198. https://doi.org/10.1523/JNEUROSCI.2218-08.2008

Benarroch, E. E. (2009). The locus ceruleus norepinephrine system: Functional organization and potential clinical significance. *Neurology*, *73*(20), 1699–1704. https://doi.org/10.1212/WNL.0b013e3181c2937c

Besnard-Guérin, C. (2020). Cytoplasmic localization of amyotrophic lateral sclerosis-related TDP-43 proteins modulates stress granule formation. *European Journal of Neuroscience*, *52*(8), 3995–4008. https://doi.org/10.1111/ejn.14762

Bi, F., Huang, C., Tong, J., Qiu, G., Huang, B., Wu, Q., Li, F., Xu, Z., Bowser, R., Xia, X. G., & Zhou, H. (2013). Reactive astrocytes secrete lcn2 to promote neuron death. *Proceedings of the National Academy of Sciences of the United States of America*, *110*(10), 4069–4074. https://doi.org/10.1073/pnas.1218497110

Bogaerts, V., Theuns, J., & Van Broeckhoven, C. (2008). Genetic findings in Parkinson's disease and translation into treatment: A leading role for mitochondria? In *Genes, Brain and Behavior* (Vol. 7, Issue 2, pp. 129–151). Blackwell Publishing Ltd. https://doi.org/10.1111/j.1601-183X.2007.00342.x

Bose, P., Armstrong, G. A. B., & Drapeau, P. (2019). Neuromuscular junction abnormalities in a zebrafish loss-of-function model of TDP-43. *Journal of Neurophysiology*, *121*(1), 285–297. https://doi.org/10.1152/jn.00265.2018

Braak, H., Del Tredici, K., Bratzke, H., Hamm-Clement, J., Sandmann-Keil, D., & Rüb, U. (2002). Staging of the intracerebral inclusion body pathology associated with idiopathic Parkinson's disease (preclinical and clinical stages). *Journal of Neurology, Supplement*, *249*(3). https://doi.org/10.1007/s00415-002-1301-4

Braak, H., Del Tredici, K., Rüb, U., De Vos, R. A. I., Jansen Steur, E. N. H., & Braak, E. (2003). Staging of brain pathology related to sporadic Parkinson's disease. *Neurobiology of Aging*, *24*(2), 197–211. https://doi.org/10.1016/S0197-4580(02)00065-9

Bridi, J. C., & Hirth, F. (2018). Mechanisms of α-Synuclein induced synaptopathy in parkinson's disease. In *Frontiers in Neuroscience* (Vol. 12, Issue FEB, p. 80). Frontiers Media S.A. https://doi.org/10.3389/fnins.2018.00080

Buratti, E., & Baralle, F. E. (2001). Characterization and Functional Implications of the RNA Binding Properties of Nuclear Factor TDP-43, a Novel Splicing Regulator of CFTR Exon 9. *Journal of Biological Chemistry*, *276*(39), 36337–36343. https://doi.org/10.1074/jbc.M104236200

Capitini, C., Fani, G., Vivoli Vega, M., Penco, A., Canale, C., Cabrita, L. D., Calamai, M., Christodoulou, J., Relini, A., & Chiti, F. (2020). Full-length TDP-43 and its C-terminal domain form filaments in vitro having non-amyloid properties. *Amyloid*, 1–10. https://doi.org/10.1080/13506129.2020.1826425

Cash, R., Dennis, T., L'Heureux, R., Raisman, R., Javoy-Agid, F., & Scatton, B. (1987). Parkinson's disease and dementia: Norepinephrine and dopamine in locus ceruleus. *Neurology*, *37*(1), 42–46. https://doi.org/10.1212/wnl.37.1.42

Cellerino, A., Valenzano, D. R., & Reichard, M. (2016). From the bush to the bench: the annual Nothobranchius fishes as a new model system in biology. *Biological Reviews*, *91*(2), 511–533. https://doi.org/10.1111/brv.12183

Chernova, T. A., Wilkinson, K. D., & Chernoff, Y. O. (2014). Physiological and environmental control of yeast prions. In *FEMS Microbiology Reviews* (Vol. 38, Issue 2, pp. 326–344). FEMS Microbiol Rev. https://doi.org/10.1111/1574-6976.12053

Chu, J. F., Majumder, P., Chatterjee, B., Huang, S. L., & Shen, C. K. J. (2019). TDP-43 Regulates Coupled Dendritic mRNA Transport-Translation Processes in Co-operation with FMRP and Staufen1. *Cell Reports*, *29*(10), 3118-3133.e6. https://doi.org/10.1016/j.celrep.2019.10.061

Cohen, T. J., Lee, V. M. Y., & Trojanowski, J. Q. (2011). TDP-43 functions and pathogenic mechanisms implicated in TDP-43 proteinopathies. In *Trends in Molecular Medicine* (Vol. 17, Issue 11, pp. 659–667). NIH Public Access. https://doi.org/10.1016/j.molmed.2011.06.004

Colacurcio, D. J., & Nixon, R. A. (2016). Disorders of lysosomal acidification—The emerging role of v-ATPase in aging and neurodegenerative disease. In *Ageing Research Reviews* (Vol. 32, pp. 75–88). Elsevier Ireland Ltd. https://doi.org/10.1016/j.arr.2016.05.004

Cox, D., Raeburn, C., Sui, X., & Hatters, D. M. (2020). Protein aggregation in cell biology: An aggregomics perspective of health and disease. In *Seminars in Cell and Developmental Biology* (Vol. 99, pp. 40–54). Elsevier Ltd. https://doi.org/10.1016/j.semcdb.2018.05.003

Cui, L., Jeong, H., Borovecki, F., Parkhurst, C. N., Tanese, N., & Krainc, D. (2006). Transcriptional Repression of PGC-1α by Mutant Huntingtin Leads to Mitochondrial Dysfunction and Neurodegeneration. *Cell*, *127*(1), 59–69. https://doi.org/10.1016/j.cell.2006.09.015

Cummings, J., Bauzon, J., & Lee, G. (2021). Who funds Alzheimer's disease drug development? *Alzheimer's & Dementia: Translational Research & Clinical Interventions*, *7*(1), e12185. https://doi.org/10.1002/trc2.12185

Daviaud, N., Garbayo, E., Lautram, N., Franconi, F., Lemaire, L., Perez-Pinzon, M., & Montero-Menei, C. N. (2014). Modeling nigrostriatal degeneration in organotypic cultures, a new ex vivo model of Parkinson's disease. *Neuroscience*, *256*, 10–22. https://doi.org/10.1016/j.neuroscience.2013.10.021

David, D. C., Ollikainen, N., Trinidad, J. C., Cary, M. P., Burlingame, A. L., & Kenyon, C. (2010). Widespread protein aggregation as an inherent part of aging in C. elegans. *PLoS Biology*, *8*(8), 47–48. https://doi.org/10.1371/journal.pbio.1000450

de Magalhães, J. P., Curado, J., & Church, G. M. (2009). Meta-analysis of age-related gene expression profiles identifies common signatures of aging. *Bioinformatics*, *25*(7), 875–881. https://doi.org/10.1093/bioinformatics/btp073

Del Tredici, K., & Braak, H. (2012). Lewy pathology and neurodegeneration in premotor Parkinson's disease. *Movement Disorders*, *27*(5), 597–607. https://doi.org/10.1002/mds.24921

Del Tredici, K., & Braak, H. (2013). Dysfunction of the locus coeruleus-norepinephrine system and related circuitry in Parkinson's disease-related dementia. In *Journal of Neurology, Neurosurgery and Psychiatry* (Vol. 84, Issue 7, pp. 774–783). BMJ Publishing Group. https://doi.org/10.1136/jnnp-2011-301817

Desplats, P., Lee, H. J., Bae, E. J., Patrick, C., Rockenstein, E., Crews, L., Spencer, B., Masliah, E., & Lee, S. J. (2009). Inclusion formation and neuronal cell death through neuron-to-neuron

transmission of α-synuclein. *Proceedings of the National Academy of Sciences of the United States of America*, *106*(31), 13010–13015. https://doi.org/10.1073/pnas.0903691106

Dickson, D. W., Fujishiro, H., DelleDonne, A., Menke, J., Ahmed, Z., Klos, K. J., Josephs, K. A., Frigerio, R., Burnett, M., Parisi, J. R., & Ahlskog, J. E. (2008). Evidence that incidental Lewy body disease is pre-symptomatic Parkinson's disease. *Acta Neuropathologica*, *115*(4), 437–444. https://doi.org/10.1007/s00401-008-0345-7

Ding, Q., Dimayuga, E., Markesbery, W. R., & Keller, J. N. (2006). Proteasome inhibition induces reversible impairments in protein synthesis. *The FASEB Journal*, *20*(8), 1055–1063. https://doi.org/10.1096/fj.05-5495com

Dolfi, L., Ripa, R., Antebi, A., Valenzano, D. R., & Cellerino, A. (2019). Cell cycle dynamics during diapause entry and exit in an annual killifish revealed by FUCCI technology. *EvoDevo 2019 10:1*, *10*(1), 1–22. https://doi.org/10.1186/S13227-019-0142-5

Dovidchenko, N. V., Leonova, E. I., & Galzitskaya, O. V. (2014). Mechanisms of amyloid fibril formation. In *Biochemistry (Moscow)* (Vol. 79, Issue 13, pp. 1515–1527). Maik Nauka Publishing / Springer SBM. https://doi.org/10.1134/S0006297914130057

Dudman, J., & Qi, X. (2020). Stress Granule Dysregulation in Amyotrophic Lateral Sclerosis. In *Frontiers in Cellular Neuroscience* (Vol. 14). Frontiers Media S.A. https://doi.org/10.3389/fncel.2020.598517

Eisenberg, D., & Jucker, M. (2012). The amyloid state of proteins in human diseases. In *Cell* (Vol. 148, Issue 6, pp. 1188–1203). Elsevier B.V. https://doi.org/10.1016/j.cell.2012.02.022

Eschbach, J., Von Einem, B., Müller, K., Bayer, H., Scheffold, A., Morrison, B. E., Rudolph, K. L., Thal, D. R., Witting, A., Weydt, P., Otto, M., Fauler, M., Liss, B., McLean, P. J., La Spada, A. R., Ludolph, A. C., Weishaupt, J. H., & Danzer, K. M. (2015). Mutual exacerbation of peroxisome proliferator-activated receptor γ coactivator 1α deregulation and α-synuclein oligomerization. *Annals of Neurology*, *77*(1), 15–32. https://doi.org/10.1002/ana.24294

Eun, S. C., So, Y. L., Park, J. Y., Hong, S. G., & Pan, D. R. (2007). Organotypic slice culture of the hypothalamic paraventricular nucleus of rat. *Journal of Veterinary Science*, *8*(1), 15–20. https://doi.org/10.4142/jvs.2007.8.1.15

Falsone, A., & Falsone, S. F. (2015). Legal but lethal: Functional protein aggregation at the verge of toxicity. In *Frontiers in Cellular Neuroscience* (Vol. 9, Issue FEB). Frontiers Research Foundation. https://doi.org/10.3389/fncel.2015.00045

Fan, A. C., & Leung, A. K. L. (2016). RNA granules and diseases: A case study of stress granules in ALS and FTLD. In *Advances in Experimental Medicine and Biology* (Vol. 907, pp. 263–296). Springer New York LLC. https://doi.org/10.1007/978-3-319-29073-7_11

Fang, Y. S., Tsai, K. J., Chang, Y. J., Kao, P., Woods, R., Kuo, P. H., Wu, C. C., Liao, J. Y., Chou, S. C., Lin, V., Jin, L. W., Yuan, H. S., Cheng, I. H., Tu, P. H., & Chen, Y. R. (2014). Full-length TDP-43 forms toxic amyloid oligomers that are present in frontotemporal lobar dementia-TDP patients. *Nature Communications*, *5*. https://doi.org/10.1038/ncomms5824

Flinn, L. J., Keatinge, M., Bretaud, S., Mortiboys, H., Matsui, H., De Felice, E., Woodroof, H. I., Brown, L., McTighe, A., Soellner, R., Allen, C. E., Heath, P. R., Milo, M., Muqit, M. M. K.,

Reichert, A. S., Köster, R. W., Ingham, P. W., & Bandmann, O. (2013). TigarB causes mitochondrial dysfunction and neuronal loss in PINK1 deficiency. *Annals of Neurology*, *74*(6), 837–847. https://doi.org/10.1002/ana.23999

Flinn, L., Mortiboys, H., Volkmann, K., Kster, R. W., Ingham, P. W., & Bandmann, O. (2009). Complex i deficiency and dopaminergic neuronal cell loss in parkin-deficient zebrafish (Danio rerio). *Brain*, *132*(6), 1613–1623. https://doi.org/10.1093/brain/awp108

Forno, L. S. (1969). Concentric hyalin intraneuronal inclusions of Lewy type in the brains of elderly persons (50 incidental cases): relationship to parkinsonism. *Journal of the American Geriatrics Society*, *17*(6), 557–575. https://doi.org/10.1111/j.1532-5415.1969.tb01316.x

Francisco, S., Ferreira, M., Moura, G., Soares, A. R., & Santos, M. A. S. (2020). Does proteostasis get lost in translation? Implications for protein aggregation across the lifespan. In *Ageing Research Reviews* (Vol. 62, p. 101119). Elsevier Ireland Ltd. https://doi.org/10.1016/j.arr.2020.101119

Freer, R., Sormanni, P., Vecchi, G., Ciryam, P., Dobson, C. M., & Vendruscolo, M. (2016). A protein homeostasis signature in healthy brains recapitulates tissue vulnerability to Alzheimer's disease. *Science Advances*, *2*(8), e1600947. https://doi.org/10.1126/sciadv.1600947

Frost, B., & Diamond, M. I. (2010). Prion-like mechanisms in neurodegenerative diseases. In *Nature Reviews Neuroscience* (Vol. 11, Issue 3, pp. 155–159). NIH Public Access. https://doi.org/10.1038/nrn2786

Fu, H., Hardy, J., & Duff, K. E. (2018). Selective vulnerability in neurodegenerative diseases. In *Nature Neuroscience* (Vol. 21, Issue 10, pp. 1350–1358). Nature Publishing Group. https://doi.org/10.1038/s41593-018-0221-2

Fumimura, Y., Ikemura, M., Saito, Y., Sengoku, R., Kanemaru, K., Sawabe, M., Arai, T., Ito, G., Iwatsubo, T., Fukayama, M., Mizusawa, H., & Murayama, S. (2007). Analysis of the adrenal gland is useful for evaluating pathology of the peripheral autonomic nervous system in Lewy body disease. *Journal of Neuropathology and Experimental Neurology*, *66*(5), 354–362. https://doi.org/10.1097/nen.0b013e3180517454

Furukawa, Y., Kaneko, K., Watanabe, S., Yamanaka, K., & Nukina, N. (2011). A seeding reaction recapitulates intracellular formation of sarkosyl-insoluble transactivation response element (TAR) DNA-binding protein-43 inclusions. *Journal of Biological Chemistry*, *286*(21), 18664–18672. https://doi.org/10.1074/jbc.M111.231209

Gähwiler, B. H. (1984). Slice cultures of cerebellar, hippocampal and hypothalamic tissue. *Experientia*, *40*(3), 235–243. https://doi.org/10.1007/BF01947561

Gancharova, O. S., Manskikh, V. N., Zamyatnin, A. A., & Philippov, P. P. (2013). Organotypic culture of neural retina as a research model of neurodegeneration of ganglion cells. *Biochemistry (Moscow)*, *78*(11), 1280–1286. https://doi.org/10.1134/S0006297913110084

Genade, T., Benedetti, M., Terzibasi, E., Roncaglia, P., Valenzano, D. R., Cattaneo, A., & Cellerino, A. (2005). Annual fishes of the genus Nothobarnchius as a model system for aging research. In *Aging Cell* (Vol. 4, Issue 5, pp. 223–233). Aging Cell. https://doi.org/10.1111/j.1474-9726.2005.00165.x

Gilks, N., Kedersha, N., Ayodele, M., Shen, L., Stoecklin, G., Dember, L. M., & Anderson, P. (2004). Stress granule assembly is mediated by prion-like aggregation of TIA-1. *Molecular Biology of the Cell*, *15*(12), 5383–5398. https://doi.org/10.1091/mbc.E04-08-0715

Glaser, T., Schwarz-Benmeir, N., Barnoy, S., Barak, S., Eshhar, Z., & Kosower, N. S. (1994). Calpain (Ca2+-dependent thiol protease) in erythrocytes of young and old individuals. *Proceedings of the National Academy of Sciences of the United States of America*, *91*(17), 7879–7883. https://doi.org/10.1073/pnas.91.17.7879

Gruber, A., Hornburg, D., Antonin, M., Krahmer, N., Collado, J., Schaffer, M., Zubaite, G., Lüchtenborg, C., Sachsenheimer, T., Brügger, B., Mann, M., Baumeister, W., Hartl, F. U., Hipp, M. S., & Fernández-Busnadiego, R. (2018). Molecular and structural architecture of polyQ aggregates in yeast. *Proceedings of the National Academy of Sciences of the United States of America*, *115*(15), E3446–E3453. https://doi.org/10.1073/pnas.1717978115

Gsponer, J., & Babu, M. M. (2012). Cellular Strategies for Regulating Functional and Nonfunctional Protein Aggregation. *Cell Reports*, *2*(5), 1425–1437. https://doi.org/10.1016/j.celrep.2012.09.036

Guo, J. L., Covell, D. J., Daniels, J. P., Iba, M., Stieber, A., Zhang, B., Riddle, D. M., Kwong, L. K., Xu, Y., Trojanowski, J. Q., & Lee, V. M. Y. (2013). Distinct α-Synuclein Strains Differentially Promote Tau Inclusions in Neurons. *Cell*, *154*(1), 103. https://doi.org/10.1016/j.cell.2013.05.057

Guo, W., Chen, Y., Zhou, X., Kar, A., Ray, P., Chen, X., Rao, E. J., Yang, M., Ye, H., Zhu, L., Liu, J., Xu, M., Yang, Y., Wang, C., Zhang, D., Bigio, E. H., Mesulam, M., Shen, Y., Xu, Q., … Wu, J. Y. (2011). An ALS-associated mutation affecting TDP-43 enhances protein aggregation, fibril formation and neurotoxicity. *Nature Structural and Molecular Biology*, *18*(7), 822–831. https://doi.org/10.1038/nsmb.2053

Halliday, M., Radford, H., Sekine, Y., Moreno, J., Verity, N., Le Quesne, J., Ortori, C. A., Barrett, D. A., Fromont, C., Fischer, P. M., Harding, H. P., Ron, D., & Mallucci, G. R. (2015). Partial restoration of protein synthesis rates by the small molecule ISRIB prevents neurodegeneration without pancreatic toxicity. *Cell Death and Disease*, *6*(3), e1672–e1672. https://doi.org/10.1038/cddis.2015.49

Hama, H., Hioki, H., Namiki, K., Hoshida, T., Kurokawa, H., Ishidate, F., Kaneko, T., Akagi, T., Saito, T., Saido, T., & Miyawaki, A. (2015). ScaleS: An optical clearing palette for biological imaging. *Nature Neuroscience*, *18*(10), 1518–1529. https://doi.org/10.1038/nn.4107

Hama, H., Kurokawa, H., Kawano, H., Ando, R., Shimogori, T., Noda, H., Fukami, K., Sakaue-Sawano, A., & Miyawaki, A. (2011). Scale: A chemical approach for fluorescence imaging and reconstruction of transparent mouse brain. *Nature Neuroscience*, *14*(11), 1481–1488. https://doi.org/10.1038/nn.2928

Harel, I., Benayoun, B. A., Machado, B., Singh, P. P., Hu, C.-K., Pech, M. F., Valenzano, D. R., Zhang, E., Sharp, S. C., Artandi, S. E., & Brunet, A. (2015). A Platform for Rapid Exploration of Aging and Diseases in a Naturally Short-Lived Vertebrate. *Cell*, *160*(5), 1013–1026. https://doi.org/10.1016/j.cell.2015.01.038

Hawkes, C. H., Del Tredici, K., & Braak, H. (2007). Parkinson's disease: A dual-hit hypothesis. In

Neuropathology and Applied Neurobiology (Vol. 33, Issue 6, pp. 599–614). John Wiley & Sons, Ltd. https://doi.org/10.1111/j.1365-2990.2007.00874.x

Hedden, T., Van Dijk, K. R. A., Becker, J. A., Mehta, A., Sperling, R. A., Johnson, K. A., & Buckner, R. L. (2009). Disruption of functional connectivity in clinically normal older adults harboring amyloid burden. *Journal of Neuroscience*, *29*(40), 12686–12694. https://doi.org/10.1523/JNEUROSCI.3189-09.2009

Hergesheimer, R. C., Chami, A. A., De Assis, D. R., Vourc'h, P., Andres, C. R., Corcia, P., Lanznaster, D., & Blasco, H. (2019). The debated toxic role of aggregated TDP-43 in amyotrophic lateral sclerosis: A resolution in sight? In *Brain* (Vol. 142, Issue 5, pp. 1176–1194). Oxford University Press. https://doi.org/10.1093/brain/awz078

Hicks, D. A., Cross, L. L., Williamson, R., & Rattray, M. (2020). Endoplasmic Reticulum Stress Signalling Induces Casein Kinase 1-Dependent Formation of Cytosolic TDP-43 Inclusions in Motor Neuron-Like Cells. *Neurochemical Research*, *45*(6), 1354–1364. https://doi.org/10.1007/s11064-019-02832-2

Hipp, M. S., Park, S. H., & Hartl, U. U. (2014). Proteostasis impairment in protein-misfolding and -aggregation diseases. In *Trends in Cell Biology* (Vol. 24, Issue 9, pp. 506–514). Elsevier Ltd. https://doi.org/10.1016/j.tcb.2014.05.003

Hosp, F., Gutiérrez-Ángel, S., Schaefer, M. H., Cox, J., Meissner, F., Hipp, M. S., Hartl, F. U., Klein, R., Dudanova, I., & Mann, M. (2017). Spatiotemporal Proteomic Profiling of Huntington's Disease Inclusions Reveals Widespread Loss of Protein Function. *Cell Reports*, *21*(8), 2291–2303. https://doi.org/10.1016/j.celrep.2017.10.097

Hou, Y., Dan, X., Babbar, M., Wei, Y., Hasselbalch, S. G., Croteau, D. L., & Bohr, V. A. (2019). Ageing as a risk factor for neurodegenerative disease. In *Nature Reviews Neurology* (Vol. 15, Issue 10, pp. 565–581). Nature Publishing Group. https://doi.org/10.1038/s41582-019-0244-7

Humpel, C. (2015). Neuroscience forefront review organotypic brain slice cultures: A review. In *Neuroscience* (Vol. 305, pp. 86–98). Elsevier Ltd. https://doi.org/10.1016/j.neuroscience.2015.07.086

Hutten, S., & Dormann, D. (2020). Nucleocytoplasmic transport defects in neurodegeneration - Cause or consequence? *Seminars in Cell & Developmental Biology*, *99*, 151–162. https://doi.org/10.1016/j.semcdb.2019.05.020

Iguchi, Y., Katsuno, M., Niwa, J. I., Takagi, S., Ishigaki, S., Ikenaka, K., Kawai, K., Watanabe, H., Yamanaka, K., Takahashi, R., Misawa, H., Sasaki, S., Tanaka, F., & Sobue, G. (2013). Loss of TDP-43 causes age-dependent progressive motor neuron degeneration. *Brain*, *136*(5), 1371–1382. https://doi.org/10.1093/brain/awt029

Ishiguro, A., Kimura, N., Watanabe, Y., Watanabe, S., & Ishihama, A. (2016). TDP-43 binds and transports G-quadruplex-containing mRNAs into neurites for local translation. *Genes to Cells*, *21*(5), 466–481. https://doi.org/10.1111/gtc.12352

Jaeger, C., Ruiz, A. G., & Llinás, R. (1989). Organotypic slice cultures of dopaminergic neurons of substantia nigra. *Brain Research Bulletin*, *22*(6), 981–991. https://doi.org/10.1016/0361-9230(89)90010-5

Jagmag, S. A., Tripathi, N., Shukla, S. D., Maiti, S., & Khurana, S. (2016). Evaluation of models of Parkinson's disease. In *Frontiers in Neuroscience* (Vol. 9, Issue JAN). Frontiers Media S.A. https://doi.org/10.3389/fnins.2015.00503

Jankovic, J. (2008). Parkinson's disease: Clinical features and diagnosis. In *Journal of Neurology, Neurosurgery and Psychiatry* (Vol. 79, Issue 4, pp. 368–376). BMJ Publishing Group. https://doi.org/10.1136/jnnp.2007.131045

Johnson, B. S., Snead, D., Lee, J. J., McCaffery, J. M., Shorter, J., & Gitler, A. D. (2009). TDP-43 is intrinsically aggregation-prone, and amyotrophic lateral sclerosis-linked mutations accelerate aggregation and increase toxicity. *Journal of Biological Chemistry*, *284*(30), 20329–20339. https://doi.org/10.1074/jbc.M109.010264

Johnson, M. E., & Bobrovskaya, L. (2015). An update on the rotenone models of Parkinson's disease: Their ability to reproduce the features of clinical disease and model gene-environment interactions. In *NeuroToxicology* (Vol. 46, pp. 101–116). Elsevier. https://doi.org/10.1016/j.neuro.2014.12.002

Kaslin, J., & Panula, P. (2001). Comparative anatomy of the histaminergic and other aminergic systems in zebrafish (Danio rerio). *Journal of Comparative Neurology*, *440*(4), 342–377. https://doi.org/10.1002/cne.1390

Kato, M., Han, T. W., Xie, S., Shi, K., Du, X., Wu, L. C., Mirzaei, H., Goldsmith, E. J., Longgood, J., Pei, J., Grishin, N. V., Frantz, D. E., Schneider, J. W., Chen, S., Li, L., Sawaya, M. R., Eisenberg, D., Tycko, R., & McKnight, S. L. (2012). Cell-free formation of RNA granules: Low complexity sequence domains form dynamic fibers within hydrogels. *Cell*, *149*(4), 753–767. https://doi.org/10.1016/j.cell.2012.04.017

Kaushik, S., & Cuervo, A. M. (2015). Proteostasis and aging. In *Nature Medicine* (Vol. 21, Issue 12, pp. 1406–1415). Nature Publishing Group. https://doi.org/10.1038/nm.4001

Kedersha, N., Cho, M. R., Li, W., Yacono, P. W., Chen, S., Gilks, N., Golan, D. E., & Anderson, P. (2000). Dynamic shuttling of TIA-1 accompanies the recruitment of mRNA to mammalian stress granules. *Journal of Cell Biology*, *151*(6), 1257–1268. https://doi.org/10.1083/jcb.151.6.1257

Kedersha, N., Ivanov, P., & Anderson, P. (2013). Stress granules and cell signaling: More than just a passing phase? In *Trends in Biochemical Sciences* (Vol. 38, Issue 10, pp. 494–506). Trends Biochem Sci. https://doi.org/10.1016/j.tibs.2013.07.004

Keeney, P. M., Xie, J., Capaldi, R. A., & Bennett, J. P. (2006). Parkinson's disease brain mitochondrial complex I has oxidatively damaged subunits and is functionally impaired and misassembled. *Journal of Neuroscience*, *26*(19), 5256–5264. https://doi.org/10.1523/JNEUROSCI.0984-06.2006

Kelmer Sacramento, E., Kirkpatrick, J. M., Mazzetto, M., Baumgart, M., Bartolome, A., Di Sanzo, S., Caterino, C., Sanguanini, M., Papaevgeniou, N., Lefaki, M., Childs, D., Bagnoli, S., Terzibasi Tozzini, E., Di Fraia, D., Romanov, N., Sudmant, P. H., Huber, W., Chondrogianni, N., Vendruscolo, M., … Ori, A. (2020). Reduced proteasome activity in the aging brain results in ribosome stoichiometry loss and aggregation. *Molecular Systems Biology*, *16*(6). https://doi.org/10.15252/msb.20209596

Khalfallah, Y., Kuta, R., Grasmuck, C., Prat, A., Durham, H. D., & Vande Velde, C. (2018). TDP-43 regulation of stress granule dynamics in neurodegenerative disease-relevant cell types /631/80/304 /631/378/87 /13/1 /13/31 /13/51 /13/109 /13/106 /13/89 /14/19 /14/32 /82/80 article. *Scientific Reports*, *8*(1), 1–13. https://doi.org/10.1038/s41598-018-25767-0

Kim, S. H., Shanware, N. P., Bowler, M. J., & Tibbetts, R. S. (2010). Amyotrophic lateral sclerosis-associated proteins TDP-43 and FUS/TLS function in a common biochemical complex to co-regulate HDAC6 mRNA. *Journal of Biological Chemistry*, *285*(44), 34097–34105. https://doi.org/10.1074/jbc.M110.154831

Knöpfel, T., Rietschin, L., & Gähwiler, B. H. (1989). Organotypic Co-Cultures of Rat Locus Coeruleus and Hippocampus. *European Journal of Neuroscience*, *1*(6), 678–689. https://doi.org/10.1111/j.1460-9568.1989.tb00374.x

Kundra, R., Dobson, C. M., & Vendruscolo, M. (2020). A Cell- and Tissue-Specific Weakness of the Protein Homeostasis System Underlies Brain Vulnerability to Protein Aggregation. *IScience*, *23*(3), 100934. https://doi.org/10.1016/j.isci.2020.100934

Kustermann, S., Schmid, S., Biehlmaier, O., & Kohler, K. (2008). Survival, excitability, and transfection of retinal neurons in an organotypic culture of mature zebrafish retina. *Cell and Tissue Research*, *332*(2), 195–209. https://doi.org/10.1007/s00441-008-0589-5

Lahne, M., Gorsuch, R. A., Nelson, C. M., & Hyde, D. R. (2017). Culture of adult transgenic zebrafish retinal explants for live-cell imaging by multiphoton microscopy. *Journal of Visualized Experiments*, *2017*(120), 55335. https://doi.org/10.3791/55335

Lam, C. S., Korzh, V., & Strahle, U. (2005). Zebrafish embryos are susceptible to the dopaminergic neurotoxin MPTP. *European Journal of Neuroscience*, *21*(6), 1758–1762. https://doi.org/10.1111/j.1460-9568.2005.03988.x

Langenberg, T., Brand, M., & Cooper, M. S. (2003). Imaging Brain Development and Organogenesis in Zebrafish Using Immobilized Embryonic Explants. *Developmental Dynamics*, *228*(3), 464–474. https://doi.org/10.1002/dvdy.10395

Leggett, C., McGehee, D. S., Mastrianni, J., Yang, W., Bai, T., & Brorson, J. R. (2012). Tunicamycin produces TDP-43 cytoplasmic inclusions in cultured brain organotypic slices. *Journal of the Neurological Sciences*, *317*(1–2), 66–73. https://doi.org/10.1016/j.jns.2012.02.027

Liu-Yesucevitz, L., Bilgutay, A., Zhang, Y. J., Vanderwyde, T., Citro, A., Mehta, T., Zaarur, N., McKee, A., Bowser, R., Sherman, M., Petrucelli, L., & Wolozin, B. (2010). Tar DNA binding protein-43 (TDP-43) associates with stress granules: Analysis of cultured cells and pathological brain tissue. *PLoS ONE*, *5*(10), 13250. https://doi.org/10.1371/journal.pone.0013250

Liu, Y. C., Chiang, P. M., & Tsai, K. J. (2013). Disease animal models of TDP-43 proteinopathy and their pre-clinical applications. In *International Journal of Molecular Sciences* (Vol. 14, Issue 10, pp. 20079–20111). Multidisciplinary Digital Publishing Institute (MDPI). https://doi.org/10.3390/ijms141020079

López-Otín, C., Blasco, M. A., Partridge, L., Serrano, M., & Kroemer, G. (2013). The hallmarks of aging. In *Cell* (Vol. 153, Issue 6, p. 1194). Elsevier B.V. https://doi.org/10.1016/j.cell.2013.05.039

Louka, A., Bagnoli, S., Rupert, J., Esapa, B., Tartaglia, G. G., Cellerino, A., Pastore, A., & Tozzini, E. T. (2021). New lessons on TDP-43 from the killifish N. furzeri. *BioRxiv*, 2021.02.04.429704. https://doi.org/10.1101/2021.02.04.429704

Louka, A., Zacco, E., Temussi, P. A., Tartaglia, G. G., & Pastore, A. (2020). RNA as the stone guest of protein aggregation. In *Nucleic Acids Research* (Vol. 48, Issue 21, pp. 11880–11889). Oxford University Press. https://doi.org/10.1093/nar/gkaa822

Luk, K. C., Kehm, V., Carroll, J., Zhang, B., O'Brien, P., Trojanowski, J. Q., & Lee, V. M. Y. (2012). Pathological α-synuclein transmission initiates Parkinson-like neurodegeneration in nontransgenic mice. *Science*, *338*(6109), 949–953. https://doi.org/10.1126/science.1227157

Mackenzie, I. R. A., & Rademakers, R. (2008). The role of transactive response DNA-binding protein-43 in amyotrophic lateral sclerosis and frontotemporal dementia. In *Current Opinion in Neurology* (Vol. 21, Issue 6, pp. 693–700). NIH Public Access. https://doi.org/10.1097/WCO.0b013e3283168d1d

Malinovska, L., Kroschwald, S., & Alberti, S. (2013). Protein disorder, prion propensities, and self-organizing macromolecular collectives. In *Biochimica et Biophysica Acta - Proteins and Proteomics* (Vol. 1834, Issue 5, pp. 918–931). Elsevier. https://doi.org/10.1016/j.bbapap.2013.01.003

Martin, S., & Tazi, J. (2014). Visualization of G3BP stress granules dynamics in live primary cells. *Journal of Visualized Experiments : JoVE*, *87*, 51197. https://doi.org/10.3791/51197

Matsui, H. (2017). The use of fish models to study human neurological disorders. *Neuroscience Research*, *120*, 1–7. https://doi.org/10.1016/j.neures.2017.02.004

Matsui, H., Gavinio, R., & Takahashi, R. (2012). Medaka Fish Parkinson's Disease Model. *Experimental Neurobiology*, *21*(3), 94–100. https://doi.org/10.5607/en.2012.21.3.94

Matsui, H., Ito, H., Taniguchi, Y., Inoue, H., Takeda, S., & Takahashi, R. (2010). Proteasome inhibition in medaka brain induces the features of Parkinson's disease. *Journal of Neurochemistry*, *115*(1), 178–187. https://doi.org/10.1111/j.1471-4159.2010.06918.x

Matsui, H., Kenmochi, N., & Namikawa, K. (2019). Age- and α-Synuclein-Dependent Degeneration of Dopamine and Noradrenaline Neurons in the Annual Killifish Nothobranchius furzeri. *Cell Reports*, *26*(7), 1727-1733.e6. https://doi.org/10.1016/j.celrep.2019.01.015

Matsui, H., Taniguchi, Y., Inoue, H., Uemura, K., Takeda, S., & Takahashi, R. (2009). A chemical neurotoxin, MPTP induces Parkinson's disease like phenotype, movement disorders and persistent loss of dopamine neurons in medaka fish. *Neuroscience Research*, *65*(3), 263–271. https://doi.org/10.1016/j.neures.2009.07.010

Mattson, M. P., & Magnus, T. (2006). Ageing and neuronal vulnerability. In *Nature Reviews Neuroscience* (Vol. 7, Issue 4, pp. 278–294). Nature Publishing Group. https://doi.org/10.1038/nrn1886

McCaughey-Chapman, A., & Connor, B. (2017). Rat brain sagittal organotypic slice cultures as an ex vivo dopamine cell loss system. *Journal of Neuroscience Methods*, *277*, 83–87. https://doi.org/10.1016/j.jneumeth.2016.12.012

McDonald, K. K., Aulas, A., Destroismaisons, L., Pickles, S., Beleac, E., Camu, W., Rouleau, G. A., & Velde, C. Vande. (2011). TAR DNA-binding protein 43 (TDP-43) regulates stress granule dynamics via differential regulation of G3BP and TIA-1. *Human Molecular Genetics*, *20*(7), 1400–1410. https://doi.org/10.1093/hmg/ddr021

McKinley, E. T., Baranowski, T. C., Blavo, D. O., Cato, C., Doan, T. N., & Rubinstein, A. L. (2005). Neuroprotection of MPTP-induced toxicity in zebrafish dopaminergic neurons. *Molecular Brain Research*, *141*(2), 128–137. https://doi.org/10.1016/j.molbrainres.2005.08.014

McMillan, P. J., White, S. S., Franklin, A., Greenup, J. L., Leverenz, J. B., Raskind, M. A., & Szot, P. (2011). Differential response of the central noradrenergic nervous system to the loss of locus coeruleus neurons in Parkinson's disease and Alzheimer's disease. *Brain Research*, *1373*, 240–252. https://doi.org/10.1016/j.brainres.2010.12.015

Meredith, G. E., & Rademacher, D. J. (2011). MPTP mouse models of Parkinson's disease: An update. In *Journal of Parkinson's Disease* (Vol. 1, Issue 1, pp. 19–33). J Parkinsons Dis. https://doi.org/10.3233/JPD-2011-11023

Merlini, G., Bellotti, V., Andreola, A., Palladini, G., Obici, L., Casarini, S., & Perfetti, V. (2001). Protein aggregation. *Clinical Chemistry and Laboratory Medicine*, *39*(11), 1065–1075. https://doi.org/10.1515/CCLM.2001.172

Neelagandan, N., Gonnella, G., Dang, S., Janiesch, P. C., Miller, K. K., Küchler, K., Marques, R. F., Indenbirken, D., Alawi, M., Grundhoff, A., Kurtz, S., & Duncan, K. E. (2019). TDP-43 enhances translation of specific mRNAs linked to neurodegenerative disease. *Nucleic Acids Research*, *47*(1), 341–361. https://doi.org/10.1093/nar/gky972

Neumann, M., Sampathu, D. M., Kwong, L. K., Truax, A. C., Micsenyi, M. C., Chou, T. T., Bruce, J., Schuck, T., Grossman, M., Clark, C. M., McCluskey, L. F., Miller, B. L., Masliah, E., Mackenzie, I. R., Feldman, H., Feiden, W., Kretzschmar, H. A., Trojanowski, J. Q., & Lee, V. M. Y. (2006). Ubiquitinated TDP-43 in frontotemporal lobar degeneration and amyotrophic lateral sclerosis. *Science*, *314*(5796), 130–133. https://doi.org/10.1126/science.1134108

Nikolaienko, O., Patil, S., Eriksen, M. S., & Bramham, C. R. (2018). Arc protein: a flexible hub for synaptic plasticity and cognition. In *Seminars in Cell and Developmental Biology* (Vol. 77, pp. 33–42). Elsevier Ltd. https://doi.org/10.1016/j.semcdb.2017.09.006

Nixon, R. A. (2020). The aging lysosome: An essential catalyst for late-onset neurodegenerative diseases. In *Biochimica et Biophysica Acta - Proteins and Proteomics* (Vol. 1868, Issue 9). Elsevier B.V. https://doi.org/10.1016/j.bbapap.2020.140443

Nonaka, T., & Hasegawa, M. (2018). TDP-43 prions. *Cold Spring Harbor Perspectives in Medicine*, *8*(3). https://doi.org/10.1101/cshperspect.a024463

Ou, S. H., Wu, F., Harrich, D., García-Martínez, L. F., & Gaynor, R. B. (1995). Cloning and characterization of a novel cellular protein, TDP-43, that binds to human immunodeficiency virus type 1 TAR DNA sequence motifs. *Journal of Virology*, *69*(6), 3584–3596. https://doi.org/10.1128/jvi.69.6.3584-3596.1995

Parker, S. J., Meyerowitz, J., James, J. L., Liddell, J. R., Crouch, P. J., Kanninen, K. M., & White, A. R. (2012). Endogenous TDP-43 localized to stress granules can subsequently form protein

aggregates. *Neurochemistry International*, *60*(4), 415–424. https://doi.org/10.1016/j.neuint.2012.01.019

Patel, D., & Kuyucak, S. (2017). Computational study of aggregation mechanism in human lysozyme[D67H]. *PLoS ONE*, *12*(5), e0176886. https://doi.org/10.1371/journal.pone.0176886

Perutz, M. F., Finch, J. T., Berriman, J., & Lesk, A. (2002). Amyloid fibers are water-filled nanotubes. *Proceedings of the National Academy of Sciences of the United States of America*, *99*(8), 5591–5595. https://doi.org/10.1073/pnas.042681399

Peterson, A. C., & Li, C. S. R. (2018). Noradrenergic dysfunction in Alzheimer's and Parkinson's Diseases-An overview of imaging studies. In *Frontiers in Aging Neuroscience* (Vol. 10, Issue MAY, p. 127). Frontiers Media S.A. https://doi.org/10.3389/fnagi.2018.00127

Pickett, J., & Brayne, C. (2019). The scale and profile of global dementia research funding. In *The Lancet* (Vol. 394, Issue 10212, pp. 1888–1889). Lancet Publishing Group. https://doi.org/10.1016/S0140-6736(19)32599-1

Platzer, M., & Englert, C. (2016). Nothobranchius furzeri: A Model for Aging Research and More. *Trends in Genetics*, *32*(9), 543–552. https://doi.org/10.1016/J.TIG.2016.06.006

Poewe, W., Seppi, K., Tanner, C. M., Halliday, G. M., Brundin, P., Volkmann, J., Schrag, A. E., & Lang, A. E. (2017). Parkinson disease. *Nature Reviews Disease Primers*, *3*, 1–21. https://doi.org/10.1038/nrdp.2017.13

Polymenidou, M., Lagier-Tourenne, C., Hutt, K. R., Huelga, S. C., Moran, J., Liang, T. Y., Ling, S. C., Sun, E., Wancewicz, E., Mazur, C., Kordasiewicz, H., Sedaghat, Y., Donohue, J. P., Shiue, L., Bennett, C. F., Yeo, G. W., & Cleveland, D. W. (2011). Long pre-mRNA depletion and RNA missplicing contribute to neuronal vulnerability from loss of TDP-43. *Nature Neuroscience*, *14*(4), 459–468. https://doi.org/10.1038/nn.2779

Prabhudesai, S., Bensabeur, F. Z., Abdullah, R., Basak, I., Baez, S., Alves, G., Holtzman, N. G., Larsen, J. P., & Møller, S. G. (2016). LRRK2 knockdown in zebrafish causes developmental defects, neuronal loss, and synuclein aggregation. *Journal of Neuroscience Research*, *94*(8), 717–735. https://doi.org/10.1002/jnr.23754

Prasad, A., Bharathi, V., Sivalingam, V., Girdhar, A., & Patel, B. K. (2019). Molecular mechanisms of TDP-43 misfolding and pathology in amyotrophic lateral sclerosis. In *Frontiers in Molecular Neuroscience* (Vol. 12, p. 25). Frontiers Media S.A. https://doi.org/10.3389/fnmol.2019.00025

Prusiner, S. B., McKinley, M. P., Bowman, K. A., Bolton, D. C., Bendheim, P. E., Groth, D. F., & Glenner, G. G. (1983). Scrapie prions aggregate to form amyloid-like birefringent rods. *Cell*, *35*(2 PART 1), 349–358. https://doi.org/10.1016/0092-8674(83)90168-X

Radford, H., Moreno, J. A., Verity, N., Halliday, M., & Mallucci, G. R. (2015). PERK inhibition prevents tau-mediated neurodegeneration in a mouse model of frontotemporal dementia. *Acta Neuropathologica*, *130*(5), 633–642. https://doi.org/10.1007/s00401-015-1487-z

Radwan, M., Wood, R. J., Sui, X., & Hatters, D. M. (2017). When proteostasis goes bad: Protein aggregation in the cell. In *IUBMB Life* (Vol. 69, Issue 2, pp. 49–54). Blackwell Publishing Ltd. https://doi.org/10.1002/iub.1597

Ray, L. B. (2017). Protein aggregation-mediated aging in yeast. In *Science (New York, N.Y.)* (Vol. 355, Issue 6330, pp. 1169–1171). NLM (Medline). https://doi.org/10.1126/science.355.6330.1169-n

Reichwald, K., Petzold, A., Koch, P., Downie, B. R., Hartmann, N., Pietsch, S., Baumgart, M., Chalopin, D., Felder, M., Bens, M., Sahm, A., Szafranski, K., Taudien, S., Groth, M., Arisi, I., Weise, A., Bhatt, S. S., Sharma, V., Kraus, J. M., … Platzer, M. (2015). Insights into Sex Chromosome Evolution and Aging from the Genome of a Short-Lived Fish. *Cell*, *163*(6), 1527–1538. https://doi.org/10.1016/j.cell.2015.10.071

Rink, E., & Wullimann, M. F. (2001). The teleostean (zebrafish) dopaminergic system ascending to the subpallium (striatum) is located in the basal diencephalon (posterior tuberculum). *Brain Research*, *889*(1–2), 316–330. https://doi.org/10.1016/S0006-8993(00)03174-7

Ripa, R., Dolfi, L., Terrigno, M., Pandolfini, L., Savino, A., Arcucci, V., Groth, M., Tozzini, E. T., Baumgart, M., & Cellerino, A. (2017). MicroRNA miR-29 controls a compensatory response to limit neuronal iron accumulation during adult life and aging. *BMC Biology 2017 15:1*, *15*(1), 1–20. https://doi.org/10.1186/S12915-017-0354-X

Robea, M. A., Balmus, I. M., Ciobica, A., Strungaru, S., Plavan, G., Gorgan, L. D., Savuca, A., & Nicoara, M. (2020). Parkinson's Disease-Induced Zebrafish Models: Focussing on Oxidative Stress Implications and Sleep Processes. In *Oxidative Medicine and Cellular Longevity* (Vol. 2020). Hindawi Limited. https://doi.org/10.1155/2020/1370837

Rocha, E. M., De Miranda, B., & Sanders, L. H. (2018). Alpha-synuclein: Pathology, mitochondrial dysfunction and neuroinflammation in Parkinson's disease. In *Neurobiology of Disease* (Vol. 109, Issue Pt B, pp. 249–257). Academic Press Inc. https://doi.org/10.1016/j.nbd.2017.04.004

Rohrbacher, J., Ichinohe, N., & Kitai, S. T. (2000). Electrophysiological characteristics of substantia nigra neurons in organotypic cultures: Spontaneous and evoked activities. *Neuroscience*, *97*(4), 703–714. https://doi.org/10.1016/S0306-4522(00)00046-4

Romero-Granados, R., Fontán-Lozano, Á., Aguilar-Montilla, F. J., & Carrión, Á. M. (2011). Postnatal proteasome inhibition induces neurodegeneration and cognitive deficiencies in adult mice: A new model of neurodevelopment syndrome. *PLoS ONE*, *6*(12), 28927. https://doi.org/10.1371/journal.pone.0028927

Rommelfanger, K. S., & Weinshenker, D. (2007). Norepinephrine: The redheaded stepchild of Parkinson's disease. In *Biochemical Pharmacology* (Vol. 74, Issue 2, pp. 177–190). Elsevier Inc. https://doi.org/10.1016/j.bcp.2007.01.036

Ross, C. A., & Poirier, M. A. (2004). Protein aggregation and neurodegenerative disease. *Nature Medicine*, *10*(7), S10. https://doi.org/10.1038/nm1066

Sallinen, V., Torkko, V., Sundvik, M., Reenilä, I., Khrustalyov, D., Kaslin, J., & Panula, P. (2009). MPTP and MPP+ target specific aminergic cell populations in larval zebrafish. *Journal of Neurochemistry*, *108*(3), 719–731. https://doi.org/10.1111/j.1471-4159.2008.05793.x

Samuel, F., Flavin, W. P., Iqbal, S., Pacelli, C., Renganathan, S. D. S., Trudeau, L. E., Campbell, E. M., Fraser, P. E., & Tandon, A. (2016). Effects of serine 129 phosphorylation on α-synuclein aggregation, membrane association, and internalization. *Journal of Biological Chemistry*,

291(9), 4374–4385. https://doi.org/10.1074/jbc.M115.705095

Sarath Babu, N., Murthy, C. L. N., Kakara, S., Sharma, R., Brahmendra Swamy, C. V., & Idris, M. M. (2016). 1-Methyl-4-phenyl-1,2,3,6-tetrahydropyridine induced Parkinson's disease in zebrafish. *Proteomics*, *16*(9), 1407–1420. https://doi.org/10.1002/pmic.201500291

Saxena, S., & Caroni, P. (2011). Selective Neuronal Vulnerability in Neurodegenerative Diseases: From Stressor Thresholds to Degeneration. In *Neuron* (Vol. 71, Issue 1, pp. 35–48). Cell Press. https://doi.org/10.1016/j.neuron.2011.06.031

Schneider, S. A., & Obeso, J. A. (2014). Clinical and pathological features of Parkinson's disease. *Current Topics in Behavioral Neurosciences*, *22*, 205–220. https://doi.org/10.1007/7854_2014_317

Shelkovnikova, T. A., Peters, O. M., Deykin, A. V., Connor-Robson, N., Robinson, H., Ustyugov, A. A., Bachurin, S. O., Ermolkevich, T. G., Goldman, I. L., Sadchikova, E. R., Kovrazhkina, E. A., Skvortsova, V. I., Ling, S. C., Da Cruz, S., Parone, P. A., Buchman, V. L., & Ninkina, N. N. (2013). Fused in sarcoma (FUS) protein lacking nuclear localization signal (NLS) and major RNA binding motifs triggers proteinopathy and severe motor phenotype in transgenic mice. *Journal of Biological Chemistry*, *288*(35), 25266–25274. https://doi.org/10.1074/jbc.M113.492017

Shen, D., Coleman, J., Chan, E., Nicholson, T. P., Dai, L., Sheppard, P. W., & Patton, W. F. (2011). Novel Cell- and Tissue-Based Assays for Detecting Misfolded and Aggregated Protein Accumulation Within Aggresomes and Inclusion Bodies. *Cell Biochemistry and Biophysics*, *60*(3), 173–185. https://doi.org/10.1007/s12013-010-9138-4

Sheng, D., Qu, D., Kwok, K. H. H., Ng, S. S., Lim, A. Y. M., Aw, S. S., Lee, C. W. H., Sung, W. K., Tan, E. K., Lufkin, T., Jesuthasan, S., Sinnakaruppan, M., & Liu, J. (2010). Deletion of the WD40 domain of LRRK2 in zebrafish causes parkinsonism-like loss of neurons and locomotive defect. *PLoS Genetics*, *6*(4), 1000914. https://doi.org/10.1371/journal.pgen.1000914

Sherer, T. B., Betarbet, R., Testa, C. M., Seo, B. B., Richardson, J. R., Kim, J. H., Miller, G. W., Yagi, T., Matsuno-Yagi, A., & Greenamyre, J. T. (2003). Mechanism of Toxicity in Rotenone Models of Parkinson's Disease. *Journal of Neuroscience*, *23*(34), 10756–10764. https://doi.org/10.1523/jneurosci.23-34-10756.2003

Stahl, K., Skare, Ø., & Torp, R. (2009). Organotypic cultures as a model of Parkinson's disease. A twist to an old model. *TheScientificWorldJournal*, *9*, 811–821. https://doi.org/10.1100/tsw.2009.68

Stoppini, L., Buchs, P. A., & Muller, D. (1991). A simple method for organotypic cultures of nervous tissue. *Journal of Neuroscience Methods*, *37*(2), 173–182. https://doi.org/10.1016/0165-0270(91)90128-M

Svahn, A. J., Don, E. K., Badrock, A. P., Cole, N. J., Graeber, M. B., Yerbury, J. J., Chung, R., & Morsch, M. (2018). Nucleo-cytoplasmic transport of TDP-43 studied in real time: impaired microglia function leads to axonal spreading of TDP-43 in degenerating motor neurons. *Acta Neuropathologica*, *136*(3), 445–459. https://doi.org/10.1007/s00401-018-1875-2

Szabadi, E. (2013). Functional neuroanatomy of the central noradrenergic system. In *Journal of*

Psychopharmacology (Vol. 27, Issue 8, pp. 659–693). J Psychopharmacol. https://doi.org/10.1177/0269881113490326

Tashiro, Y., Urushitani, M., Inoue, H., Koike, M., Uchiyama, Y., Komatsu, M., Tanaka, K., Yamazaki, M., Abe, M., Misawa, H., Sakimura, K., Ito, H., & Takahashia, R. (2012). Motor neuron-specific disruption of proteasomes, but not autophagy, replicates amyotrophic lateral sclerosis. *Journal of Biological Chemistry*, *287*(51), 42984–42994. https://doi.org/10.1074/jbc.M112.417600

Terzibasi, E., Valenzano, D. R., Benedetti, M., Roncaglia, P., Cattaneo, A., Domenici, L., & Cellerino, A. (2008). Large Differences in Aging Phenotype between Strains of the Short-Lived Annual Fish Nothobranchius furzeri. *PLOS ONE*, *3*(12), e3866.

Terzibasi Tozzini, E., Dorn, A., Ng'Oma, E., Polačik, M., Blažek, R., Reichwald, K., Petzold, A., Watters, B., Reichard, M., & Cellerino, A. (2013). Parallel evolution of senescence in annual fishes in response to extrinsic mortality. *BMC Evolutionary Biology*, *13*(1). https://doi.org/10.1186/1471-2148-13-77

Testa, C. M., Sherer, T. B., & Greenamyre, J. T. (2005). Rotenone induces oxidative stress and dopaminergic neuron damage in organotypic substantia nigra cultures. *Molecular Brain Research*, *134*(1), 109–118. https://doi.org/10.1016/j.molbrainres.2004.11.007

Thomas, R. R., Keeney, P. M., & Bennett, J. P. (2012). Impaired complex-I mitochondrial biogenesis in parkinson disease frontal cortex. *Journal of Parkinson's Disease*, *2*(1), 67–76. https://doi.org/10.3233/JPD-2012-11074

Tomizawa, K., Kunieda, J. ichi, & Nakayasu, H. (2001). Ex vivo culture of isolated zebrafish whole brain. *Journal of Neuroscience Methods*, *107*(1–2), 31–38. https://doi.org/10.1016/S0165-0270(01)00349-1

Tourrière, H., Chebli, K., Zekri, L., Courselaud, B., Blanchard, J. M., Bertrand, E., & Tazi, J. (2003). The RasGAP-associated endoribonuclease G3BP assembles stress granules. *Journal of Cell Biology*, *160*(6), 823–831. https://doi.org/10.1083/jcb.200212128

Tozzini, E. T., Baumgart, M., Battistoni, G., & Cellerino, A. (2012). Adult neurogenesis in the short-lived teleost Nothobranchius furzeri: Localization of neurogenic niches, molecular characterization and effects of aging. *Aging Cell*, *11*(2), 241–251. https://doi.org/10.1111/j.1474-9726.2011.00781.x

Tran, M., & Reddy, P. H. (2021). Defective Autophagy and Mitophagy in Aging and Alzheimer's Disease. In *Frontiers in Neuroscience* (Vol. 14). Frontiers Media S.A. https://doi.org/10.3389/fnins.2020.612757

Udan, M., & Baloh, R. H. (2011). Implications of the prion-related Q/N domains in TDP-43 and FUS. In *Prion* (Vol. 5, Issue 1, pp. 1–5). Prion. https://doi.org/10.4161/pri.5.1.14265

Uemura, N., Koike, M., Ansai, S., Kinoshita, M., Ishikawa-Fujiwara, T., Matsui, H., Naruse, K., Sakamoto, N., Uchiyama, Y., Todo, T., Takeda, S., Yamakado, H., & Takahashi, R. (2015). Viable Neuronopathic Gaucher Disease Model in Medaka (Oryzias latipes) Displays Axonal Accumulation of Alpha-Synuclein. *PLoS Genetics*, *11*(4). https://doi.org/10.1371/journal.pgen.1005065

Valdesalici, S., & Cellerino, A. (2003). Extremely short lifespan in the annual fish Nothobranchius furzeri. *Proceedings of the Royal Society of London. Series B: Biological Sciences*, *270*(SUPPL. 2). https://doi.org/10.1098/RSBL.2003.0048

Vaquer-Alicea, J., & Diamond, M. I. (2019). Propagation of protein aggregation in neurodegenerative diseases. *Annual Review of Biochemistry*, *88*, 785–810. https://doi.org/10.1146/annurev-biochem-061516-045049

Vega, M. V., Nigro, A., Luti, S., Capitini, C., Fani, G., Gonnelli, L., Boscaro, F., & Chiti, F. (2019). Isolation and characterization of soluble human full-length TDP-43 associated with neurodegeneration. *The FASEB Journal*, *33*(10), 10780–10793. https://doi.org/https://doi.org/10.1096/fj.201900474R

Volpicelli-Daley, L. A., Luk, K. C., Patel, T. P., Tanik, S. A., Riddle, D. M., Stieber, A., Meaney, D. F., Trojanowski, J. Q., & Lee, V. M. Y. (2011). Exogenous α-Synuclein Fibrils Induce Lewy Body Pathology Leading to Synaptic Dysfunction and Neuron Death. *Neuron*, *72*(1), 57–71. https://doi.org/10.1016/j.neuron.2011.08.033

Walther, D. M., Kasturi, P., Zheng, M., Pinkert, S., Vecchi, G., Ciryam, P., Morimoto, R. I., Dobson, C. M., Vendruscolo, M., Mann, M., & Hartl, F. U. (2015). Widespread proteome remodeling and aggregation in aging C. elegans. *Cell*, *161*(4), 919–932. https://doi.org/10.1016/j.cell.2015.03.032

Waxman, E. A., & Giasson, B. I. (2011). Characterization of kinases involved in the phosphorylation of aggregated α-synuclein. *Journal of Neuroscience Research*, *89*(2), 231. https://doi.org/10.1002/JNR.22537

Wen, L., Wei, W., Gu, W., Huang, P., Ren, X., Zhang, Z., Zhu, Z., Lin, S., & Zhang, B. (2008). Visualization of monoaminergic neurons and neurotoxicity of MPTP in live transgenic zebrafish. *Developmental Biology*, *314*(1), 84–92. https://doi.org/10.1016/j.ydbio.2007.11.012

Wolf, M. K. (1970). Anatomy of cultured mouse cerebellum. II. Organotypic migration of granule cells demonstrated by silver impregnation of normal and mutant cultures. *Journal of Comparative Neurology*, *140*(3), 281–297. https://doi.org/10.1002/cne.901400304

Wolters, F. J., & Arfan Ikram, M. (2019). Epidemiology of Vascular Dementia: Nosology in a Time of Epiomics. *Arteriosclerosis, Thrombosis, and Vascular Biology*, *39*(8), 1542–1549. https://doi.org/10.1161/ATVBAHA.119.311908

Xu, Z.-S. (2012). Does a loss of TDP-43 function cause neurodegeneration? *Molecular Neurodegeneration*, *7*, 27. https://doi.org/10.1186/1750-1326-7-27

Yang, H., Hu, H.-Y., & Hu, -Y. (2016). Sequestration of cellular interacting partners by protein aggregates: implication in a loss-of-function pathology. *The FEBS Journal*, *283*(20), 3705–3717. https://doi.org/10.1111/febs.13722

Žák, J., & Reichard, M. (2020). Fluctuating temperatures extend median lifespan, improve reproduction and reduce growth in turquoise killifish. *Experimental Gerontology*, *140*. https://doi.org/10.1016/j.exger.2020.111073

Zarow, C., Lyness, S. A., Mortimer, J. A., & Chui, H. C. (2003). Neuronal loss is greater in the locus

coeruleus than nucleus basalis and substantia nigra in Alzheimer and Parkinson diseases. *Archives of Neurology*, *60*(3), 337–341. https://doi.org/10.1001/archneur.60.3.337

Zhang, F., Liu, C. L., & Hu, B. R. (2006). Irreversible aggregation of protein synthesis machinery after focal brain ischemia. *Journal of Neurochemistry*, *98*(1), 102–112. https://doi.org/10.1111/j.1471-4159.2006.03838.x

Zhang, K., Daigle, J. G., Cunningham, K. M., Coyne, A. N., Ruan, K., Grima, J. C., Bowen, K. E., Wadhwa, H., Yang, P., Rigo, F., Taylor, J. P., Gitler, A. D., Rothstein, J. D., & Lloyd, T. E. (2018). Stress Granule Assembly Disrupts Nucleocytoplasmic Transport. *Cell*, *173*(4), 958-971.e17. https://doi.org/10.1016/j.cell.2018.03.025

Zhang, S., Hu, S., Chao, H. H., & Li, C. S. R. (2016). Resting-State Functional Connectivity of the Locus Coeruleus in Humans: In Comparison with the Ventral Tegmental Area/Substantia Nigra Pars Compacta and the Effects of Age. *Cerebral Cortex*, *26*(8), 3413–3427. https://doi.org/10.1093/cercor/bhv172